Christensenella minuta has minor effects on gut microbiome composition but modulates host energy expenditure in mice

Dissertation

der Mathematisch-Naturwissenschaftlichen Fakultät

der Eberhard Karls Universität Tübingen

zur Erlangung des Grades eines

Doktors der Naturwissenschaften

(Dr. rer. nat.)

vorgelegt von

Tanja Schön

aus Hannover

Tübingen

2023

Gedruckt mit Genehmigung der Mathematisch-Naturwissenschaftlichen Fakultät der Eberhard Karls Universität Tübingen.

Tag der mündlichen Qualifikation:	17.05.2023
Dekan:	Prof. Dr. Thilo Stehle
1. Berichterstatter/-in:	Prof. Ruth Ley, Ph.D.
2. Berichterstatter/-in:	Prof. Dr. Boris Maček

Acknowledgements

I am truly lucky that I received so much support from several people without whom this thesis would not have been possible. I would like to thank:

My supervisors:

Ruth E. Ley for the opportunity she gave me to do my Ph.D. in the Department of Microbiome Science, even though I was a stranger to the field of microbiology. Jillian L. Waters for her support, the regular meetings, her confidence in me and my work, and for teaching me so much: starting from how to inoculate microbial cultures up to all the steps related to working with mice. The other members of my thesis advisory committee, Boris Maček and Frank Chan. Collectively, you have all followed my progress and contributed to my thesis with discussions and valuable feedback while encouraging me to continue my work.

My lab mates:

Taichi Suzuki for all his support in my mouse experiment, for the vivid and animating discussions about science, cooking, art, plants, and fish tanks. Claudia Mirretta-Barone, for all the lunch conversations and her caring personality. Jacobo de la Cuesta, Leo Moreno, Andrea Borbón, Guillermo Luque, and Albane Ruaud for the many coffee breaks, shared laughs and tears, and all the time spent together. Liam Fitzstevens, my SWAG buddy, for the jokes, keeping me motivated, and the mental support in the final sprint of this thesis. Tony Walters, Daphne Welter, and Jess Sutter for long conversations, and delicious meals. The Banff crew, Hagay Enav, Kelsey Hus, Stacey Heaver, and a few people already mentioned, for an unforgettable trip to the winter wonderland of Canada. Silke Dauser, Sophie Maisch, and Annkatrin Geisel for our chats and bantering that made my days start with a smile. Dai Long Vu, Dennis Jakob, Christa Lanz, George Deffner, Xiaoying Liu, and all the other people I enjoyed a break with. Karin Klein, Heike Budde, and Ursula Schach, for all the support that keeps the department and lab running. Matthias Neuscheler and Christin Eitel for preparing the mouse equipment and their assistance during my mouse experiments. Moreover, all in my lab for answering my questions, sharing your knowledge, the bioinformatic support, and the feedback after

every presentation.

My Family and Friends:

Elena Schön, Andrej Schön, and Marica Schön, for never stopping to believe in me and for their endless support, patience, and love. Danke für alles, ich liebe euch. Rabiye Akbuğa and Ali Akbuğa for cooking food, when we were too tired. Tanja Akbuğa, Aytekin Akbuğa, and their children, Milas, Ella, Nora, and the next one on the way, for being a source of endless joy in my life. Christian Krüger and Sebastian Pirk, for all the amazing trips around the world, the delicious food cooked together, the shared movie and board game nights. The University-Hohenheim crew, Barbara Peixoto Pinheiro, Esther Lehmann, Viviane Hönig, and Oliver Täffner, for all the laughs in the past years. May many more follow!

Last, but not least:

Rıfat Akbuğa, who I love with all my heart. Who is my rock and makes me a better person every day. His support and patience keep me going and growing in the long journey of my academic career and adult life. Whose guidance made me see the light during the darkest moments of my Ph.D. and the pandemic. Without you, this thesis would not exist. Seni çok seviyorum aşkım!

Summary

The gut microbiome is a complex microbial community comprising archaea, bacteria, viruses, and fungi inhabiting the gastrointestinal tract. Mounting evidence implies it plays a causal role in host health and disease, prompting an intensive search for key taxa driving these associations. Human metabolic health and a healthy BMI are consistently associated with the gut bacterial family *Christensenellaceae*, a highly heritable family within the Firmicutes. Our group, and subsequently others, have demonstrated a causal role of *Christensenella minuta* in reducing host adiposity gain. Despite this strong evidence for a central role of *C. minuta* in host health, little is known about its interactions with other microbial community members and the host, limiting understanding of its effect on host body composition and health. This work aimed to provide insights into the effect of *C. minuta* on both the microbial community and the host *in vivo*. To accomplish this, I adopted two approaches.

First, I examined how *C. minuta* affected the microbial community in mice. I investigated this question in the context of a simplified and complex microbial community, the latter obtained by fecal transplants from a human obese donor to recipient germfree mice. My findings show an increase in the abundance of *C. minuta* in the presence of other taxa in the murine gut. While *C. minuta* had only minor effects on the composition of a complex microbial community, I observed a consistent pattern of lower abundances of taxa belonging to the family *Lachnospiraceae*.

Further, I assessed the impact of *C. minuta* amendment on host energy expenditure in recipient male and female mice. Strikingly, *C. minuta* proved to be linked with murine physical activity, energy expenditure, and circulating metabolites, the latter partly correlated to changes in the microbial community. These effects of *C. minuta* on both the microbiome and the host differed depending on host sex, adding another level of complexity to these interactions.

My research sheds light on the interactions of *C. minuta* with the microbiome and the host, uncovering a potential mechanism for the association of *Christensenellaceae* with metabolic health and lean BMI.

Zusammenfassung

Das Darmmikrobiom ist eine komplexe mikrobielle Gemeinschaft aus Archaeen, Bakterien, Viren und Pilzen, die den Magen-Darm-Trakt bewohnen. Zunehmende Erkenntnisse belegen eine kausale Rolle des Darmmikrobioms für die Gesundheit und Krankheit des Wirtes und veranlassten eine intensive Suche nach den treibenden Schlüssel-Taxa. Ein gesunder Stoffwechsel und BMI des Menschen werden durchweg mit der Darmbakterienfamilie *Christensenellaceae* in Verbindung gebracht. Die Häufigkeit dieser Familie innerhalb der Firmicuten wird stark von den Genen des Wirtes bestimmt. Unsere Arbeitsgruppe, gefolgt von anderen, wies eine ursächliche Rolle von *Christensenella minuta* bei der Reduktion der Fettzunahme des Wirtes nach. Trotz dieser aussagekräftigen Beweise für eine zentrale Rolle von *C. minuta* für die Gesundheit des Wirts, ist nur wenig über die Interaktionen von *C. minuta* mit anderen Mitgliedern der mikrobiellen Gemeinschaft und dem Wirt bekannt, was eine Einschränkung für das Verständnis auf dessen Auswirkungen auf die Körperzusammensetzung und Gesundheit des Wirtes darstellt. Ziel dieser Dissertation war es, Einblicke in die Wirkung von *C. minuta* auf die mikrobielle Gemeinschaft und den Wirt *in vivo* zu gewinnen. Um dies zu erreichen, habe ich zwei Ansätze verfolgt.

Zunächst untersuchte ich den Einfluss von *C. minuta* auf die mikrobielle Gemeinschaft in Mäusen. Diese Fragestellung betrachtete ich im Zusammenhang einer vereinfachten oder komplexen mikrobiellen Gemeinschaft, letztere bezogen aus Stuhltransplantation eines fettleibigen menschlichen Spenders auf keimfreie Empfänger-Mäuse. Meine Resultate zeigen, dass die Häufigkeit von *C. minuta* in Gegenwart anderer Taxa im Mäusedarm zunimmt. Während *C. minuta* nur geringfügige Auswirkungen auf die Gesamtzusammensetzung einer komplexen mikrobiellen Gemeinschaft hatte, stellte ich ein konsistentes Muster geringerer Häufigkeiten von Taxa aus der Familie der *Lachnospiraceae* fest.

Des Weiteren untersuchte ich die Auswirkungen einer Zugabe von *C. minuta* auf den Energieverbrauch männlicher und weiblicher Empfänger-Mäuse. Dabei zeigte sich ein Zusammenhang zwischen *C. minuta* und der physischen Aktivität, dem Energieverbrauch und den zirkulierenden Metaboliten von Mäusen. Ein Teil

dieser Metaboliten korrelierte mit Veränderungen in der mikrobiellen Gemeinschaft. Diese Auswirkungen von *C. minuta* auf das Mikrobiom und den Wirt variierten je nach Geschlecht der Mäuse, was diesen Wechselwirkungen eine weitere Komplexitätsebene verlieh.

Meine Forschung liefert neue Erkenntnisse über die Wechselwirkungen von *C. minuta* mit dem Mikrobiom und dem Wirt und deckt einen möglichen Mechanismus für die Assoziation von *Christensenellaceae* mit einem gesunden Stoffwechsel und BMI auf.

Table of Contents

Abbreviations

ASF	Altered Schaedler Flora
BMI	Body mass index
DAA	Differential abundance analysis
EE	Energy expenditure
FMT	Fecal microbiota transplantation
GE	genome equivalents
HF	High-fat
NC	Normal-chow
OTU	Operational taxonomic unit
SCFA	Short-chain fatty acid

Chapter 1. Background

The human microbiome can be considered a “microbial organ” [1], with a profound influence on our body processes and health [2], including host obesity [3]. In 2012 the microbial family of *Christensenellaceae* was first discovered through the isolation of one member, *Christensenella minuta* [4]. Two years later my research group discovered a causal role for *C. minuta* in reducing host adiposity gain [5] and submitted the patent, “Modulation of fat storage in a subject by altering population levels of *Christensenellaceae* in the GI tract” [6]. But open questions remain - what is the mechanism behind the adiposity decreasing effect of *C. minuta* and can it be traced back to the interactions of *C. minuta* with the host or the microbial community?

1.1. The human microbiome

At the cellular level, the human body is only half-human: it consists of as many microbial cells as human cells, including bacteria, archaea, viruses, and fungi [7]. Collectively, these microbes colonizing our bodies, with their distinct properties, functions, and interactions with their environment, are known as the human microbiome [8]. The majority of these microbes are harbored by the intestinal tract, the largest interface of the human body with its external environment [9]. The dense population of 10^{11} microbes $gram^{-1}$ in this area and the ease of sampling have led to a comprehensive characterization of the gut microbiome [7]. A description of the microbiome is provided by two complementary perspectives, one ecological and the other physiological. An ecologist defines a microbiome as an ecosystem exposed to changes in nutrients [10] or environmental stressors [11], where its members interact with each other and with their environment [8]. It is this interaction with the environment, the intestinal tract of a living organism, that leads to the physiological significance of the gut microbiome. The host can actively influence interactions with the microbial community in favor of commensal species [12] while benefiting from compounds produced by the microbiome [13] and the protective effects of the microbiome against pathogen invasion [14]. It is due to this strong interplay between

the host and the intestinal microbes that researchers portray the gut microbiome as a microbial organ, a structural unit residing within the body of the host with a physiological relevant function [1].

1.2. The interplay between the gut microbiome and obesity

In recent years, studies have revealed the importance of the gut microbiome for human health by discovering its involvement in several diseases beyond the gastrointestinal tract, including metabolic syndrome [15,16], autoimmune conditions [17], cancer [18], as well as psychological and neurological diseases [19–21]. Fecal microbiota transplantation (FMT) studies have demonstrated causal relationships of the gut microbiome in several disease phenotypes: disease parameters, including accelerated gastrointestinal transit time [22], permeability [23], inflammation [22,23], and conditions such as obesity [24,25] can be transferred from the microbiome donor to a healthy recipient.

Obesity is a non-communicable disease causing approximately 2.8 million deaths each year, and this number is rising at an alarming rate [26]. While obesity was previously associated with industrialized, high-income countries, it is now spreading to low- and middle-income countries [27]. As a risk factor for a wide range of multiple diseases, including type 2 diabetes, cardiovascular disease, coronary heart disease, stroke, and various cancers, obesity dramatically impacts quality of life and life expectancy [28]. The condition of obesity is the outcome of an imbalanced host energy homeostasis, an important mechanism maintaining host health and survival. Energy homeostasis consists of two principal factors, energy intake and energy expenditure (EE), each of which includes physiological and behavioral aspects [29]. Energy intake is primarily driven by the feeling of appetite, which is regulated in the hypothalamus and the nucleus of the solitary tract of the brain. Here, nervous and endocrine signals related to nutritional status are translated into neuropeptides controlling feeding behavior [30]. The four key determinants of EE are: (i) the basal metabolic rate, (ii) energy costs of thermoregulation, (iii) the thermic effect of food, and (iv) physical activity [31]. The basal metabolic rate refers to the obligatory energy cost of self-maintenance at thermoneutrality in an inactive state

[32], while thermoregulation ensures body temperature remains between certain boundaries regardless of the surrounding temperature [33]. The less well-known term “thermic effect of food” describes the increment in energy costs caused by absorbing and processing food for storage [34]. Finally, the physical activity proportion of EE is equivalent to heat production by muscle movements [35]. Although these components are separately defined, they are not independent. For example, heat generated by physical activity or feeding can substitute for heat production by thermoregulation [31]. The balance between energy intake and EE is vital for human health and survival, as imbalances can lead to the development of metabolic disorders [36].

Interestingly, the gut microbiome can affect multiple aspects of energy homeostasis in the host [30]. In this context, the best-studied effect of the microbiome is its contribution to energy harvested from our daily food intake. A major proportion of nutritional energy is inaccessible to the human body without the additional fermentative metabolic conversions contributed by our gut microbiome [24,37]. This is clearly illustrated by a lower adiposity of 42% in germfree mice compared to conventionally raised mice, despite their greater food intake [38]. The energy harvest capability of the gut microbiome differs dramatically from person to person and has been identified as a crucial factor for obesity [24]. Further, our gut microbes are vital for metabolic-induced thermogenesis, as demonstrated by the higher risk of hypothermia in germfree animals or animals treated with antibiotics when exposed to cold stress [39]. More recently, researchers described the communication of our microbial gut inhabitants with the brain and vice versa, the microbiome-gut-brain axis [20]. Here, studies have identified how microbes influence aspects of energy homeostasis controlled by the host brain. Several pre- and probiotics were found to modulate concentrations of molecules regulating appetite, including the pancreatic polypeptide in the intestine, leptin in adipose tissue, and serum ghrelin concentrations [40]. Multiple studies have also shown an influence of individual gut microbial species [41,42] on voluntary physical exercise or the whole microbial community on exercise capacity and exhaustion [43], implying effects on muscle metabolism and behavior.

Collectively, these findings highlight the microbiome as a key player in the development and maintenance of obesity, indicating that modulating its community will aid the treatment or prevention of obesity. We thus need to move beyond pure associations and identify causal relationships, including the key taxa [44].

1.3. The connection between *Christensenella minuta* and obesity

In the context of the microbiome and obesity, the bacterial family *Christensenellaceae* of the Firmicutes phylum is a promising candidate causal agent. Earlier work from our lab uncovered an association between *Christensenellaceae* and a healthy body max index (BMI) [5]. Subsequently, studies worldwide reinforced this link and discovered associations with further parameters of health (Figure 1.1) [5,45–85]. Moreover, researchers connected a reduction in the relative abundance of *Christensenellaceae* to several diseases, such as inflammatory bowel disease [86–88], irritable bowel syndrome [89,90], and metabolic syndrome [54,78,91]. An additional property rendering this family an even more interesting study subject is its high heritability across multiple populations worldwide. In other words, the abundance of this microbial family in the human gut is partially dictated by the host genome [5,92].

This thesis focuses on a specific member of the *Christensenellaceae, Christensenella minuta* DSM 22607. *C. minuta* was the first representative of this bacterial family isolated from the feces of a healthy Japanese male in 2012 [4], with its complete genome being published in 2017 [93]. It is a non-sporulating, non-motile, strictly anaerobic [4], gram-positive [94] gut bacterium, capable of producing short-chain fatty acids (SCFAs), acetate, and butyrate [4], as well as hydrogen [95]. Interest in this species stems from its causal role in reducing adiposity gain in the host: in 2014, my lab performed transplantation studies using germfree mice, demonstrating that the addition of live *C. minuta* to obese human donor stool significantly diminished weight and adiposity gains compared to mice receiving the same unamended donor stool [5]. In 2021, Mazier et al. reproduced this reduction in adiposity gain by amending a different strain of *C. minuta* to mice on a high-fat diet,

suggesting that the causal role of *C. minuta* in host leanness is not limited to the exact mode of obesity induction [96]. Although both studies imply a causal role of *C. minuta* regulating host body composition, the underlying mechanism remains unclear.

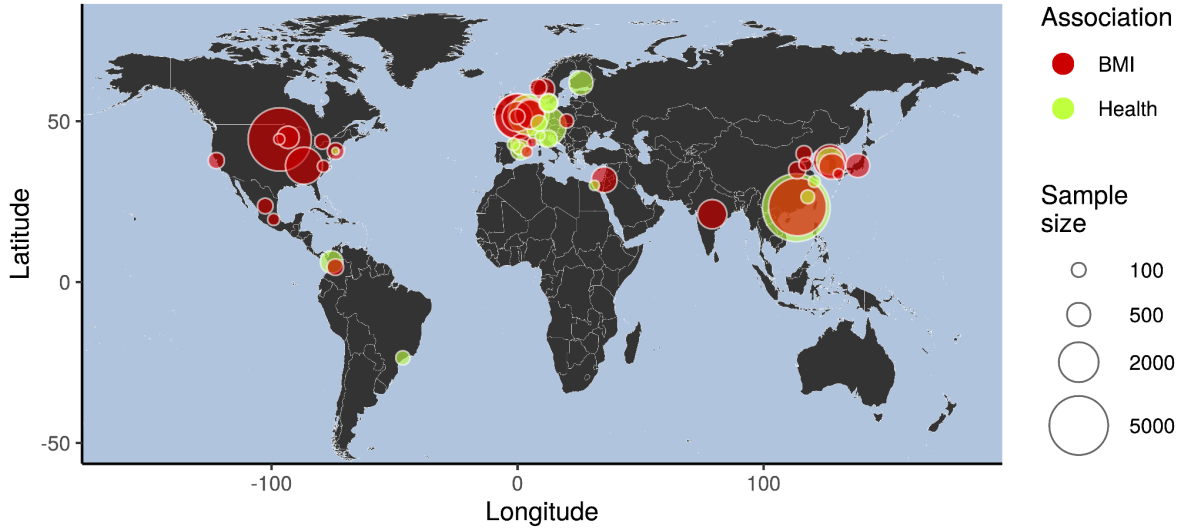

Figure 1.1: Global map of studies associating the gut bacterial family *Christensenellaceae* with healthy body mass index or metabolic health in humans. Sampling locations of 42 studies associating the abundance of *Christensenellaceae* in the gut with a healthy BMI (red) or metabolic health (green) in humans to the world map [5,45–85]. Circle size indicates study cohort size.

1.4. Aims and contributions

In this work, I aim to gain a deeper insight into the adiposity-decreasing mechanism of *C. minuta* in the host by investigating its effect on (i) the microbial community *in vivo* and (ii) the host, with a focus on host energy expenditure. For these investigations, I used datasets of murine studies conducted by Dr. Jillian L. Waters, a former project leader and my co-supervisor in the lab, and performed my own set of murine experiments.

(i) To accomplish my aim, I analyzed simplified or complex microbial communities in mice. In the case of the simplified community experiments (Chapter 2), I quantified *C. minuta* and *Blautia hydrogenotrophica* in the murine cecal content of a study conducted by Dr. Waters. To overcome the challenge of low microbial biomass in the samples, I developed a protocol to accurately quantify the two

microbial species by qPCR using species-specific primers. Further, I analyzed how the addition of *C. minuta* modulated a complex microbial community obtained via fecal transplants from an obese human donor inoculated into recipient germfree mice (Chapters 3 + 4). Here, I analyzed existing datasets of amplicon-sequenced fecal microbiomes from murine pilot studies performed by Dr. Waters (Chapter 3) and conducted my own murine experiments, including microbial shotgun sequences of the murine cecal content (Chapter 4). My results revealed a higher fitness of *C. minuta* in the presence of other microbial taxa in the murine gut (Chapter 2). Meanwhile, *C. minuta* had only minor effects on the complex microbial community when focusing on the overall community structure. Switching attention to individual taxa, an interesting pattern arose in both studies, with taxa belonging to *Lachnospiraceae* being less abundant in mice with *C. minuta* than the controls (Chapters 3 + 4).

(ii) To investigate how the *C. minuta* amendment affected host energy expenditure, I analyzed murine behavior, activity, and indirect calorimetry data collected by a behavioral phenotyping respirometry cage system in my mouse experiment (Chapter 4). Here, I uncovered evidence that *C. minuta* modulates behavioral and metabolic aspects of host EE in a sex-dimorphic manner. These phenotypes were associated with changes in metabolites involved in the gut-microbiome-brain axis and were partly traceable to modulations of the microbial community and its functional profile.

Overall, my research provides further insights into how *C. minuta* interacts with the microbiome and the host, expanding our understanding of its role in the mammalian gut habitat. I revealed a potential mechanism for the association of *Christensenellaceae* with metabolic health and lean BMI, taking an additional step toward fully understanding the impact of the microbiome on host health.

Chapter 2. Quantitative qPCR of *Christensenella minuta* in samples with low microbial biomass

2.1. Introduction

C. minuta plays a demonstrably important role in host health, reducing host adiposity gain [5,96], However, knowledge of this microbial species is scarce, particularly regarding its activities *in vivo*. The high complexity of the intestinal microbiome [97], combined with the influence of host genetics [5,98] and various environmental factors [99], complicates efforts to determine functions and interactions of individual community members in human and animal studies. To obtain a better understanding of specific species of interest, a simplification of the whole system is necessary. Such a simplified *in vivo* approach in microbiome research can be achieved through use of a gnotobiotic animal model containing an exact number of known microbial species [100–102]. Predominantly, gnotobiotic animals are created by colonizing germfree animals with the microbes of interest. This technique of studying the microbes in a gnotobiotic model organism *in vivo,* has enabled researchers to reveal multiple microbe-host and microbe-microbe interactions, including their molecular pathways [103–108]. Despite the immense advantages of gnotobiotic model organisms, completely eradicating microbial species in the body has its drawbacks. Germfree animals exhibit deficits in certain physiological, anatomical, behavioral, and metabolic attributes compared to conventionally raised mice [109]. To avoid such deficits in germfree mice, researchers developed a minimal microbial community called the Altered Schaedler Flora (ASF). The ASF consists of eight murine gut microbes selected to recapitulate the microbiome characteristics of conventional mice in a simplified manner [110], and colonizing murine guts with this community bypasses many of the deficits shown by germfree mice.

Dr. Waters aimed to study *C. minuta* in gnotobiotic mouse experiments. Although *C. minuta* had been shown to successfully colonize the murine intestine in combination with a human microbial community [5], it was uncertain if *C. minuta* could colonize gnotobiotic mice. Considerable alterations of colonization success in absence of a complex microbial community can arise due to limited availability of microbial products that can facilitate colonization [111,112]. Therefore, Dr. Waters investigated *C. minuta*, capable of producing hydrogen [95], in combination with *Blautia hydrogenotrophica,* an acetogenic microbe that utilizes hydrogen to produce acetate [113]. The idea here was that the metabolic intersection between the two microbes would lead to interactions aiding the colonization success of one or both species. To study both species, Dr. Waters conducted two gnotobiotic mouse experiments. In both experiments, she inoculated either germfree mice or mice with an ASF background [114] with *C. minuta* and *B. hydrogenotrophica* alone or in combination. Together we hypothesized that, should successful colonization occur, *B. hydrogenotrophica* would benefit from the hydrogen produced by *C. minuta,* which would be reflected in its higher abundance and increased acetate production.

To assess the colonization success of *C. minuta* and *B. hydrogenotrophica* in Dr. Waters' two murine experiments, I needed to optimize the DNA extraction and qPCR methods to quantify the microbial genome equivalents (GE) in the murine ceca via qPCR. The methods commonly used in our lab failed due to the dual challenge of low microbial biomass and limited quantities of the cecal content from the gnotobiotic mice. Such challenges are not uncommon in microbiome studies [115,116]. To address the challenges presented by my samples, I designed a DNA extraction protocol (detailed in the Appendix), yielding a sufficient amount of DNA with a purity suitable for qPCR. For the qPCR protocol, I performed typical adjustments for each primer, including annealing temperature, annealing time, and primer concentrations. To quantify the starting concentrations of each sample, I applied the One-Point-Calibration method [117] rather than the widespread standard curve method. This calibration method corrected for differences in primer efficiencies and variabilities between individual samples, ensuring proper quantification of the microbial species in the murine guts. For an analysis of metabolic interactions between the microbes, I obtained metabolomics data from Dr. Waters containing

information on SCFA concentrations in the murine guts and examined how the different colonization scenarios affected the metabolic production of acetate.

My results show that neither *C. minuta*, nor the ASF community affected the abundance of *B. hydrogenotrophica.* By contrast, fitness of *C. minuta* increased in the presence of either *B. hydrogenotrophica* or the ASF-community. Acetate was highly associated with the microbial biomass in the murine cecal contents, without evident effects by the presence of *C. minuta*. With this study, I provide a protocol for exact quantification of microbial species in low biomass samples with a high load of qPCR-inhibitors. Moreover, I offer first insights into the microbial interactions of *C. minuta in vivo*, broadening our understanding of this microbial species.

2.2. Material & Methods

Mouse experiments

Dr. Waters conducted two gnotobiotic mouse studies with male C57BL/J6 mice. The first study was performed with germfree mice (GF-study) and the second with mice containing the ASF (ASF-study). The mice were inoculated with *C. minuta* and *B. hydrogenotrophica* alone or in combination. A non-inoculated group of mice served as controls. During the experiment, mice were co-housed in groups of three to five animals. Further information can be found in Table 2.1.

Table 2.1: Information for murine gnotobiotic experiments

Experiment	Diet	age at inoculation	Duration	Lab performed at
GF-study	NIH 7017	4 weeks	6 weeks	Cornell & Tübingen
ASF-study	NC 5001	4 weeks	7 weeks	Georgia State University

ASF = Altered Schaedler Flora; GF = germfree

Nucleic acid extraction and quantification

Bacterial Standards

A pelleted 10 mL turbulent culture of *C. minuta* or *B. hydrogenotrophica,* grown in supplemented brain-heart-infusion media, was used for DNA extraction with

the DNeasy PowerSoil kit (Qiagen). The pellets were resuspended in 200 µL beating-tube buffer and transferred back into the bead-beating tubes. After homogenization of contents using the FastPrep-24 5G-device (MP Biomedicals, LLC; Settings= Speed: 7 m/s, Time: 90 s, Cycles: 2, Pause: 30 s), I spun down the tube content before adding 20 µL Proteinase K (20 mg/mL) to each sample, followed by incubation for 30 min at 60°C. Further extraction steps were carried out according to the instructions of the kit manufacturer. DNA was eluted with 80 µL PCR-grade H_2O.

Germfree mouse

I extracted DNA from germfree mouse tails with the DNeasy Blood and Tissue kit (Qiagen) according to the manufacturer's instructions.

Murine cecal contents

DNA extraction was performed by physical and enzymatic disruption of the cecal contents, followed by phenol/chloroform/iso-amyl alcohol DNA extraction and a clean-up step. I optimized this protocol for input samples with low DNA quantities. The detailed protocol is included in the Appendix (Appendix Chapter 2: Detailed DNA extraction protocol). In brief, approximately 30 mg of frozen cecal contents were aliquoted into prefilled 0.1 mm Zirconium-bead-tubes. The samples were suspended in 915 µL freshly prepared lysis solution (0.04 M sodium acetate (pH 7), 1% SDS, and 2 mM EDTA (pH 8)), and incubated at 60 °C for 30 min. Next, samples were cooled on ice prior to homogenization in a bead beater (FastPrep-24 5G, MP Biomedicals, LLC; Settings = Speed: 7 m/s, Time: 90 s, Cycles: 2, Pause: 30 s). After spinning the tube content down, I added 20 µL Proteinase K (20 mg/ml) to each tube following incubation of 30 min at 60 °C. After centrifugation, supernatants were transferred into 2 mL tubes. DNA was extracted by phenol/chloroform/iso-amyl alcohol and chloroform/iso-amyl alcohol, following ethanol precipitation at −20 °C overnight [118]. Precipitated DNA was resuspended in 220 µL PCR-grade water. Finally, DNA was cleaned up using the DNeasy Blood and Tissue kit (Qiagen) according to the manufacturer's protocol. DNA was eluted in 50 µL PCR-grade H_2O.

Quantification

I quantified DNA using a Qubit® 3.0 Fluorometer (HS Assay kit/ BR Assay kit) and checked its purity using a DS-11+ µVolume Nanodrop.

qPCR

I used the KiCqStart® SYBR® Green qPCR ReadyMix™, optimized the qPCR settings by gradient-qPCRs, and estimated the LOD for each primer. Undiluted murine samples, including three 10-fold dilutions of each, were pipetted in triplicates into the qPCR well plates. Extraction blanks, as well as germ-free murine DNA samples, were not diluted. Bacterial DNA from *C. minuta* and *B. hydrogenotrophica* cultures was diluted to ~ 0.2 ng/µL (*C. minuta*: 0.19 ng/µL; *B. hydrogenotrophica*: 0.2 ng/µL) and used as standards for quantification. The total reaction volume per well was 20 µL with a primer concentration of 200 nM, and a DNA volume of 3 µL. While the master-mixes and sample dilutions were prepared manually, loading of the 384 well plates was performed robotically (TECAN 780 ROBOT FLUENT 780 BASE UNIT). The qPCR run was performed on a BioRad CFX384 Touch™ Real-Time PCR Detection System. The cycling conditions consisted of a 95 °C incubation for 3 min, followed by a total of 40 cycles of 95 °C incubations for 10 s, 10 s annealing, and incubations at 72 °C for 30 s. Annealing temperature differed between the primers: universal 16S = 55 °C; *C. minuta* = 56.5 °C; *B. hydrogenotrophica* = 60 °C. A melting curve analysis followed from 55 to 95°C (5 s). After checking the amplification, melting curves, and fragment size by gel-electrophoresis, data were analyzed with Bio-Rad CFX96 Manager (Version: 3.1.1517.0823)

Table 2.2: Primer used for quantification of bacterial GE in murine cecal contents

Publication	Species	Direction	Sequence
[119]	*C. minuta*	forward	TTCGGGAGGAACTGTGGGTAT
	C. minuta	reverse	GGTTGCTCACGCGTTACTCA
[113]	*B. hydrogenotrophica*	forward	GAACGGAGATTTCGGTTGAA
	B. hydrogenotrophica	reverse	GTGCAATATTCCCCACTGCT
[120]	bacteria (universal)	16S rRNA 926 - forward	AAACTCAAAKGAATTGACGG
	bacteria (universal)	16S rRNA 16S 1062 - reverse	CTCACRRCACGAGCTGAC

qPCR Quantification

Calculation of genome equivalents in the reference controls

Using an online calculator [121], I calculated the copy numbers of the reference controls by their genome size and DNA concentration. To obtain the genome equivalents, I divided the copy numbers by the 16S rRNA copies in the genome.

Table 2.3: GE calculation of the qPCR positive controls

Species	*C. minuta*	*B. hydrogenotrophica*
Genome size [bp]	2969292	3565428
Accession number	NZ_CP029256.1	NZ_ACBZ00000000.1
conc. control (ng)	0.594	0.606
16S rRNA copies/genome	2	1
Genome equivalents	$9.25*10^4$	$1.57*10^5$

Starting quantity calculation

For the final quantification, I used only diluted cecal-DNA samples due to detectable PCR inhibition in the undiluted samples. The exclusion of individual outliers was determined from the standard deviation of the Cq values. I quantified my samples using the One-Point-Calibration method [117] with the 0.6 ng standards as references. The efficiency of the PCR reaction of each well was calculated with the *qpcR* package [122]. These efficiencies were used to estimate starting quantities of each sample, which were normalized by the input amounts.

Statistical analysis

Differences in abundances were estimated by analysis of variance (ANOVA) followed by the TukeyHSD test. The Spearman method was used for the correlation analyses. *p*-values <0.05 were considered statistically significant.

2.3. Results and Discussion

Fitness of *C. minuta* increases in the presence of *B. hydrogenotrophica* or the ASF community

Dr. Waters conducted two gnotobiotic murine studies investigating *C. minuta* and *B. hydrogenotrophica* in a simplified *in vivo* environment. She inoculated either germfree mice (GF-study) or mice containing the ASF-community (ASF-study) with *C. minuta* and *B. hydrogenotrophica* alone or in combination. We hypothesized an increase of fitness in *B. hydrogenotrophica* in the presence of *C. minuta* caused by the latter's hydrogen production.

To test this hypothesis, I assessed microbial abundances in the different *in vivo* colonization conditions (GF, GF + *C. minuta*, GF + *B. hydrogenotrophica*, GF + *C. minuta* + *B. hydrogenotrophica*, ASF, ASF + *C. minuta*, ASF + *B. hydrogenotrophica*, ASF + *C. minuta* + *B. hydrogenotrophica*) with three sets of primers via qPCR, universal 16S rRNA primers [120], and specific primers for each microbial species of interest [113,119]. As stated above, the commonly used extraction method within the lab failed due to the challenge of low microbial biomass. To overcome this obstacle, I developed a DNA-extraction protocol optimized for low-

biomass samples (detailed in the Appendix) and adjusted the qPCR parameters for a confident absolute quantification of the two target microbes in the murine cecal contents. My results showed the presence of *C. minuta* had no effect on the abundance of *B. hydrogenotrophica* (Figure 2.1A), leading me to reject the initial hypothesis. A weakly significant lower abundance of *B. hydrogenotrophica* was present in the dual association in the GF-study compared to the *B. hydrogenotrophica*-ASF mice ($p = 0.045$, Figure 2.1A). Aside from this one small fluctuation, *B. hydrogenotrophica* exhibited a consistent abundance independent of additional microbial community members. This might be due to its metabolic flexibility [113]. Most microbes can use various substrates as energy sources, enabling them to switch substrate usage depending on their availability. In the absence of hydrogen*, B. hydrogenotrophica* can generate energy via a hydrogen-independent pathway by using organic carbon sources provided by the host or their diet as substrates. In the presence of *C. minuta,* it can switch to hydrogen-dependent acetogenesis using hydrogen and CO_2 [113].

Meanwhile, *C. minuta* showed higher abundances in the presence of *B. hydrogenotrophica* ($p = 3e^{-4}$, Figure 2.1A), in the ASF alone ($p = 1e^{-4}$, Figure 2.1A), and in the ASF combined with *B. hydrogenotrophica* ($p = 4e^{-5}$, Figure 2.1A) compared to the mono-association of *C. minuta* in the GF-study. In all cases, the additional microbial members increased the abundance of C. minuta by the same magnitude (Figure 2.1A). The increase in *C. minuta's* biomass may be a consequence of a reduction in the hydrogen partial pressure. A reduction in hydrogen partial pressure has been reported to increase the microbial biomass of other hydrogen-producing microbes, like *Clostridium thermolacticum* [123]. An alternative explanation is a nutrient-based cross-feeding between *C. minuta* and the other gut microbes, a common phenomenon in microbiomes [124,125].

In the ASF-study, the total microbial biomass is approximately ten times higher than the quantities of *C. minuta* or *B. hydrogenotrophica* (Figure 2.1A, universal primers). Nevertheless, *C. minuta* and *B. hydrogenotrophica* show similar abundances across both studies (Figure 2.1A, species specific primers). This outcome was unexpected, as no other bacteria were present in the GF mice, potentially outcompeting these two microbes. These results might imply a host-

dependent growth limit for those two microbial species, but further investigations are needed to test this assumption.

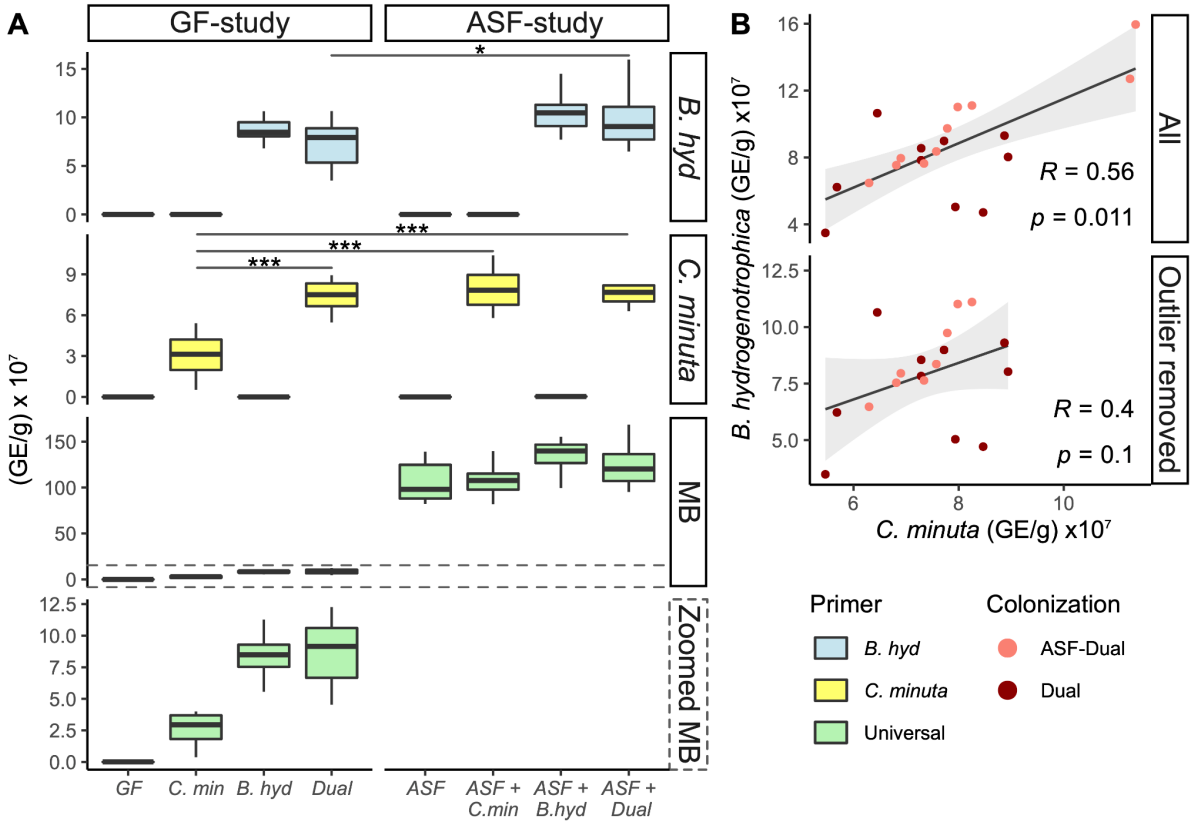

Figure 2.1 - Microbial abundances quantified via qPCR. Microbial abundances of *B. hydrogenotrophica*, *C. minuta*, and all microbes were quantified using species-specific [113,119] and universal primers [120] in two murine gnotobiotic experiments. Mice of a germfree- or ASF-background were inoculated with *C. minuta* and *B. hydrogenotrophica* (*B. hyd*) alone or in combination (Dual). (A) Boxplots showing the microbial abundances for each treatment group, for each set of primers. The two bottom rows depict total microbial biomass with a zoomed-in section at the bottom. (B) Correlation of the abundances of *B. hydrogenotrophica* and *C. minuta* in the dual associated groups of both studies. The upper plot contains the whole dataset, while the two outliers were removed in the lower plot. Statistical analyses were performed using (A) ANOVA corrected by TukeyHSD and (B) Spearman correlations. ASF = Altered Schaedler Flora; *B. hyd* = *B. hydrogenotrophica*; GE = genome equivalents; MB = microbial biomass.

A correlation analysis showed that the abundance of *C. minuta* and *B. hydrogenotrophica* correlated positively in dual-associated mice of both studies (p = 0.011, Figure 2.1B), but this correlation was mainly driven by two outliers. After outlier removal, a non-significant trend for a positive correlation remained (p = 0.1,

Figure 2.1B). Due to the sparsity of samples, no final conclusions regarding the dependence of microbial abundances between both species could be drawn.

In conclusion, my data provided evidence for syntrophic interactions between *C. minuta* and *B. hydrogenotrophica* or the ASF microbial members, raising the abundance of *C. minuta*.

Correlation between microbial biomass and microbial acetate

To investigate microbial interaction on a metabolic level, I analyzed acetate levels in dependence on microbial biomass. Acetate is the simplest SCFA produced by the host and microbes [30]. Here, I observed a significant association between acetate and total microbial biomass in the combined dataset of both studies (p = 2.2e-16, Figure 2.2A) and in each study independently (GF-study: p = 1.9e-5; ASF-study: p = 0.007; Figure 2.2B). None of the other SCFAs was associated with microbial biomass (data not shown).

A closer inspection of the correlation plots shows that the cecal contents of GF-*B. hydrogenotrophica* mice contained three times higher levels of acetate than GF-*C. minuta* mice, an expected pattern according to published *in vitro* data [4,126]. Adding *C. minuta* to the murine guts of mice colonized with other microbes did not alter acetate levels in any constellation tested, implying the absence of metabolic syntrophic interactions affecting acetate levels produced by the remaining microbial community in the murine guts.

This data demonstrated the dependence of intestinal acetate on microbial biomass in mice. No effects beyond the linear range were evident, implying the absence of additional syntrophic effects boosting acetate levels.

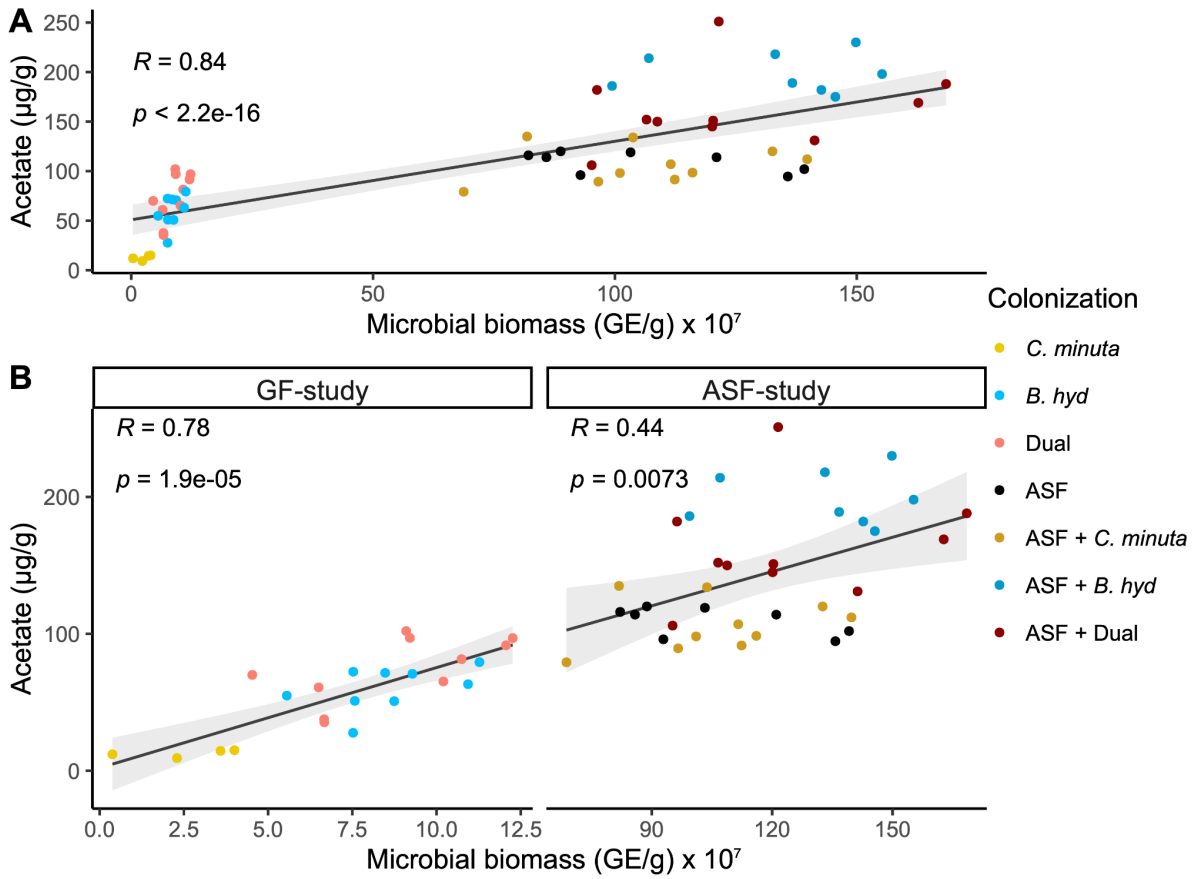

Figure 2.2 - Correlation of microbial biomass with cecal acetate concentrations. (A-B) Correlation of cecal acetate with total microbial biomass in two gnotobiotic murine studies, (A) combined, or (B) separately per study. Color of dots indicate the murine colonization group. ASF = Altered Schaedler Flora; *B. hyd* = *B. hydrogenotrophica*; GE = genome equivalents.

2.4. Conclusion

This chapter provided evidence for microbe-microbe interactions resulting in increased abundances of *C. minuta,* with no evidence of a syntrophic boost in microbial acetate metabolism in the context of a simplified microbial community *in vivo*. In the next chapter, I proceed to investigate the effect of *C. minuta* on complex microbial compositions in a meta-analysis of murine FMT studies.

Chapter 3. Meta-analysis of the gut microbiome in murine pilot studies with *Christensenella minuta*

3.1. Introduction

Christensenellaceae are sparsely present in the human gut microbiome, with an average abundance of 0.01% [5]. Yet their reported association with a lean human BMI is one of the most consistent associations in the human microbiome field (Figure 1.1) [5,45–85]. How can microbes with such a low abundance have such pronounced associations with human health?

Beyond the abundance of *Christensenellaceae,* various changes in the microbial community structure are associated with obesity and metabolic disease [65]. This gives rise to the theory that this family has no direct effect on the host, instead exerting an indirect impact by modulating the microbial community. Such a change in the microbial community could then mediate the health-promoting influence of *Christensenellaceae* upon the host. The ability of the genus *Christensenella,* and particularly the species *C. minuta,* to produce hydrogen [95] highlights this species as a possible mediator. Hydrogen is an essential compound for the gut microbiome with community-shaping properties [124,127]. Lending support to this potential community-shaping effect of *C. minuta*, Goodrich et al. showed a distinct clustering of microbial communities in mice receiving an inoculum containing live *C. minuta* compared to controls without such a *C. minuta* amendment in PCoA plots [5]. However, such a pattern might be a product of mere chance rather than a direct influence by the microbe of interest. Testing for a consistent change in the gut microbiome with an amendment of living *C. minuta*, I performed a meta-analysis of several murine pilot studies. Dr. Waters conducted a total of 18 individual murine pilot studies with *C. minuta*, investigating a different question in each study. This variation of the issue under investigation leads to variability of experimental parameters. Many of these variable parameters, for example diet, sex, genotype, and host age, are known to alter the microbial community [5,98,128,129]. Thus, these experimental variations may conceal a treatment effect on the microbial communities in the available studies.

From the 18 studies, I selected seven that I considered similar enough to allow for comparison and obtained their amplicon sequences and metadata to analyze the dataset using QIIME2 [130]. Reanalyzing the experiment published by Goodrich et al. [5], I was able to reproduce their results they obtained using QIIME 1.7.0 [131]. In the whole data set from the seven studies, batch effects of the individual studies were the main driving force shaping β-diversity of the microbial communities. These batch effects also influenced the abundance of *C. minuta* in the murine fecal samples. Statistical analyses of β-diversity metrics revealed minor differences between murine treatment groups in the microbial community composition of the whole data set. Differential abundance analysis (DAA) revealed seven significantly differentially abundant taxa, with five of these taxa belonging to the family of *Lachnospiraceae*.

In conclusion, while experimental batch effects dominated the differences in the microbial communities, I detected minor, common signals in the microbiome composition of mice in response to the amendment of *live C. minuta*. The reproducibility of those changes in the microbial communities and their relevance for the host, including host health and body composition, need to be investigated in further experiments.

3.2. Materials and Methods

Data acquiring

Dr. Waters performed 18 murine pilot studies at the University of Cornell between 2014 and 2016, including 16S rRNA (V4) amplicon sequencing on collected murine fecal samples. The precise procedures of DNA extraction, library preparation, and sequencing are described in detail elsewhere [5]. Dr. Waters provided all sequencing data, including experimental metadata.

Reanalysis of E1 and meta-analysis

The 18 studies performed by Dr. Waters included the murine experiment published in 2014 by Goodrich et al. [5], here called E1. Examining the experimental metadata, I selected six more studies similar to the experimental design of E1 for a meta-analysis. Table 3.1 displays information about the parameters of the seven included experiments. Manual creation of a merged metadata file was followed by meta-analysis of the amplicon sequences with QIIME2 2019.10 [130]. Samples were rarefied to 13.000 sequences to calculate α-diversity metrics (Faith PD, observed operational taxonomic units (OTUs), Pielou Evenness, Shannon Entropy) and β-diversity (unweighted and weighted UniFrac distances) using the SILVA v.132 phylogenetic trees where necessary. Statistical analysis of ß-diversity distances was performed using PERMANOVA [132,133]. I used linear mixed models for comparisons of *C. minuta* levels between treatments and MaAsLin2 [134] for DAAs.

3.3. Results and Discussion

Reanalysis of E1 reproduces the published results

First, I sought to confirm the reproducibility of *C. minuta's* effect on the microbial community composition in the experiment published by Goodrich et al. (2014) [5], in this thesis referred to as E1. To accomplish this, I compared principal coordinate plots of unweighted UniFrac distances generated with QIIME2 2019.10 [130] (Figure 3.1B, D), with the results in the original publication obtained with QIIME 1.7.0 [131] (Figure 3.1A, C). Striking differences between my own results and the results of the original publication included the inversion of the axes and the higher variance, evident from the PC-axes. Further, inoculum samples clustered closer to the murine samples from later time points in my analysis compared to the published version. Despite these discrepancies, the same treatment effects were observable in both sets of results: fecal microbiomes 20 hours post-inoculation clustered distinctly from all the other samples on PC1 regardless of treatment group. Meanwhile, later time point samples formed a distinct cluster separated by treatment in PC2. Analyzing the QIIME2 2019.10 generated unweighted UniFrac distances by PERMANOVA, both parameters "day after inoculation" and "treatment" were

statistically significant (day: R_2 = 0.43, p = 0.001; treatment: R_2 = 0.05, p = 0.001) [132,133].

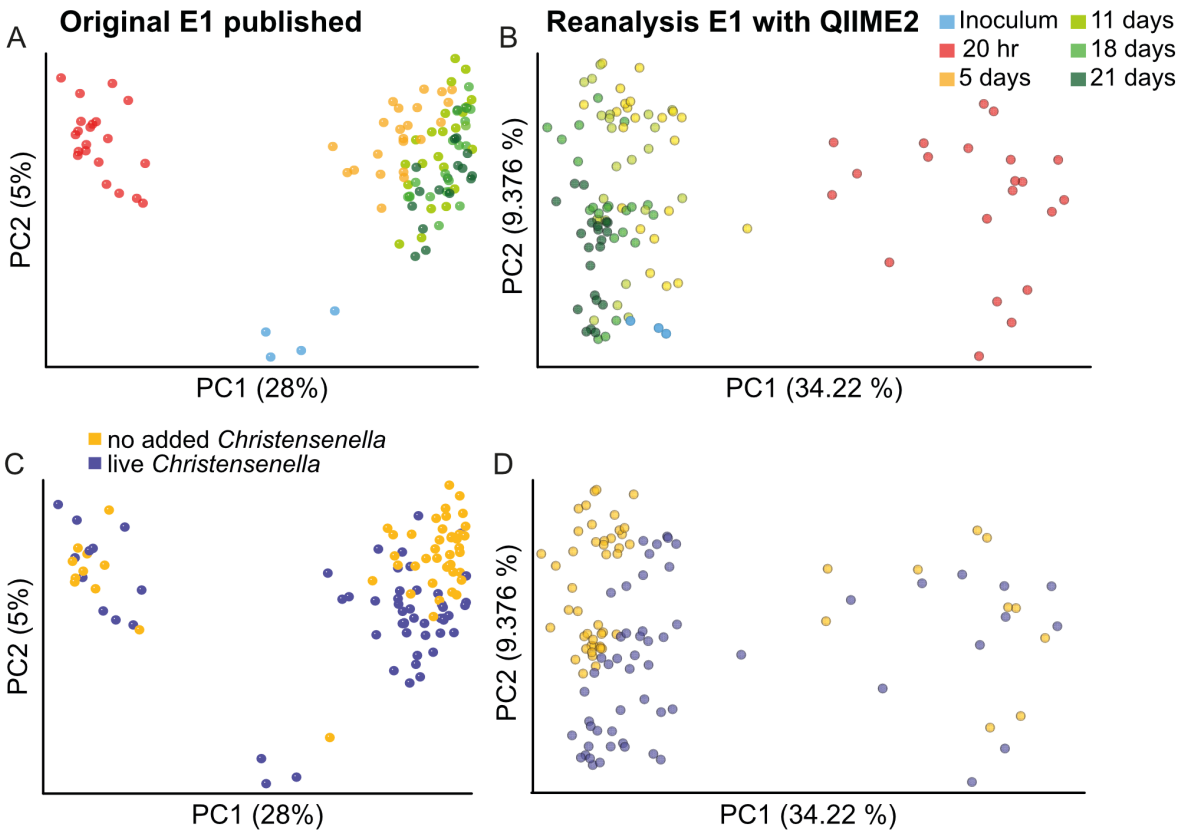

Figure 3.1 - Reproduction of published treatment effects on microbial fecal β-diversity by *C. minuta* with QIIME2. Principal coordinate analyses of unweighted UniFrac distances in fecal microbiomes of mice receiving a fecal microbiota transplant from an obese human donor stool alone or amended with living *C. minuta*. Phylogenetic profiling and analyses were performed using (A, C) QIIME 1.7.0 [131], published in [5], and (B, D) QIIME2 2019.10 [130]. Each point represents a sample and is colored by (A, B) time point or (C, D) treatment. (B, D) Statistical analysis performed with PERMANOVA [132,133] shows a significant difference in β-diversity between treatment (R_2 = 0.05, p = 0.001) and time post-inoculation (R_2 = 0.43, p = 0.001).

In conclusion, E1 showed a separation of the microbial community structure by the amendment of live *C. minuta* independently of the software used for analysis.

Strong batch effects in the microbial communities

Dr. Waters performed a total number of 18 murine studies with *C. minuta* at Cornell University. For the meta-analysis, I selected a subset of those 18 studies comprising experiments with comparable designs. I focused on FMT studies using a stool sample of an obese human donor amended with no (Minus), heat-killed (HK), or living *C. minuta* (Plus) prior to the inoculation to recipient germfree mice. These criteria resulted in the inclusion of seven studies. The selected data set still contained variations in experimental parameters between the studies, as evident in Table 3.1.

Table 3.1: Experimental parameters of selected studies in meta-analysis data set

Study	Treatment groups	Mouse strain	Donor of stool sample	Mouse sex	Mouse diet	Study duration (days)
E1	Plus Minus	Swiss Webster	A	♀	NC	21
E2	Plus Minus HK	Swiss Webster	A	♀	NC	30
E3	Plus HK	Swiss Webster	A	♀	NC	21
E4	Plus HK	Swiss Webster	A	♀	NC	132
E5	Plus HK	Swiss Webster	B	♀	NC	26
E6	Plus HK	C57BL/6	A	♂	NC → HF	81
E7	Plus Minus	C57BL/6	A	♂	HF	28

Minus = FMT with pure stool inoculum; HK= FMT with stool amended with heat-killed *C. minuta*; Plus = FMT with stool amended with living *C. minuta;* NC = normal-chow diet; HF = high-fat diet

For comparability, I combined the HK and Minus groups into a new group called “no live *C. minuta*” and renamed the Plus group “live *C. minuta*”. With this new data set, I performed a meta-analysis using QIIME2 2019.10 [130] to investigate the effect of living *C. minuta* amendment to the initial inoculum on the microbial community structure in mice. My results showed that microbial communities were indistinguishable in terms of α-diversity in all four accessed metrics (Faith PD: p = 0.86; Observed OTUs: p = 0.88; Pielou evenness: p = 0.44; Shannon entropy: p = 0.53; Figure 3.2).

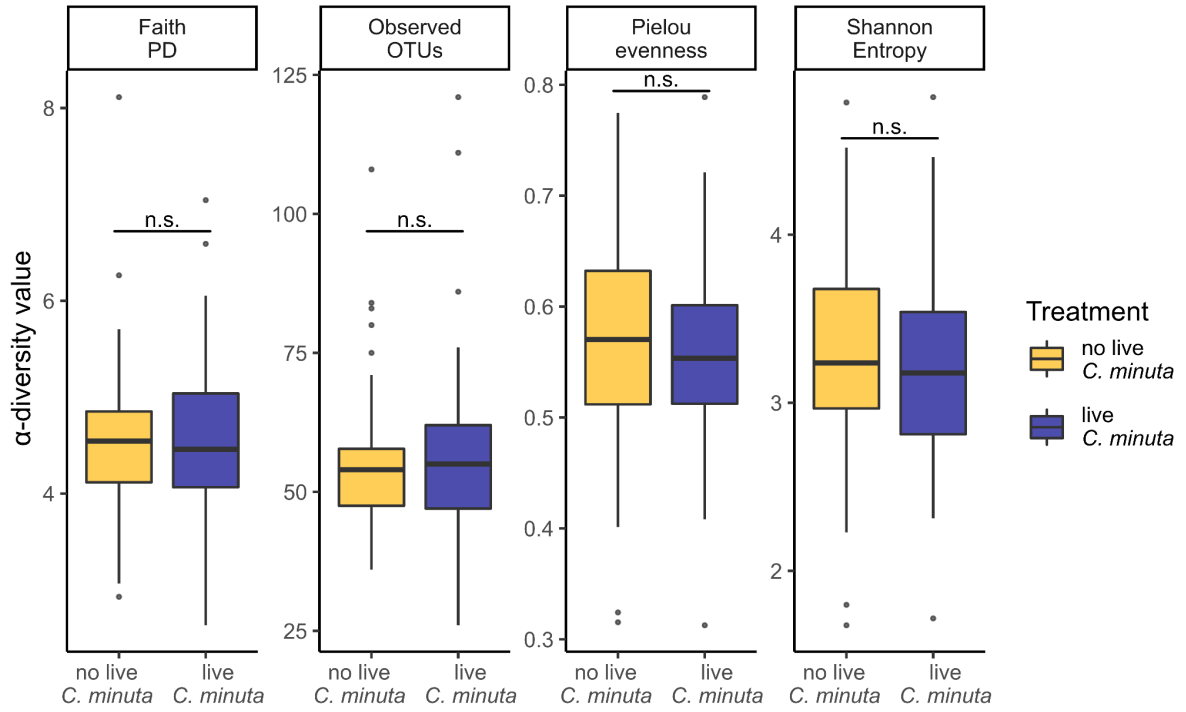

Figure 3.2 - No differences in α-diversity between treatment groups in meta-analysis. α-diversity metrics boxplots of fecal microbiomes of a meta-analysis dataset containing seven murine experiments. Mice received a fecal microbiota transplant from an obese human donor stool amended with either no or heat-killed *C. minuta* (no live *C. minuta*), or living *C. minuta*. α-diversity was calculated using QIIME2 2019.10 [130] and statistical analyses were performed with linear mixed models correcting for study effects. n.s. = not significant.

Visual inspection of microbial β-diversity using unweighted UniFrac distances between the fecal microbiomes revealed a pronounced clustering of the individual experiments. This clustering is observable in the analysis of all collected fecal samples from each murine experiment (Figure 3.3A) and in the endpoint samples of

each experiment (Figure 3.3B). No patterns according to treatment or diet were evident (Figure 3.3A-B). The absence of a distinction by diet was surprising as the literature reports a strong influence of diet on the microbiome communities in humans and mice [10,135]. A distinct clustering by experimental studies is also present in the inoculum samples prior to transplantation (Figure 3.2C). These results imply that the strong batch effects in the murine samples emerged from the inoculum samples. As all inoculum samples, except E5, were prepared from the same donor stool sample, it is likely that these differences stemmed from minor variations in the preparation of the initial inoculum or the heterogeneity within a stool sample [136].

Statistical analysis of weighted and unweighted UniFrac distances with PERMANOVA reinforced the evident patterns in the PCoA plots with the significant influence of murine study batch effects on the microbial β-diversity (Table 3.2). However, in these analyses, I also uncovered small but significant differences in β-diversity between murine treatment groups and by murine diet (Table 3.2), which were not evident from the PCoA plots in Figure 3.2. These small but significant differences by treatment group suggest that *C. minuta* may, as hypothesized, affect the microbial community. Based on the small effect size, explaining only up to 2% of the total variance between the microbial communities, I suspect subtle effects on individual microbial species.

Taken together, *C. minuta* exerted a minor effect on the overall microbial community, while strong batch effects of the individual studies dominated the variance in the data set.

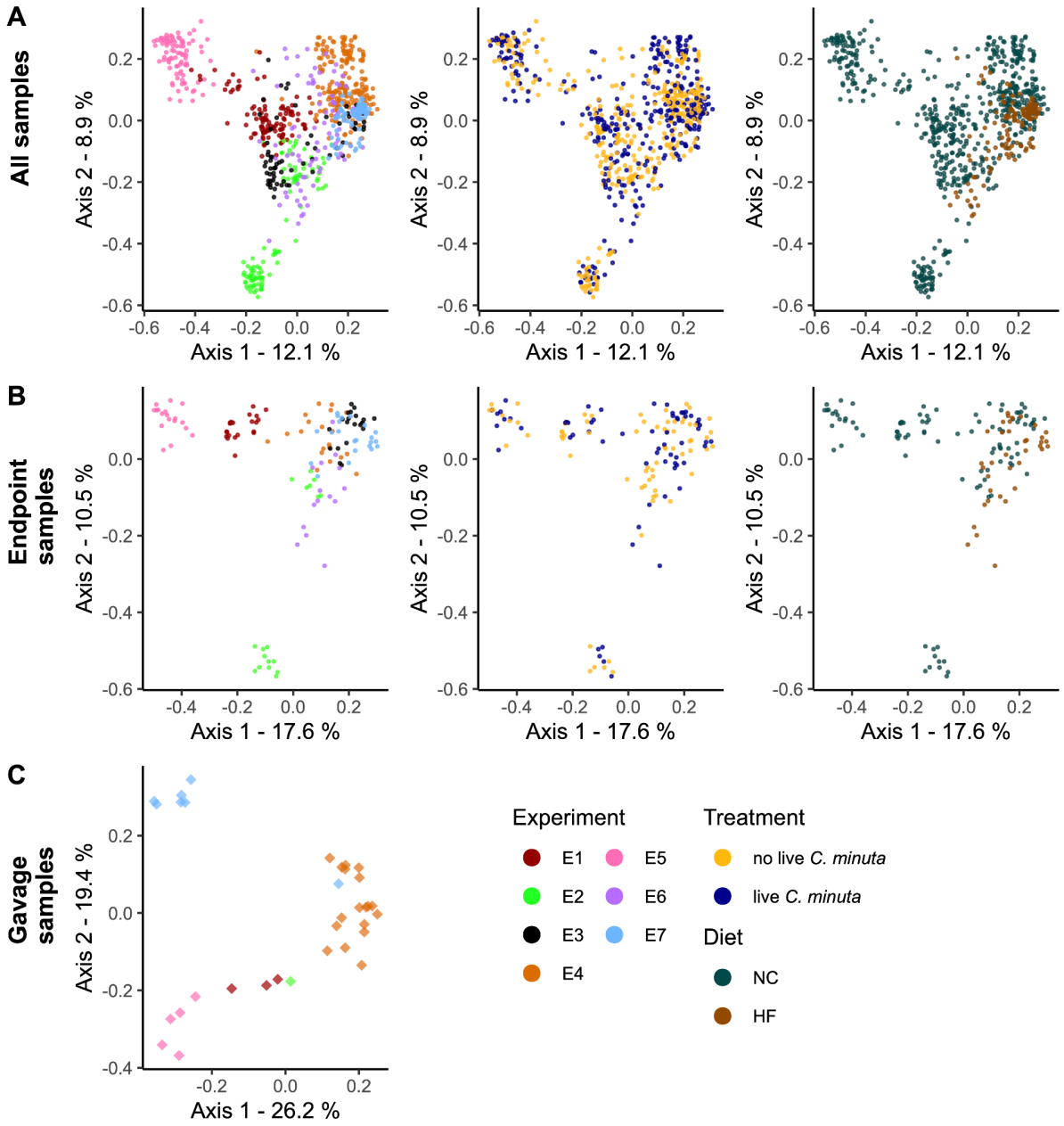

Figure 3.3 - Strong batch effects by experimental study in meta-analysis. Principal coordinate analysis plots of unweighted UniFrac distances in fecal microbiomes of mice receiving a fecal microbiota transplant from an obese human donor stool amended with either no or heat-killed *C. minuta* (no live *C. minuta*), or living *C. minuta*. Phylogenetic profiling and analyses were performed using QIIME2 2019.10 [130]. Each point represents a (A,B) murine sample or (C) inoculum sample prior to transplantation. Points are colored by murine study, treatment group and murine diet. NC = normal-chow diet; HF = high-fat diet.

Table 3.2: PERMANOVA results of weighted and unweighted UniFrac distances.

Samples	Distance metric	Study	Treatment	Diet
All mouse samples	uwUF	F(6 | 739) = 80.8 R^2 = 0.39 *p* = 0.001	F(1 | 739) = 4.2 R^2 = 0.003 *p* = 0.001	F(1 | 745) = 51.2 R^2 = 0.06 *p* = 0.001
	wUF	F(6 | 739) = 50.7 R^2 = 0.29 *p* = 0.001	F(1 | 739) = 2.9 R^2 = 0.003 *p* = 0.033	F(1 | 745) = 37.8 R^2 = 0.05 *p* = 0.001
Endpoint samples	uwUF	F(6 | 127) = 23.6 R^2 = 0.52 *p* = 0.001	F(1 | 127) = 1.6 R^2 = 0.006 *p* = 0.097	F(1 | 133) = 14.1 R^2 = 0.1 *p* = 0.001
	wUF	F(6 | 127) = 16 R^2 = 0.42 *p* = 0.001	F(1 | 127) = 5.6 R^2 = 0.02 *p* = 0.001	F(1 | 133) = 11.4 R^2 = 0.08 *p* = 0.001
inoculum samples	uwUF	F(4 | 28) = 10.7 R^2 = 0.54 *p* = 0.001	F(1 | 28) = 5.5 R^2 = 0.07 *p* = 0.001	-
	wUF	F(4 | 28) = 12.9 R^2 = 0.46 *p* = 0.001	F(1 | 28) = 28 R^2 = 0.25 *p* = 0.001	-

uwUF = unweighted UniFrac distances; wUF = weighted UniFrac distances.

Strong batch effects in the abundance of *C. minuta*

Given the strong batch effects in the microbial community composition, I continued to investigate to what extent the abundance of *C. minuta*, the protagonist of all these studies, was affected. Boxplots of *C. minuta's* relative abundance in the murine fecal samples revealed dramatic differences between the seven studies (Figure 3.4A). As already observed by Goodrich et al., *C. minuta* was present at similar levels in both treatment groups in the majority of the studies (Figure 3.4B). A possible explanation is that these bacteria stem from the low levels of *C. minuta* present in the donor stool microbiome (Chapter 4), detectable by metagenomic sequencing. Of all seven studies, only E6 depicted a higher abundance of *C. minuta*

in the mice amendment with live *C. minuta* compared to the controls from the same study (*q* = 1.8e-8, Figure 3.3B).

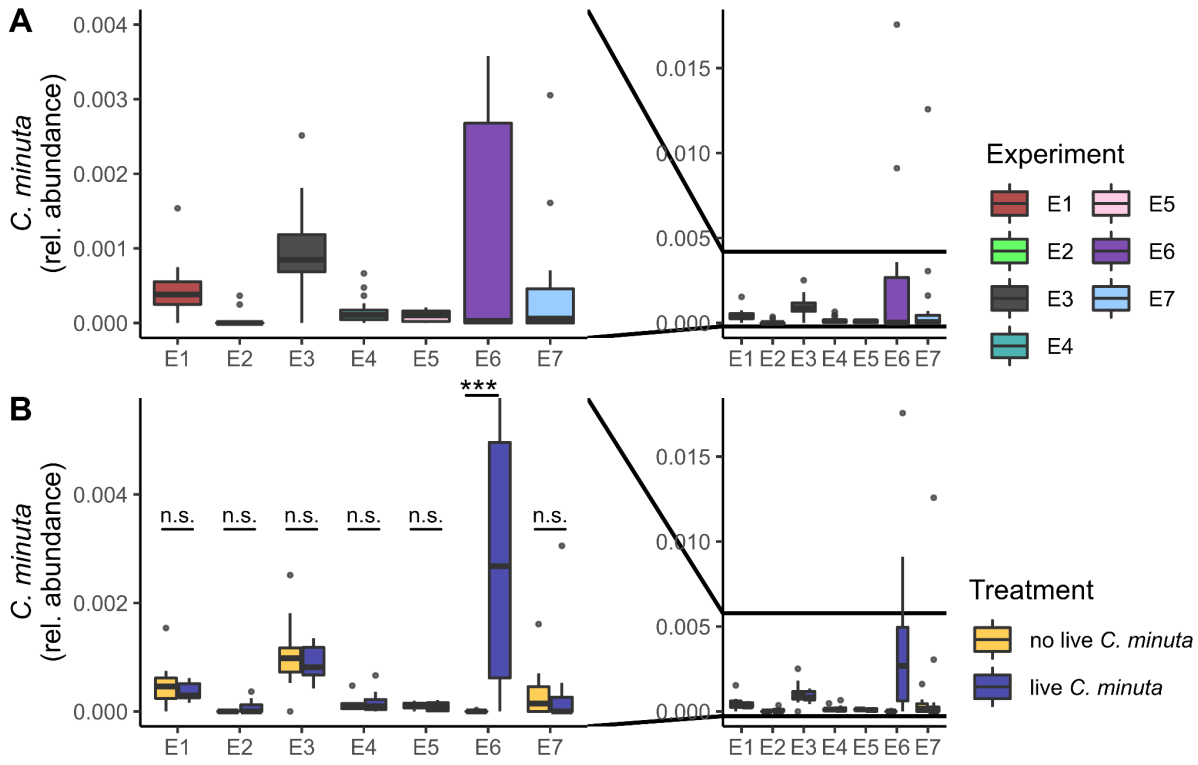

Figure 3.4 - High variation in abundance of *C. minuta* between studies of the meta-analysis. (A, B) *C. minuta* abundances in fecal microbiomes of the studies comprising the meta-analysis (A) for each experiment and (B) for each treatment group within each experiment. Phylogenetic profiling was performed with QIIME2 2019.10 [130] and statistical analyses were conducted with linear mixed models and corrected for multiple hypothesis testing using the Benjamini-Hochberg Procedure. *** = $p < 0.001$; n.s. = not significant.

Moreover, *C. minuta* reached the highest abundance in E6 compared to the other pilot studies (Figure 3.4B). The driving force behind this effect is unknown. Available literature reported that the abundance of *C. minuta* is modulated by (i) host sex [47,61,137], (ii) host genetics [5], and (iii) diet [138–140]. Those reports aggregated the expectations of a similar abundance of *C. minuta* in closely related individuals and a higher abundance of *C. minuta* in females fed a high-fat (HF) diet. The depicted data was not in line with those expectations: (i) Despite the reports of higher abundances of *C. minuta* in females, here, the average abundances in female mice (E1-E5) were lower compared to the studies with male mice (E6-E7). (ii) Mice in E6 and E7 had a highly reduced variability in host genetics, being mice from the

C57BL/6 inbred line, whereas mice from E1 to E5 were from an outbred line (SwissWebster). Nevertheless, the abundance of *C. minuta* varied substantially between these two studies. (iii) Even though mice in E7 were fed an HF diet over the whole study, these mice exhibited abundances of *C. minuta* comparable to those mice in the normal-chow (NC) diet studies (E1-E5). Meanwhile, in E6, mice were fed an NC diet for the first 28 days before transitioning to an HF diet. Whether or not this transition in the murine diet caused the observed bloom of *C. minuta* in the live *C. minuta* mice of E6 is unclear though it would not explain why the mice of the no live *C. minuta* group had such a low abundance in comparison.

In summary, the abundances of *C. minuta* varied considerably between the murine studies, reflecting the variation of the total microbial community, discussed in the previous paragraph.

***C. minuta* amendment modulated abundances of individual microbial OTUs**

I revealed strong batch effects between experiments in my investigations into the effects of live *C. minuta* amendment to the murine inoculum on the overall microbial community and the stability of *C. minuta's* abundance. Nevertheless, statistical analyses of weighted and unweighted UniFrac distances uncovered significant differences between the microbial communities of the different treatments. To explore whether these significant differences in the microbial communities arose from a common change of individual taxa, I performed three sets of DAAs using MaAsLin2 [134]. I first used the whole data set, while in my second analysis I only included the NC diet studies (E1-E5). The last analysis comprised the remaining HF diet studies (E6 & E7).

Using the complete data, I detected two differentially abundant taxa (Figure 3.5). Using the NC data set, I identified five more differential abundant taxa in addition to the two taxa detected in the complete data set (Figure 3.5). The HF data set contained no differentially abundant taxa between treatments. Interestingly, the significantly differentially-abundant taxa showed lower abundances in the mice amended with live *C. minuta*. The majority of these seven taxa belonged to the family of *Lachnospiraceae*, indicating an increased influence of *C. minuta* upon certain taxonomically-related species compared to others. Unfortunately, it is not

possible to determine which variables drove the differences between the NC-diet and HF-diet studies due to the multiple parameter differences between these studies (Table 3.1).

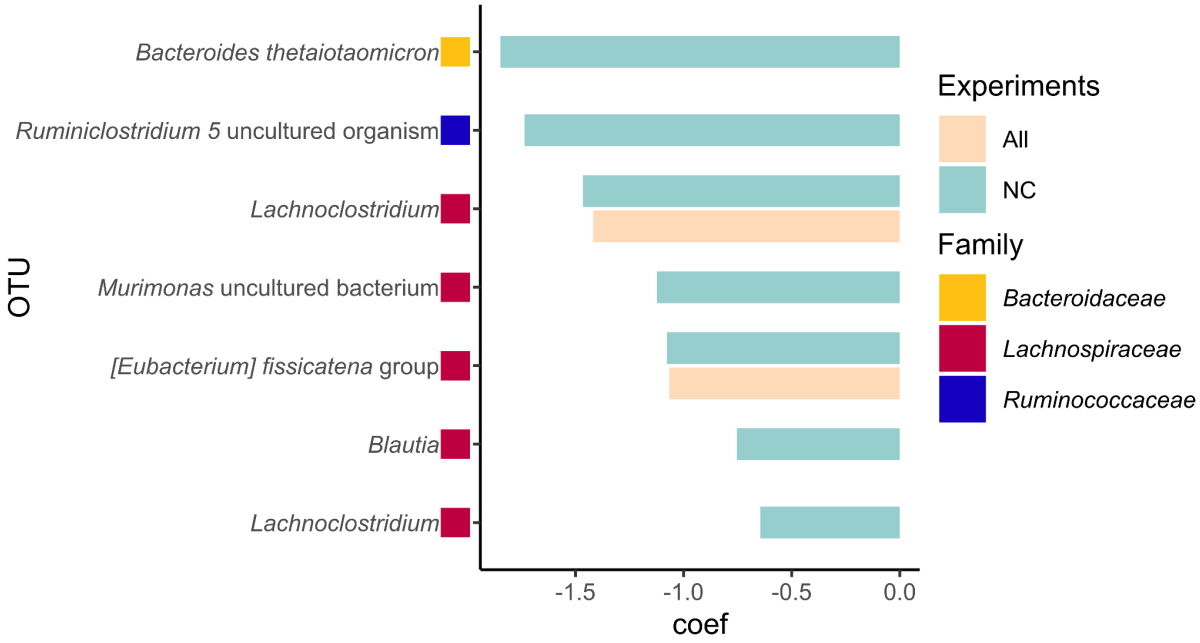

Figure 3.5 - Lower abundance of several OTUs by the amendment of live *C. minuta*. Bar plot of significantly differentially-abundant OTUs between treatments in the meta-analysis of seven murine pilot studies. Phylogenetic profiling was performed with QIIME2 2019.10 [130]. Cream-colored bars are the significant OTUs using the whole meta-analysis dataset; turquoise-colored bars are the significant OTUs using the five normal-chow diet studies in the meta-analysis dataset. Color next to the OTU-name in the x-axis indicates the taxonomic family of the OTU. Negative coefficients represent taxa with a lower abundance in the live *C. minuta* treatment group compared to those with no live *C. minuta*. Statistical analyses were performed using MaAsLin2 [134], and results were corrected with the Benjamini-Hochberg Procedure. NC = normal-chow.

These results, combined with the results from the β-diversity analyses, suggest that *C. minuta* selectively reduced the abundance of specific OTUs, without affecting the remaining microbial community. The exact mechanism involved in this reduced abundance remains unknown and requires further investigation.

3.4. Conclusion

This chapter presents results suggesting an effect of *C. minuta* on a small subset of the intestinal microbiome in mice using a meta-analysis of seven independent murine pilot studies. Only minor changes in the overall microbial community composition were observed in response to the amendment of live *C. minuta*. However, DAA revealed that live *C. minuta* resulted in a lower abundance of taxa primarily belonging to the *Lachnospiraceae*. In the next chapter, I tested the reproducibility of these microbial changes due to *C. minuta* in my murine studies and further explored the impact of *C. minuta* on host energy expenditure.

Chapter 4: Sex-dependent effects of the gut bacterium *Christensenella minuta* on physical activity in mice

4.1. Abstract

The gut bacterial family *Christensenellaceae* is consistently associated with human metabolic health and a healthy BMI. Amendment of *Christensenella minuta* to the gut microbiome in mice is associated with reduced adiposity, but the mechanism remains unclear. Here, we assessed the impact of *C. minuta* amendment to fecal transplantation from an obese human donor on the energy expenditure (EE) of recipient male and female germfree mice. We observed that mice receiving live *C. minuta* showed a lower feed efficiency without changes in weight gain, adiposity gain, or fecal energy content. We hypothesized compensation by higher host EE. In support of this, we observed higher physical activity levels in mice with live *C. minuta*: both sexes displayed higher overall activity, with significantly greater locomotion in males. Females with live *C. minuta* had a significantly higher resting metabolic rate, with a trend of higher total EE, which correlated with circulating markers of glucocorticoid metabolism. In males, we observed an association between locomotion and cecal total short-chain fatty acids, of which butyrate was lower in males with live *C. minuta*. Differences between male treatments in the microbial community composition and functional profile reflected the lower cecal butyrate concentrations. Our results show a link of live *C. minuta* amendment with physical activity and metabolic EE in mice. These results indicate that the metabolic health and lean BMI association with *Christensenellaceae* in the gut microbiome may be due to a causal effect on physical activity levels in the host.

4.2. Author contributions

Authors are listed in the order to be used for publication.

1. Tanja Schön, Max Planck Institute for Biology, Tübingen, Germany.
   Devised the study, performed and supervised all experiments, performed all data analyses, wrote the manuscript.
2. Taichi Suzuki, Max Planck Institute for Biology, Tübingen, Germany.
   Helped to perform all experiments, provided input for the manuscript.
3. Jillian L. Waters, Max Planck Institute for Biology, Tübingen, Germany.
   Devised the study, helped to perform all experiments, provided input for the manuscript.
4. Ruth E. Ley, Max Planck Institute for Biology, Tübingen, Germany.
   Devised the study, provided input for the manuscript. Corresponding author.

Status in publication process

Advanced manuscript, awaiting submission to target journal.

4.3. Manuscript

IMPORTANCE

The human gut microbiome is made of trillions of microbial cells, influencing host health. The bacterial family *Christensenellaceae* correlates with metabolic health and a lean body type. Moreover, a causal role of the species *Christensenella minuta* in regulation of host body composition has been shown. How this species can affect host body type is an unanswered question. Here, we show that *C. minuta* influences host physical activity and metabolic energy expenditure, accompanied by changes in murine metabolism and the gut microbial community in a sex-dependent manner. These observations hint to potential mechanisms for its causal role in host leanness.

INTRODUCTION

The bacterial family of *Christensenellaceae* is a highly heritable and prevalent family of Firmicutes within the human gut microbiome [1]. The abundance of this family has been connected to metabolic health, and in particular to a healthy body mass index (BMI), in human metagenomic studies worldwide (Figure 1) [1–42]. Previous work from our group has shown a causal role of *Christensenellaceae* for low host BMI: the addition of live *Christensenella minuta* diminished adiposity gain mediated by an obesity-inducing microbiome in mice [1]. Mazier et al. reproduced the reduction in adiposity gain by amending *C. minuta* to mice fed a high-fat diet, suggesting that the causal role of *C. minuta* in host leanness is not limited to the exact mode of obesity induction [43].

Furthermore, Mazier et al. reported a decrease in feed efficiency, body weight gain per total ingested calories, in the mice receiving the *C. minuta* inoculum, without further elucidations on the causal mechanism [43]. Lower feed efficiency can arise from lower energy harvest from consumed food or a higher energy expenditure (EE) of the host. Interestingly, the gut microbiome influences both those aspects [44–46]. Gut microbes ferment dietary-indigestible components and provide additional energy to the host [45]. Moreover, the gut microbiome communicates with the host brain via blood-borne microbial products, microbially produced metabolites, as well as

afferent-spinal and vagal nerves [46]. This gut-microbiome-brain axis enables the gut microbiome to modulate host metabolic energy homeostasis, including host physical activity [46–49]. Studies reported the capability of the whole microbial gut community [50] or even single microbial species [51,52] to modulate host physical activity. Several human studies associated host physical activity with *Christensenellaceae*. Subjects with high fitness levels of various cohorts of different ages worldwide showed higher abundances of *Christensenellaceae* [25,53,54]. Also, rodent studies linked physical activity to the abundance of *Christensenellaceae*. High-capacity runner rats had higher levels of *Christensenellaceae*, and its abundance was positively correlated with running distance [55]. In a study of obesity-induced mice, mice had higher abundances of *Christensenellaceae* after eight weeks of daily exercise compared to the non-exercised group [56]. Another link between *Christensenella* and physical activity is its production of hydrogen [57], a metabolite linked to physical activity and recovery after exercise [58–60].

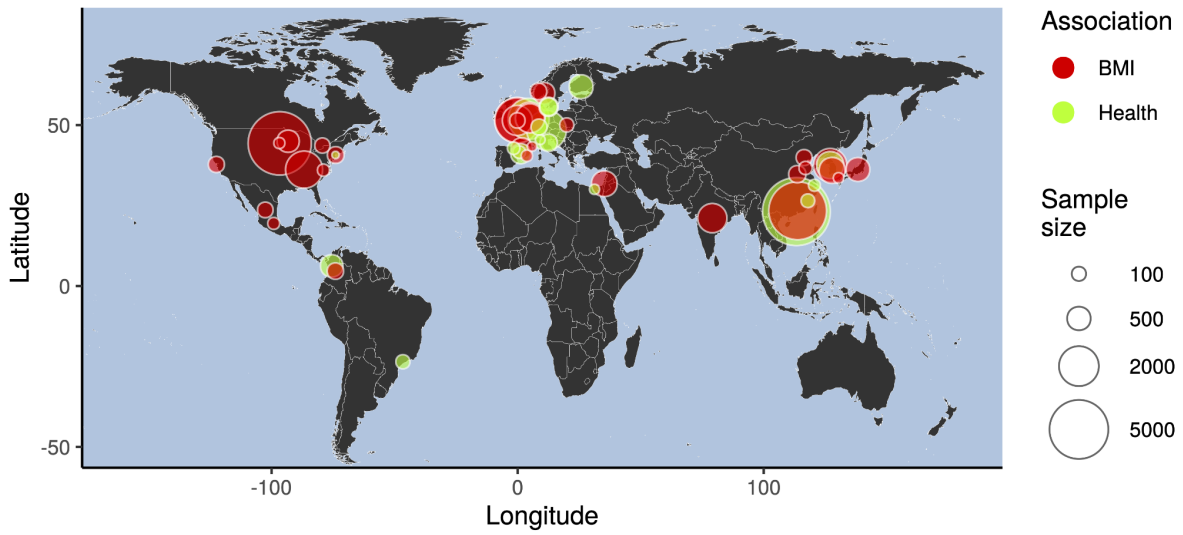

Figure 1 - Global map of studies associating the gut bacterial family *Christensenellaceae* with healthy body mass index or metabolic health in humans. Sampling locations of 42 studies associating the abundance of *Christensenellaceae* in the gut with a healthy BMI (red) or metabolic health (green) in humans to the world map [1–42]. Circle size indicates study cohort size.

Here, we hypothesize that *C. minuta* modulates host EE, in particular physical activity, to regulate host body composition. Instead of the standard approach to measure solely host body composition as the outcome of an imbalanced energy homeostasis, we assessed individual aspects of energy homeostasis, including food

intake, activity, behavior, and EE using a behavioral phenotyping respirometry cage system. For this, we conducted a fecal transplant experiment with 184 male and female germfree mice receiving feces from an obese human donor amended with live or heat-killed *C. minuta*. We investigated alterations in host metabolism and the microbial gut community and how these changes correlated with the observed activity and EE phenotypes. Our results show that treatment with live *C. minuta* resulted in lower host feed efficiency, higher host activity and EE, in addition to modulated host metabolism and gut microbial community composition. The observed phenotypes varied between host sexes, demonstrating a sex-dependent effect of *C. minuta* on the host.

RESULTS

Live *C. minuta* decreases feed efficiency independently of fecal energy loss

To investigate the effect of *C. minuta* on the host and the microbial gut community, we conducted a large-scale series of fecal transplant experiments (184 mice total). Here, we inoculated male and female 5-6 week old germfree SwissWebster mice with an anoxic slurry derived from a single stool sample obtained from an obese human donor [1]. This donor stool microbiome contained low levels of *C. minuta* (Figure S1A). Prior to inoculation into the germ-free recipient mice by gavage, we amended the fecal slurry with either live (*Live-CM*) or heat-killed *C. minuta* (*Killed-CM*) (1010 CFUs per dose/mouse). For the first 25 days post-inoculation, we housed mice singly (males) or in groups of four per cage (females) and provided normal polysaccharide-rich chow ad libitum. After 25 days, we transferred the mice singly to a behavioral phenotyping respirometry cage system (Promethion Sable Line, NV, USA) to collect data on mouse behavior via a light beam break system and energy expenditure (EE) using indirect calorimetry. We assessed body weight of the mice weekly, as well as body composition at inoculation and at day 25 post-inoculation. In each experiment, we used 16 mice of one sex, 8 for each treatment group. For each sex we replicated the experiment 6 times, resulting in a combined sample size of 90 male and 94 female mice (Figure 2A).

To evaluate if live *C. minuta* amendment to the inoculum resulted in elevated levels of *C. minuta* relative to the *Killed-CM* control, we quantified its abundance by

qPCR using species-specific primers [61] in murine cecal contents at day 28 post-inoculation. Administration of live *C. minuta* was associated with higher levels of *C. minuta* abundance (p = 2.2e-4, Figure 2B) compared to heat-killed.

We evaluated how the live *C. minuta* treatment impacted murine body composition, food intake, and feed efficiency. We observed no differences between treatments for adiposity (Figure 2C) or weight gain (Figure S1B). However, we detected a trend for higher food intake (by 5%) in the *Live-CM* versus *Killed-CM* mice for both sexes (p = 0.055, Figure 2D, E). Extrapolating these measurements over the whole duration of the experiment resulted in a lower feed efficiency (by 8%) of the *Live-CM* vs. *Killed-CM* treatments (p = 0.045, Figure 2F). To test, if live *C. minuta* affected fecal energy loss, we quantified the energy content of all murine feces excreted between day 25 and 28 post-inoculation by bomb calorimetry. No difference in the fecal energy content was present between the treatments (p = 0.48, Figure 2G).

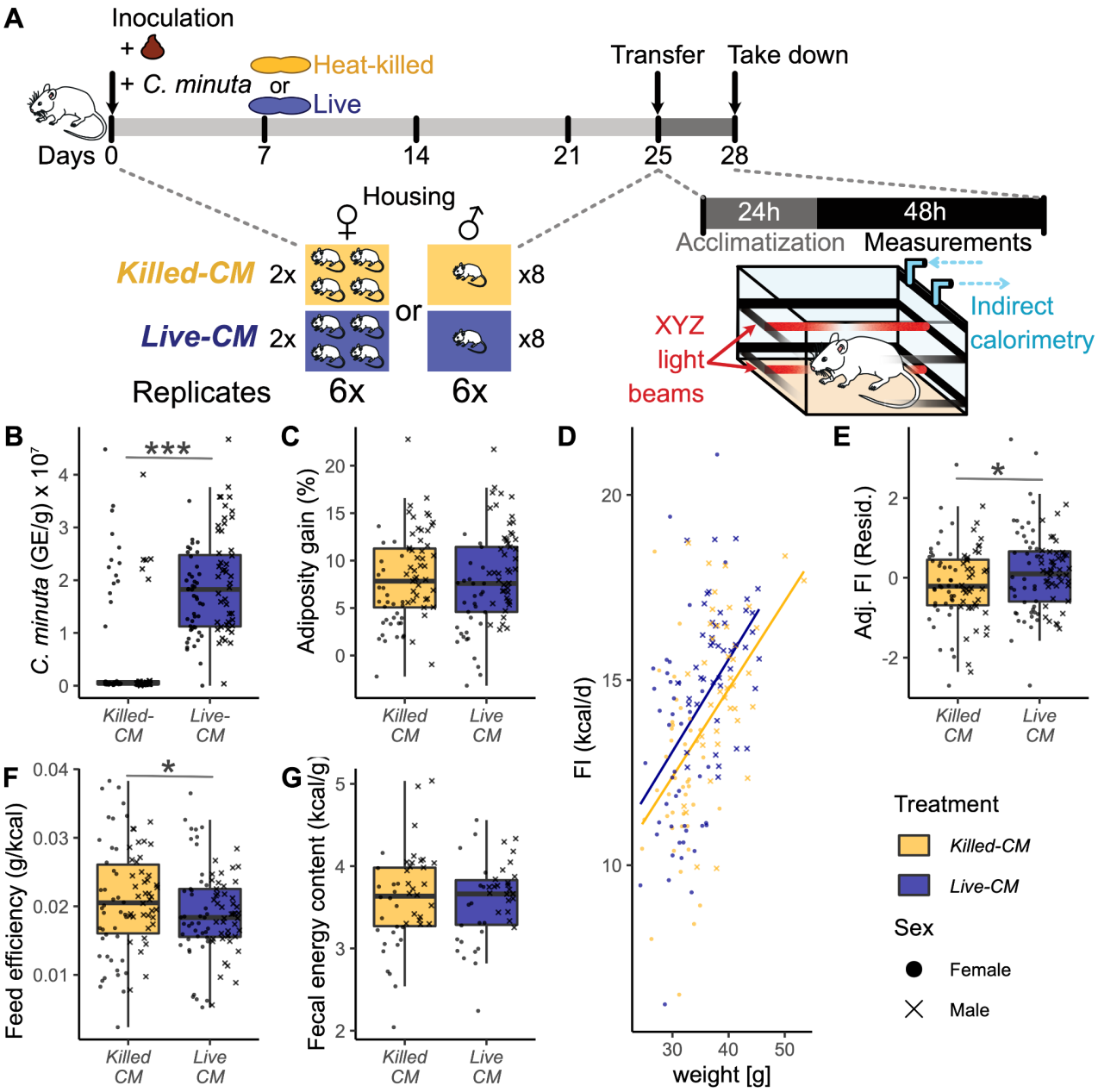

Figure 2 - Lower feed efficiency in mice amended with live *C. minuta*. (A) Experimental procedure of FMT- experiment with male and female germfree mice. Inoculums contained a fecal sample from an obese human donor amended with living (*Live-CM*) or heat-killed *C. minuta* (*Killed-CM*). Each experiment consisted of 16 mice of one sex, 8 for each treatment group, and was replicated 6 times. During the first 25 days, mice were housed in groups of 4 (females) or alone (males). 25 days after inoculation, the mice were transferred to a behavioral phenotyping respirometry cage system (Promethion Sable Line, NV, USA). The first 24 hours of the recording were excluded from the analysis for acclimatization. (B) Quantification of *C. minuta* in murine cecal contents on day 28 post-inoculation via qPCR using species-specific primers [67]. (C) Murine adiposity gain from day 0 to day 25 post-inoculation. (D-E) Average daily food intake from day 25 to day 28 post-inoculation as (D) raw values correlated with murine body weight and (E) residuals adjusted for sex, batch and weight. (F) Feed efficiency over the duration of the experiment, calculated using murine weight gain

from day 0 to day 28 post-inoculation and (D) measured food intake. (G) Energy content of all murine feces from day 25 to day 28 post-inoculation measured via bomb calorimetry. Asterisks indicate statistical significance of the linear mixed model correcting for sex, batch and (D-E) mouse weight. * : $p < 0.1$; ** : $p < 0.01$; *** : $p < 0.001$. Adj. = adjusted; FI = food intake; GE = genome equivalents; Resid. = residuals.

C. minuta increases host activity and metabolic energy expenditure in a sex-dependent manner

Given that the lower feed efficiency was not linked to elevated fecal energy content, we hypothesized energy expenditure (EE), especially physical activity, to be higher in the *Live-CM* compared to the *Killed-CM* group. We assessed two forms of EE, physical activity and indirect calorimetry estimated total EE using behavioral phenotyping respirometry cages. A light beam break system in the cage system assessed physical activity. Additionally, we measured oxygen consumption and carbon dioxide production via indirect calorimetry and calculated EE using the Weir equation [62]. While physical activity is a behavior that results in an elevation of energy expenditure above resting levels [63], EE measurements by indirect calorimetry include all aerobic processes contributing to total EE [64,65]. As none of both measurements represent the exact EE, only measurable by direct calorimetry, we considered both as complementary. To allow the mice to acclimate to the new cage environment, we excluded the first 24h of the measurements collected in the behavioral phenotyping respirometry cage system for all following metrics.

To test our hypothesis with the collected murine physical activity data, we obtained two activity metrics monitored by the light-beam-break system, overall activity (number of beam breaks independent of movement size in the XYZ-axes) and locomotion (total distance traveled within the XY-axes in m). We estimated the differences between treatments of those metrics, their association with the abundance of *C. minuta* and their correlation to murine feed efficiency. In support of our hypothesis, we observed higher overall activity with *Live-CM* treatment. The *Live-CM* groups of both sexes were associated with a higher overall activity compared to the *Killed-CM* groups (6.8% higher beam breaks, $p = 0.009$, Figure 3A). Overall activity was significantly associated with the abundance of *C. minuta* in

murine cecal contents (p = 0.03, Figure 3B), but not with murine feed efficiency (p = 0.41, Figure 3C). In contrast, solely *Live-CM* males showed greater locomotion (total distance traveled within the XY-axes in m) by 8.5 % compared to the *Killed-CM* males (p = 0.025, Figure 3D), whereas it was indistinguishable between female treatments (p = 0.708, Figure 3D). The abundance of *C. minuta* was correlated with the locomotion of male mice (p = 0.03, Figure 3E), not of females (p = 0.8, Figure 3E). Further, we observed a negative correlation between feed efficiency and locomotion in males (p = 0.04, Figure 3F), and no association in females (p = 0.4, Figure 3F). We detected no differences in activity between the treatments during the first 24h of acclimatization to the novel cage environment, suggesting that the observed behavior changes are not stress-induced (Fig S2A, B).

Further supporting our hypothesis, total EE trended to be 2.2 % higher in the *Live-CM* females compared to the *Killed-CM* females (p = 0.06, Figure 3G, H), but was indistinguishable between the male treatments (p = 0.71, Figure 3G, H). To evaluate if physical or metabolic processes mediated the higher EE in females with live *C. minuta*, we examined murine EE collected while the animal was physically at rest, an approximation of the resting metabolic rate (RMR). The average RMR of both sexes showed no difference between the treatment groups (females: p = 0.51, males: p = 0.63, Fig S2C). But an examination of the the RMR in dependence of the circadian cycles, revealed a higher RMR in the *Live-CM* females compared the *Killed-CM* females during the light cycle by 0.02 kcal/h, corresponding to a higher RMR by 4.3% (p = 0.042, Figure 3I). We observed no difference between the female treatments during the night cycle (p = 0.29, Figure 3I) or in male treatments during either light (p = 0.6, Figure 3I) or dark cycle (p = 0.69, Figure 3I).

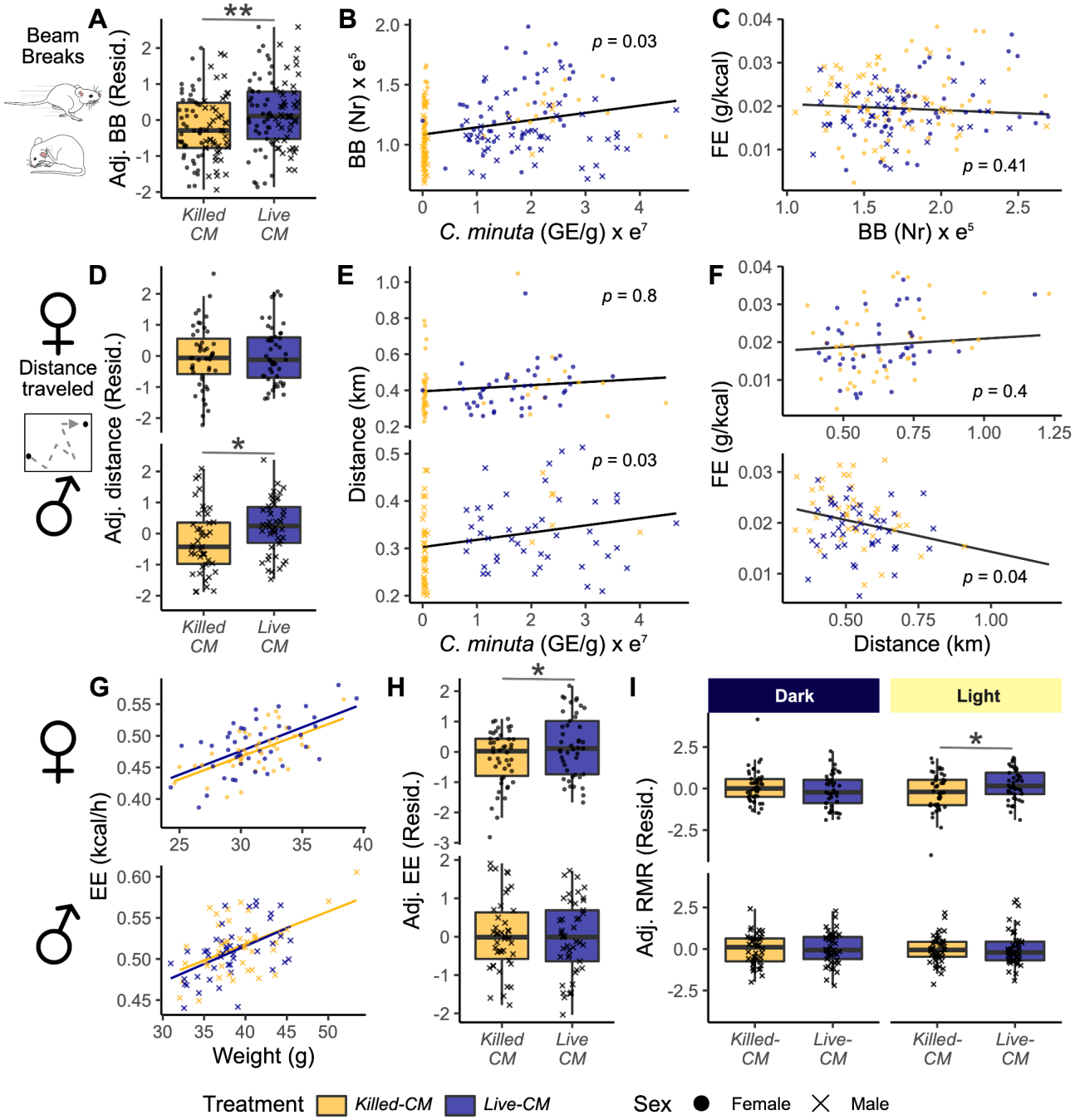

Figure 3 - Higher physical activity and metabolic EE in mice with live *C. minuta*. (A-D) Activity and (G-I) indirect calorimetry measurements of the mice in the metabolic cage system. (A, D) Residual activity metrics adjusted for batch- and sex-effects. (A-C) Number of beam breaks (A) per treatment group, (B-C) raw values associated with (B) the abundance of *C. minuta* and (C) murine feed efficiency. (D-F) For each sex, total distance traveled (D) per treatment group, (E-F) raw values associated with (E) the abundance of *C. minuta* and (F) feed efficiency. (G-H) Average hourly energy expenditure and (I) resting metabolic rate during the dark and light circle calculated using the Weir equation [68] as (G) raw values correlated to murine body weight and (H, I) residuals adjusted for body weight, sex, and batch effects. Asterisks indicate statistical significance of the linear mixed model correcting for sex, batch and (E-G) mouse weight. In correlation analyses, *p*-values of linear

mixed models are stated in the figure. * : p < 0.1; ** : p < 0.01; *** : p < 0.001. Adj. = adjusted; BB = beam breaks; EE = energy expenditure; FE = feed efficiency; GE = genome equivalents; Resid. = residuals; RMR = resting metabolic rate.

Addition of *C. minuta* resulted in sex-dimorphic metabolomic changes in the host associated with physical activity and EE

To assess the potential for involvement of microbially produced or modified metabolites in the described phenotypes, we performed two metabolomics screens with samples collected at day 28 post-inoculation: a SCFA screen in murine cecal contents, and a combination of targeted and untargeted metabolomics of murine sera.

In the murine cecal contents, we measured five SCFAs and three branched chain fatty acids (Figure 4A, Figure S3A, B), of which only butyrate was significantly lower in the *Live-CM* males compared to the *Killed-CM* males (q = 0.008, Figure 4A). As butyrate has been associated with murine activity [66] we analyzed if it correlated to the murine activity metrics, but found no association (overall activity: p = 0.37; locomotion: p = 0.16; Figure S3C, D). Instead, we observed a correlation of total SCFAs with murine locomotion (p = 0.001, Figure 4B) and to a weaker extent with overall activity (p = 0.02, Figure S3 E). Compared to *Killed-CM* males, *Live-CM* males showed a trend for lower total SCFAs (p = 0.11, Figure 4C) and a weaker trend in the opposite direction in females (p = 0.15, Figure 4C).

Additionally, we targeted 11 compounds, known to be influenced by the gut microbiome and capable of affecting host behavior (Table S1), in serum samples by liquid-chromatography mass-spectrometry (LC-MS) (Figure 4D, Figure S3E). Of all metabolites we assessed, only one showed a trend of being modulated by live *C. minuta*: females showed a trend for lower corticosterone, the main rodent stress hormone, in the *Live-CM* group compared to the *Killed-CM* group (q = 0.12, Figure 4D). For the pathway analysis we used the entire peak spectrum of the same LC-MS run. Here, we observed associations between female EE and pathways involved in glucocorticoid synthesis, including steroid hormone biosynthesis (p = 2e-4, Figure 4E) and primary bile acid biosynthesis (p = 0.012, Figure 4E).

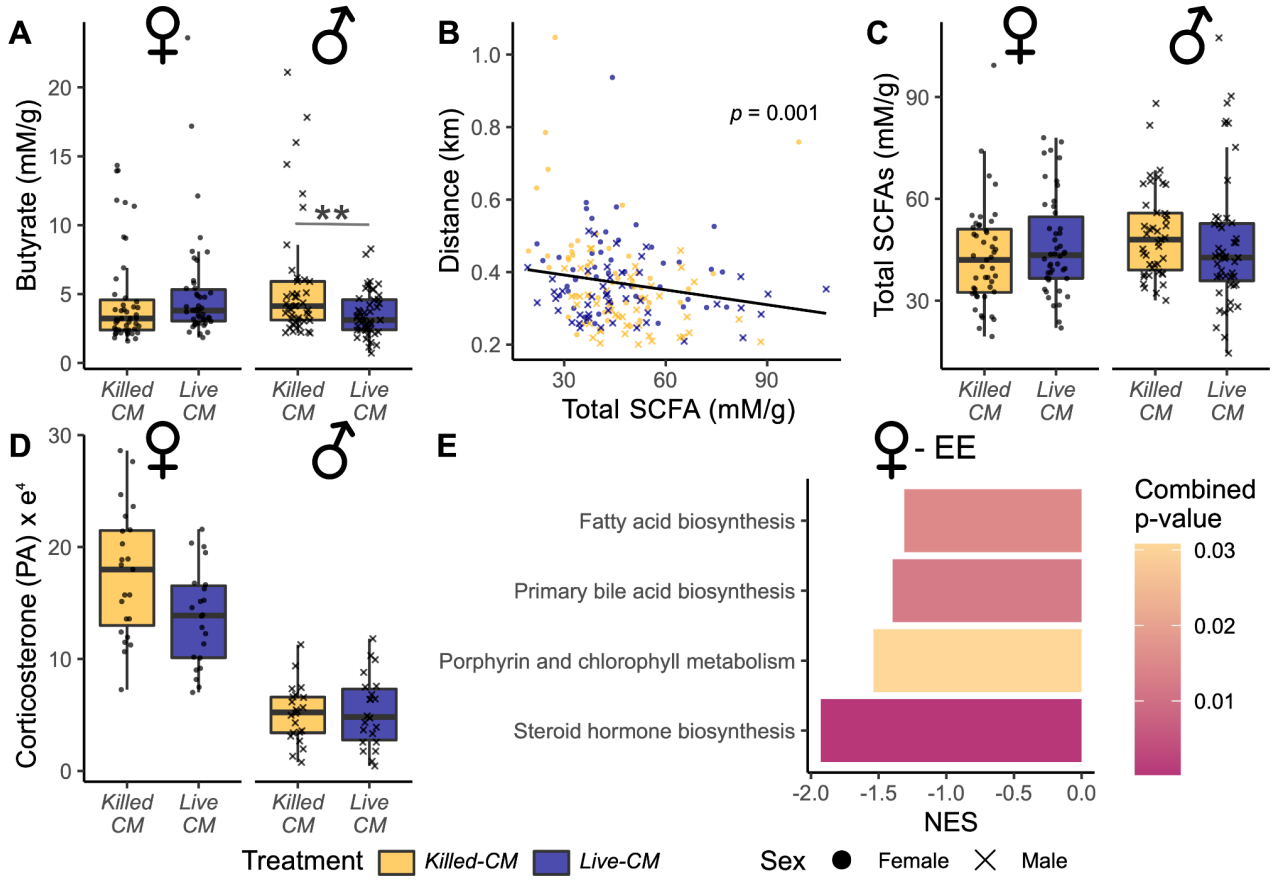

Figure 4 - Changes of metabolism in relation to energy expenditure metrics. (A-C) SCFA concentrations in murine cecal contents on day 28 post-inoculation measured via GC-MS with (A) butyrate, and (B-C) the sum of all five SCFA measured (B) correlated to murine locomotion and (C) by treatment. (D) Serum corticosterone levels at day 28 post-inoculation measured via LC-MS. (E) Metabolic pathways significantly associated with female EE, determined by analyzing the entire LC-MS peak spectrum of murine serum samples with XCMS (v.2.7.2) [101], MaAsLin2 [99], and MetaboAnalyst5.0 (www.metaboanalyst.ca)[102]. Pathways with a combined p-value (GSEA & mummichog) < 0.05 were considered significant. (A-D) Asterisks indicate statistical significance of the linear mixed model correcting for sex and batch. In correlation analyses, p-values of linear mixed models are stated in the figure. ** : p < 0.01. EE = energy expenditure; NES = normalized enrichment score; PA = peak area; SCFA = short chain fatty acid.

Shifts in the microbial community composition of male treatments reflect cecal butyrate levels

To further investigate the changes in murine activity, EE and metabolism, we analyzed the microbial community. First, we performed qPCR using universal 16S rRNA primers to quantify the microbial biomass in the murine cecal contents. We observed that mice with live *C. minuta* were associated with a higher microbial biomass by 10% (p = 0.008, Figure 5A) compared to the *Killed-CM* group. We normalized the phylogenetic profiled metagenomic cecal sequences by the total microbial genome equivalents per mouse determined by qPCR (Figure S4A) and used those normalized reads for further analyses. Examining the microbial community using four different α-diversity metrics, microbial richness (MR), Shannon Entropy (SE), microbial evenness (ME), and phylogenetic diversity (PD), revealed a significant lower α-diversity in the *Live-CM* males compared to *Killed-CM* males in all metrics (MR: p = 0.028, SE: p = 0.009, Figure 5B; ME: p = 2e-4, PD: p = 0.035; Figure S4B). Females showed no differences in α-diversity between the treatments (Figure 5B, Figure S4B). Similar to α-diversity, statistical β-diversity analyses using weighted and unweighted UniFrac (UF) distances revealed small but significant changes in the microbial communities between male treatments (weighted UF: F(1|81) = 8, R2 = 0.077, p = 0.003; unweighted UF: F(1|81) = 4.3, R2 = 0.032, p = 0.002). Again, females displayed no differences between the treatments (weighted UF: F(1|85) = 0.5, R2 = 0.001, p = 0.55; unweighted UF: F(1|85) = 1.9, R2 = 0.009, p = 0.08).

Using differential abundance analyses (DAA), we analyzed the treatment effect on the level of individual taxa and the functional profile of the microbial community. Further, we estimated the association of these taxa and functional profiles to cecal butyrate concentrations, a metabolite mainly produced by the microbial community with a significant difference between male treatments (Figure 4A). We observed 37 differentially-abundant genera between mice with live and heat-killed *C. minuta* in either females or males (Figure 5D). The majority of these 37 genera belonged to two main phylogenetically related groups, *Bacteroidales* and *Lachnospirales*. Within the *Bacteroidales*, all genera showed a lower abundance in the *Live-CM* mice of both sexes. The second and larger cluster incorporated 20 genera belonging to the *Lachnospirales*, of which 18 were members of the family

Lachnospiraceae. Males with live *C. minuta* showed a consistently lower abundance of *Lachnospirales* compared to *Killed-CM* males. In contrast, several genera of *Lachnospirales* showed higher abundances in *Live-CM* females compared to the female heat-killed control. Of the 37 differentially-abundant taxa between treatments, 16 taxa correlated significantly with cecal butyrate concentration. Especially the *Lachnospirales*, with lower abundance in the male *Live-CM* mice, showed a strong positive association with cecal butyrate concentrations (Figure 5D).

In line with the results of the α- and β-diversity analyses, DAA of microbial functional profiles resulted in significant differential abundant pathways between treatments exclusively in males or the combined dataset. The significant pathways with the highest effect size were involved in fermentation, carbohydrate degradation and amino acid biosynthesis (Figure 5E). Most strikingly, the majority of these pathways were oppositely associated with cecal butyrate concentration, again solely in males or the combined dataset (Figure 5E).

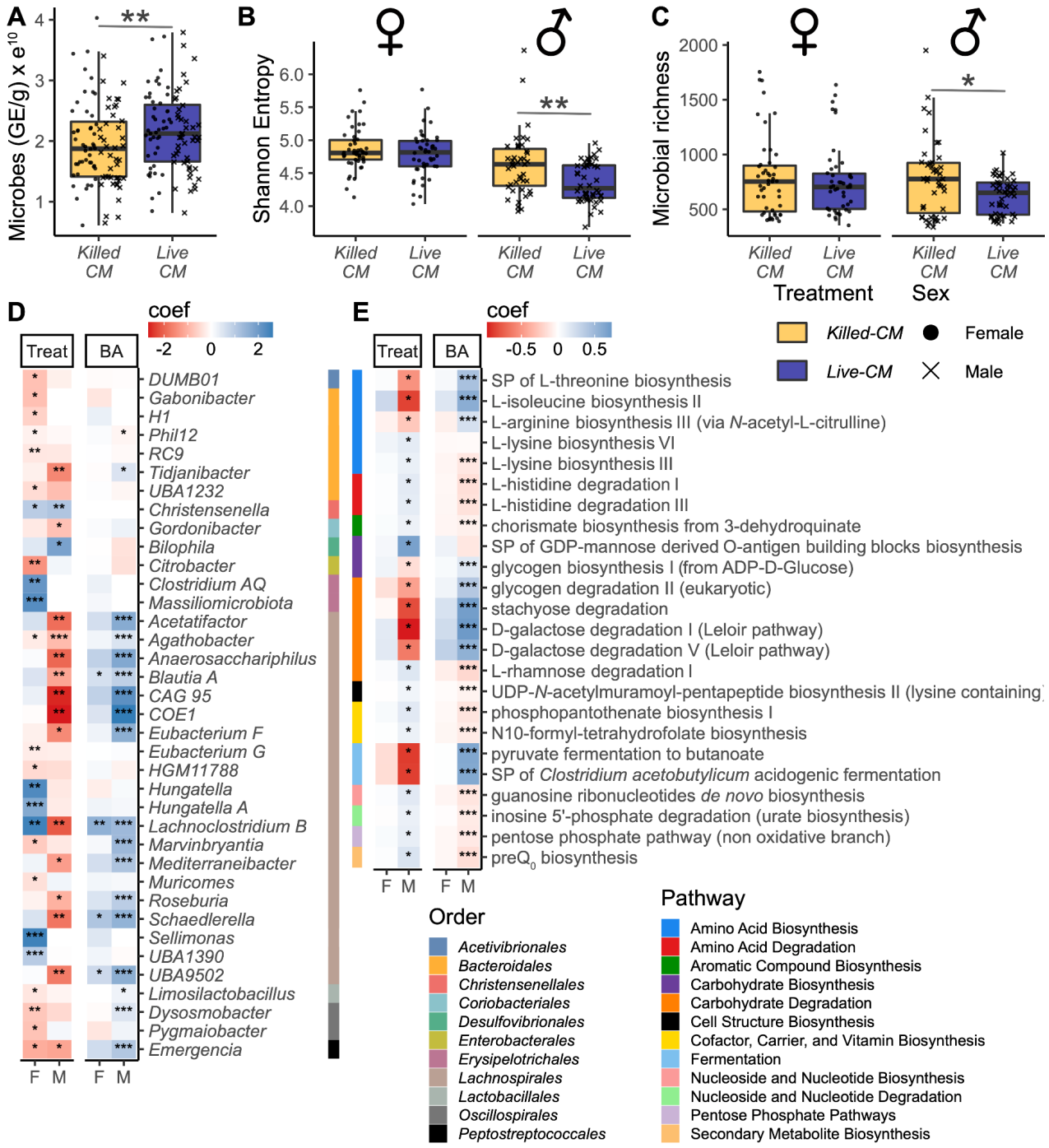

Figure 5 - *C. minuta* amendment resulted in sex-dimorphic effects of microbial community composition in recipient mice. (A) Quantification of microbial biomass via qPCR with universal 16S rRNA primers. (B-C) α-diversity of phylogenetically-profiled metagenomic cecal sequences. (D-E) Differential abundance analysis of (D) microbial taxa and (E) microbial functional profiles using MaAsLin2 [99]. Coefficients indicate associations with treatments (red: negative values = higher in *Killed-CM*, blue: positive values = higher in *Live-CM*) or cecal butyrate concentrations (red: negative values = negative association, blue: positive values = positive association). Asterisks indicate statistical significance of the linear mixed model correcting for sex and batch. * : $p < 0.1$; ** : $p < 0.01$; *** : $p < 0.001$. BA= Butyrate; F= females; GE = genome equivalents; M = males ; Treat = treatment.

DISCUSSION

Here, we studied the effect of *C. minuta* on the host's EE. Our previous study and Mazier et al. showed that treatment with live *C. minuta* decreased host adiposity gain [1,43]. Even though we did not observe such an effect in our current study, we detected a lower feed efficiency. Likewise, Mazier et al. reported a lower feed efficiency by the amendment of *C. minuta*, even though our studies differed in many parameters, including the strain of *C. minuta*, the mouse strain, mouse sex, the origin of the gut microbial community, and the mode of obesity induction. While Mazier et al. measured food intake, body weight and body composition, revealing the lower feed efficiency [43], they did not examine the causal mechanism. We designed our experiments to get a deeper insight into how *C. minuta* can influence host energy homeostasis by measuring fecal energy loss, physical activity, and metabolic energy expenditure, in addition to food intake, body weight and body composition. A lower feed efficiency can be achieved by lower energy absorption in the gut or a higher host EE [67,68]. We observed the latter in our study in the form of higher voluntary physical activity and metabolic EE.

Physical exercise is beneficial for host health and affects the microbial community [69]. While several studies associated a higher abundance of *C. minuta* with increased physical activity of the host [25,53–56], we are the first to report that *C. minuta* influences the voluntary physical activity of the host. In our experiment, we distinguish between overall activity, counting the number of beam breaks independent of movement size in the XYZ-axes, and locomotion, measuring the total distance traveled within the XY-axes in m. Despite the high correlation of both metrics, we observed differences in how the amendment of *C. minuta* affected those two metrics. Both sexes showed higher overall activity with live *C. minuta* compared to heat-killed. In contrast, we only observed greater locomotion in *Live-CM* males compared to *Killed-CM* males. These data suggest that the main driver for higher activity in males was their greater locomotion and in females a higher amount of fine-movement patterns, such as scratching and grooming.

A possible mechanism of how *C. minuta* is able to modulate host physical activity is via microbial metabolites. Szentirmai et al. reported lower murine activity by intraportal injection of butyrate [66]. In line with this report, we observed greater

locomotion and lower concentration of cecal butyrate in *Live-CM* males compared to *Killed-CM* males. Nonetheless, no correlation between these two parameters was present. In contrast, total SCFAs and locomotion showed a significant association. SCFAs are microbially produced metabolites, and changes in the microbial community composition can lead to changes in the SCFA profile in the host gut. Here, males with live *C. minuta* showed a lower α-diversity and differences in the microbial community composition and functional profile compared to the *Killed-CM* males. Butyrate was associated with differentially abundant taxa between male treatments and changes in the functional profiles of the male microbiome. According to our data, we hypothesize that live *C. minuta* induced a shift in the microbial community of male mice, which resulted in a modulation of microbial-derived SCFA, causing changes in host voluntary activity.

We observed a negative correlation between the locomotion of male mice with feed efficiency, but not in females, hinting at a causal connection between both metrics in male mice and suggesting another mechanism for lowering feed efficiency in females. Indeed, our data showed a higher energy expenditure in females with live *C. minuta* compared to heat-killed. While we observed only a trend of higher average EE, we observed a significantly higher RMR during the light cycle by 4.3% in *Live-CM* females compared to *Killed-CM* females. These data imply a modulation of metabolic EE in females by the amendment with live *C. minuta*. In search of a possible mechanism, we observed a modulation of glucocorticoid metabolism in the females between treatments reflected in lower levels of corticosterone in *Live-CM* females compared to the female heat-killed control. Further, female EE was associated with glucocorticoid metabolism pathways. A connection between glucocorticoid metabolism and metabolic energy expenditure is well described [70,71], together with an influence of microbial community upon both [44,72–77]. So far, our data indicate that *C. minuta* is capable of modulating host EE, possibly by affecting host glucocorticoid metabolism in females.

In our experiments, we used mice of both sexes. Here, we observed multiple sex-dimorphic effects by the addition of *C. minuta* to the initial inoculum in terms of (i) host activity, (ii) metabolic parameters, and (iii) microbial community composition. Our observations reflect literature reporting sex-dimorphic phenotypes. (i) In general,

females show higher activity levels than male mice [78,79], and reports imply a higher susceptibility of male mice to dietary or microbial modulation of locomotor activity [80–83]. (ii) Host sex hormones modulate multiple metabolic pathways, including SCFAs and glucocorticoid biosynthesis [84–87], and (iii) the gut microbiome [88]. For example, the response to dietary [89] or antibiotic [84] manipulations of the microbial community depends upon host sex. Though this is the first study to report that *C. minuta* affects the host dependent on sex, we are familiar with a sexually dimorphic pattern in the abundance of Christensenellaceae, with higher abundances in females [4,18,83]. Even though differences between sexes are well known, animal experiments show a sex bias toward using only male animals [90]. The use of only one sex, commonly males, simplifies the experimental design but impacts their informative value for the other sex, a fact mostly ignored in the discussion of study results.

The major strength of this study is a large number of animals of an outbred line, including both sexes (182 in total) and experimental replicates (12 in total, 6 per sex). This design comes with costs of high batch effects but the advantage of robust results and reproducibility. Nevertheless, we only used one donor stool sample in our experiments to avoid another level of complexity. Hence, more investigation is needed to examine the role of *C. minuta* in host behavior and energy homeostasis in the context of variations in the composition of the microbial community of the donor.

In conclusion, we show that *C. minuta* increased recipient physical activity and metabolic EE, potential mechanisms for its causal role in host leanness and lower feed efficiency. So far, our data suggest that *C. minuta* alters EE in females potentially by modulating host glucocorticoid metabolism. In males, *C. minuta* amendment is associated with greater locomotion, possibly connected to the changes in the microbial community and their production of SCFAs. These two hypotheses and the sex-dependent effects of *C. minuta* on the host need further investigation.

MATERIAL AND METHODS

Mouse experiments

All animal experimental procedures were reviewed and approved by the German RP. We purchased female and male five- to six-week-old germ-free (GF) Swiss Webster mice from Taconic Biosciences Inc. (Hudson, NY) or bred them in our facility.

Inoculation

We inoculated all mice with 200 µL resuspended feces, from a healthy obese human donor, amended with living or heat-killed *C. minuta* by oral gavage. To prepare the inoculum, we obtained *C. minuta* (DSM 22607) from the German Collection of Microorganisms and Cell Cultures (DSMZ; Braunschweig, Germany). We grew *C. minuta* in brain heart infusion media BHIS media supplemented with yeast extract (5 g/l), reduced with L-cysteine-HCl (0.5 g/l) at 37°C under anaerobic conditions without shaking for 3 days. For the control group, the culture was heat-killed by autoclaving (20 min at 121 °C) just before the preparation of the inoculum. In an anoxic glove box, we resuspended 0.3 g of stool in 4 mL of anaerobic PBS that contained 2 mM DTT by 5 min of vortexing. 80 mL of each *C. minuta* culture was pelleted by centrifugation and added to half of the resuspended feces. The final inoculum contained approximately 1 × 10^{10} live or heat-killed *C. minuta* cells per mouse.

Housing and euthanization

We performed experiments with 16 mice of the same sex, with 8 mice per treatment group. For each sex we replicated the experiment 6 times, resulting in a combined number of 12 experiments with 192 mice (96 male, 96 female) total. Because of sickness or death, we excluded 8 mice. For the first 25 days post-inoculation, we housed all mice at 22 °C under a 12 h light/dark cycle in Digital Ventilated Cages (Tecniplast, Buguggiate, Italy), which recorded murine activity. We co-housed female mice from the same treatment group in groups of 4, whereas male mice were single-housed. Autoclaved water and polysaccharide-rich chow (Altromin, NIH31M) were provided *ad libitum*. During the weekly cage change, we monitored murine body weight. Before inoculation and at day 25 post-inoculation, we measured fat mass and lean mass in the mice by quantitative magnetic resonance using an

EchoMRI-100 (Echo Medical Systems, LLC., TX, USA). On day 25 post-inoculation, we transferred the mice into the behavioral phenotyping respirometry cage system (Promethion Sable Line, NV, USA), in which all mice were single-housed at 26 °C under a 12 h light/dark cycle. Here, we monitored murine body weight, activity, behavior, food and water intake, and EE using indirect calorimetry. On day 28 post-colonization, the mice were euthanized, half by CO_2 and the other half by decapitation. Before euthanization, we fasted the mice for 5h. Tissues were immediately collected, flash-frozen, and stored at −80 °C. Blood was directly collected after decapitation. All blood samples were coagulated for 20 min at RT, centrifuged at 12.000 g for 20 min at 4 °C, after which the supernatant was collected and flash-frozen.

Bomb calorimetry

Gross energy content of fecal samples from mice were analyzed with the calorimeter bomb IKA C5003 (IKA-Werke GMBH & co.KG, Staufen, Germany) at the Center of PhenoGenomics of the EPFL (Switzerland). Prior to the adiabatic measurement, the samples were dried under a PSM class II hood overnight. The calibration of the machine was performed with 0.5g of benzoic acid.

Metagenomics and qPCR

gDNA extraction

We isolated genomic DNA from frozen mouse cecal contents and aliquots of the gavage preparation (inoculum), using the PowerSoil® - htp DNA isolation kit (Qiagen, Valencia, CA, USA). We assessed the wet-weight of cecal samples before loading to the extraction plate.

Absolute quantification by qPCR

We quantified genome equivalents from all bacteria and *C. minuta* in cecal genomic DNA by qPCR. We used the the KiCqStart® SYBR® Green qPCR ReadyMix™ and universal 16S rRNA primers (515 Forward: 5'-TCG TCG GCA GCG TCA GAT GTG TAT AAG AGA CAG GTG CCA GCM GCC GCG GTA A -3', 806 Reverse: 5'-GTC TCG TGG GCT CGG AGA TGT GTA TAA GAG ACA GGG ACT ACH VGG GTW TCT AAT-3') or primers specific for *C. minuta* [61] (Forward: 5'-TTC

GGG AGG AAC TGT GGG TAT-3', Reverse: 5'-GGT TGC TCA CGC GTT ACT CA-3'). For the standard curve we used genomic DNA from *Blautia hydrogenotrophica* or *C. minuta* extracted from pure cultures quantified with a Qubit® 3.0 Fluorometer (high sensitivity assay kit).

The total reaction volume per well was 20 µL with a primer concentration of 200 nM. The DNA volume per well was 3 µL, which we diluted priorly 1:10 for the quantification of *C. minuta* and 1:100 for the quantification of all bacteria. We prepared the master-mixes and sample-dilutions manually, but loaded the 384 well plates robotically (TECAN 780 ROBOT FLUENT 780 BASE UNIT). The qPCR run was performed in the BioRad CFX384 Touch™ Real-Time PCR Detection System. The cycling conditions consisted of a 3 min incubation at 95 °C, followed by a total of 40 cycles of 95 °C incubations for 10 s, 10 s annealing at 55 °C, and extension at 72 °C for 30 s. Annealing temperature differed between the primers: universal 16S rRNA = 55 °C; *C. minuta* = 56.5 °C. After the PCR melting curve analysis was performed from 55 to 95°C (5 s). Data were analyzed by Bio-Rad CFX96 Manager (Version: 3.1.1517.0823). We normalized the results by the wet weight of cecal content used for the DNA extraction.

Shotgun metagenomics

Shotgun metagenomic sequencing

We prepared shotgun metagenome libraries with a modified Nextera protocol, as described elsewhere [91]. Briefly, 5 ng gDNA were tagmented with Nextera Tn5. After purification with Agencourt AMPure XP beads (Beckman Coulter, Brea, CA, USA), we normalized and pooled the samples. Fragments in sizes from 400 to 700 bp were selected by BluePippin (Sage Sciences). We sequenced the barcoded pools on an Illumina HiSeq3000 or NextSeq2000 instrument with 2x150 bp paired-end sequencing. Library preparation and sequencing was performed at the Max Planck Institute for Biology Tübingen, Tübingen, Germany.

Sequence quality control

For the validation of the raw reads we used fqtools v.2.0 [92]. Next, we de-duplicated the reads with the clumpify module of bbtools v.37.78 (https://jgi.doe.gov/data-and-tools/bbtools/). Adapter trimming and read quality

control were performed with skewer v.0.2.2 [93] and the bbduk module of bbtools. We filtered reads mapping to the human or mouse genome out by using the bbmap module of bbtools. Finally, fastqc v.0.11.7 (https://github.com/s-andrews/FastQC) and multiQC v.1.5a [94] generated QC reports for all reads.

Metagenomic profiling

Post-QC reads were taxonomically profiled with Kraken v.2.0 [95] and Bracken v.2.2 [96] against the custom databases generated using the Struo2 pipeline [97] based on GTDB release 202 (available at http://ftp.tue.mpg.de/ebio/projects/struo2/GTDB_release202/). We performed functional profiling using HUMANn3 v.3.0.0.alpha.3 [98].

Metagenomic analyses

We rarefied the microbial reads to 460.000 sequences, calculated relative frequencies from the rarefied reads, and multiplied them with the genome equivalents per g cecal content to obtain an estimation of microbial absolute abundance. Normalized unstratified HUMANn3 v.3.0.0.alpha.3 [98] output was used for the functional analysis. We used MaAsLin2 [99] to detect differentially abundant microbes or microbial pathways between treatments and their association to cecal butyrate concentrations. Here, we considered taxa with a median relative abundance lower than 0.00001 as absent and set the prevalence threshold for taxa and pathways to 0.5. Multiple-hypothesis corrected (Benjamini-Hochberg) p-values < 0.05 were considered significant.

Serum Metabolomics

Targeted metabolites

We measured 11 selected metabolites known to be modulated by the gut microbiome and affecting host behavior, in the collected serum samples via LC-MS (Table S1).

Serum-metabolites were extracted by mixing pre-chilled methanol containing isotopic standards (13C11 L-tryptophan, kynurenic acid ring-D5) with serum at the ratio of 2:1 (v:v). The mixture with the final concentration of isotopic standards of 0.5 µg/mL was cooled for 30 min at -20°C before centrifuging at 11,000 g at 4°C for 15

min. The supernatant was filtered through a regenerated carbon filter with a pore size of 0.2 µm. LC-MS analysis of metabolites of interest was performed using a HPLC system (Dionex UltiMate 3000, Thermo Fisher, USA) coupled with a high-resolution mass spectrometer with an electrospray ionization source (Impact II, Bruker, Germany). Reverse phase chromatography was executed using a C-18 column (L × inner diameter 250 cm × 4.6 mm, 5 µm particle size, Agilent P/N 990967-902) held at a constant temperature of 20°C. The mobile phase consisted of solvent A (0.1% formic acid in water) and solvent B (0.1% formic acid in acetonitrile). Gradient elution was applied with following conditions: the chromatographic gradient started at 3% B for 3 min, increased linearly to 100% B at 20 min, held at 100% B for 3 min, decreased linearly to 3% B at 27 min, followed by an equilibrating time of 3 min. The flow rate was kept constantly at 0.5 mL/min. The injection volume was 40 µL. Samples were stored in the autosampler at 8°C for a maximum period of 72 h prior to injection. A dilution series of standards with a concentration range from 0.000128 to 10 µg/mL was measured to build the linear regression model. The weighting factor of 1, 1/x, or 1/x2 was selected depending on lowest sum percent relative error [100]. The operating parameters of the mass spectrometer were as follows: the spray needle voltage at 3.5 kV, nitrogen was used as nebulizing gas (1.5 bar) and drying gas (5 L/min), and the drying temperature was at 200°C. The data were acquired in Full-MS mode with a scanning range of 50-1,000 m/z and scanning rate of 2 Hz in the positive ion mode. Each measurement included a 30s-segment for automated internal calibration using sodium formate 5 mM. Peak integration of Full-MS data was performed using Skyline (v.21.1). The internal isotopic standards were used for quality control and for normalization purposes.

Untargeted pathway analysis

We analyzed our data with XCMS (v.2.7.2) [101], MaAsLin2 [99], and MetaboAnalyst5.0 (www.metaboanalyst.ca)[102]. Briefly, LC-MS raw data files were converted into the mzML format using ProteoWizard MS converter (v.3.0) applying peak picking on MS1 level [103] and then processed by XCMS software (v.2.7.2), to perform peak extraction, baseline calibration, peak alignment, peak identification, retention time (RT) correction and integration of peak area. The parameters setting was as follows: centWave method setting for feature detection (ppm = 20, peak width = 12.8 - 80 s, signal/noise threshold = 10, mzdiff = -0.001, prefilter intensity = 100,

and prefilter peaks = 3); Obiwarp method setting for RT correction (ProfStep = 0.5), parameters for chromatogram alignment (mzwid = 0.01, minfrac = 1, bw = 1, and minsamp = 1). The output data matrix including RTs, m/z values and peak intensity was further analyzed with MaAsLin2, correcting for batch effects. The calculated t-values and multiple hypothesis corrected *p*-values (Benjamini-Hochberg) for each m/z and RT pair were exported and analyzed with the functional analysis in MetaboAnalyst5.0. The parameters setting was as follows: ion mode: positive; mass tolerance: 5 ppm; algorithms: GSEA and mummichog v.2; *p*-value cutoff: 0.05; adducts: M+, [M+H]+, [M+2H]2+, [M+Na]+, [M+K]+, [M-H2O+H]+, [M+NH4+, [2M+H]+; pathway library: Mus musculus [KEGG]. Pathways with a combined p-value smaller than 0.05 were considered significant.

Cecal Metabolomics

The samples and SCFA standard mix tubes were treated as reported by Furuhashi et al, with few modifications[104]. Briefly, 3-methyl pentanoate was added as an internal standard. Then, 125 µL of 20 mM NaOH, 100 µL of pyridine and 80 µL of isobutanol was added and the final volume was adjusted to 650 µL with ultrahigh quality water. Next, we derivatized the solution with 50 µL of isobutyl-chloroformate and kept the lid open for 1 min to release generated gasses. The sample was vortexed for 30 s, spun down and 150 µL of hexane was added. We vortexed the sample for 10 s and centrifuged it at 21,000 x g for 3 min. Thereafter, we transferred the upper hexane phase into an autosampler vial. 1 µL of sample was injected into gas chromatography mass spectrometry (GC-MS) in split mode (1:50) with helium as a carrier gas at a flow rate of 1 mL/min. Measurements were carried out on a single quadrupole mass spectrometer (5977B-MSD;) equipped with 7890B GC and 7693 autosampler, all from Agilent Technologies, Santa Clara, CA, USA. We set the temperature of the GC-MS ion source and the transfer line for the samples to 280 °C. A VF-5ms column (60 m, 0.25 mm, 0.25 µm; CP8961, Agilent, USA) was used. The oven temperature gradient for the samples was as follows: after 5 min at 40 °C, the oven was programmed to rise to 300°C at a rate of 10°C/min. We set the temperature of the GC-MS ion source to 250°C and the transfer line to 350 °C. The scan range was between m/z 30–600. A 70 eV EI mode (Extractor ion source; Agilent Technologies Santa Clara, CA, USA) was used and SCFAs were quantified

by peak areas estimations in the extracted ion chromatogram (MassHunter; Agilent Technologies, Santa Clara, CA, USA).

Statistical analysis

We applied linear mixed models to analyze the statistical difference using lmerTest [105]. Here, we corrected for the batch of the experimental replicates, sex, technical variables and in case of EE or food intake additionally for murine weight [74].

In case of the targeted metabolites in murine sera and the SCFAs in murine cecal contents, we used MaAsLin2 [99] to perform the linear mixed model analysis followed by a multiple-hypothesis correction (Benjamini-Hochberg). Metabolites with a $q < 0.05$ were considered significant.

ACKNOWLEDGEMENTS

We thank Silke Dauser for the preparation of the shotgun libraries and Sophie Maisch for the media-preparation. We thank Claudia Miretta-Barone, Matthias Neuscheler and Christin Eitel for their help with the mouse experiments. We thank Carolina Nishi for assisting with the SCFA GC-MS measurements. We thank Dai Long Vu and Dennis Jakob for the help and management of the targeted and untargeted LC-MS metabolomics measurements. This work was supported by the Max Planck Society.

REFERENCES

1. Goodrich JK, Waters JL, Poole AC, Sutter JL, Koren O, Blekhman R, et al. Human genetics shape the gut microbiome. Cell. 2014;159: 789–799.

2. Turnbaugh PJ, Hamady M, Yatsunenko T, Cantarel BL, Duncan A, Ley RE, et al. A core gut microbiome in obese and lean twins. Nature. 2009;457: 480–484.

3. Peters BA, Shapiro JA, Church TR, Miller G, Trinh-Shevrin C, Yuen E, et al. A taxonomic signature of obesity in a large study of American adults. Sci Rep. 2018;8: 9749.

4. Brooks AW, Priya S, Blekhman R, Bordenstein SR. Gut microbiota diversity across ethnicities in the United States. PLoS Biol. 2018;16: e2006842.

5. López-Contreras BE, Morán-Ramos S, Villarruel-Vázquez R, Macías-Kauffer L, Villamil-Ramírez H, León-Mimila P, et al. Composition of gut microbiota in obese and normal-weight Mexican school-age children and its association with metabolic traits. Pediatr Obes. 2018;13: 381–388.

6. Jackson MA, Bonder MJ, Kuncheva Z, Zierer J, Fu J, Kurilshikov A, et al. Detection of stable community structures within gut microbiota co-occurrence networks from different human populations. PeerJ. 2018;6: e4303.

7. Ferrer M, Ruiz A, Lanza F, Haange S-B, Oberbach A, Till H, et al. Microbiota from the distal guts of lean and obese adolescents exhibit partial functional redundancy besides clear differences in community structure. Environ Microbiol. 2013;15: 211–226.

8. Fu J, Bonder MJ, Cenit MC, Tigchelaar EF, Maatman A, Dekens JAM, et al. The Gut Microbiome Contributes to a Substantial Proportion of the Variation in Blood Lipids. Circ Res. 2015;117: 817–824.

9. Kummen M, Holm K, Anmarkrud JA, Nygård S, Vesterhus M, Høivik ML, et al. The gut microbial profile in patients with primary sclerosing cholangitis is distinct from patients with ulcerative colitis without biliary disease and healthy controls. Gut. 2017;66: 611–619.

10. Stanislawski MA, Dabelea D, Wagner BD, Sontag MK, Lozupone CA, Eggesbø M. Pre-pregnancy weight, gestational weight gain, and the gut microbiota of mothers and their infants. Microbiome. 2017;5: 113.

11. Lim MY, You HJ, Yoon HS, Kwon B, Lee JY, Lee S, et al. The effect of heritability and host genetics on the gut microbiota and metabolic syndrome. Gut. 2017;66: 1031–1038.

12. Yun Y, Kim H-N, Kim SE, Heo SG, Chang Y, Ryu S, et al. Comparative analysis of gut microbiota associated with body mass index in a large Korean cohort. BMC Microbiol. 2017;17: 151.

13. Oki K, Toyama M, Banno T, Chonan O, Benno Y, Watanabe K. Comprehensive analysis of the fecal microbiota of healthy Japanese adults reveals a new bacterial lineage associated with a phenotype characterized by a high frequency of bowel movements and a lean body type. BMC Microbiol. 2016;16: 284.

14. Li X, Yuan X, Pang L, Miao Y, Wang S, Zhang X, et al. Gut Microbiota markers for antipsychotics induced metabolic disturbance in drug naïve patients with first episode schizophrenia – A 24 weeks follow-up study. bioRxiv. medRxiv; 2021. doi:10.1101/2020.12.26.20248886

15. Vujkovic-Cvijin I, Sklar J, Jiang L, Natarajan L, Knight R, Belkaid Y. Host variables confound gut microbiota studies of human disease. Nature. 2020;587: 448–454.

16. Nogacka AM, de Los Reyes-Gavilán CG, Martínez-Faedo C, Ruas-Madiedo P, Suarez A, Mancabelli L, et al. Impact of Extreme Obesity and Diet-Induced Weight Loss on the Fecal Metabolome and Gut Microbiota. Mol Nutr Food Res. 2021;65: e2000030.

17. Dhakal S, McCormack L, Dey M. Association of the Gut Microbiota with Weight-Loss Response within a Retail Weight-Management Program. Microorganisms. 2020;8. doi:10.3390/microorganisms8081246

18. Li X, Li Z, He Y, Li P, Zhou H, Zeng N. Regional distribution of Christensenellaceae and its associations with metabolic syndrome based on a population-level analysis. PeerJ. 2020;8: e9591.

19. Cuevas-Sierra A, Riezu-Boj JI, Guruceaga E, Milagro FI, Martínez JA. Sex-Specific Associations between Gut Prevotellaceae and Host Genetics on Adiposity. Microorganisms. 2020;8. doi:10.3390/microorganisms8060938

20. McCann JR, Bihlmeyer NA, Roche K, Catherine C, Jawahar J, Kwee LC, et al. The pediatric obesity microbiome and metabolism study (POMMS): Methods, baseline data, and early insights. bioRxiv. medRxiv; 2020. doi:10.1101/2020.06.09.20126763

21. Ikeda T, Aida M, Yoshida Y, Matsumoto S, Tanaka M, Nakayama J, et al. Alteration in faecal bile acids, gut microbial composition and diversity after laparoscopic sleeve gastrectomy. Br J Surg. 2020;107: 1673–1685.

22. Gong J, Shen Y, Zhang H, Cao M, Guo M, He J, et al. Gut Microbiota Characteristics of People with Obesity by Meta-Analysis of Existing Datasets. Nutrients. 2022;14. doi:10.3390/nu14142993

23. Stefura T, Zapała B, Gosiewski T, Skomarovska O, Dudek A, Pędziwiatr M, et al. Differences in Compositions of Oral and Fecal Microbiota between Patients with Obesity and Controls. Medicina . 2021;57. doi:10.3390/medicina57070678

24. Allin KH, Tremaroli V, Caesar R, Jensen BAH, Damgaard MTF, Bahl MI, et al. Aberrant intestinal microbiota in individuals with prediabetes. Diabetologia. 2018;61: 810–820.

25. Castro-Mejía JL, Khakimov B, Krych Ł, Bülow J, Bechshøft RL, Højfeldt G, et al. Physical fitness in community-dwelling older adults is linked to dietary intake, gut microbiota, and metabolomic signatures. Aging Cell. 2020;19: e13105.

26. Yuan X, Chen R, McCormick KL, Zhang Y, Lin X, Yang X. Metabolically healthy obese children and the role of the gut Microbiota. Research Square. Research Square; 2020. doi:10.21203/rs.3.rs-127205/v1

27. Kim M-H, Yun KE, Kim J, Park E, Chang Y, Ryu S, et al. Gut microbiota and metabolic health among overweight and obese individuals. Sci Rep. 2020;10: 19417.

28. Calderón-Pérez L, Llauradó E, Companys J, Pla-Pagà L, Pedret A, Rubió L, et al. Interplay between dietary phenolic compound intake and the human gut microbiome in hypertension: A cross-sectional study. Food Chem. 2021;344: 128567.

29. Radwan S, Gilfillan D, Eklund B, Radwan HM, El Menofy NG, Lee J, et al. A comparative study of the gut microbiome in Egyptian patients with Type I and Type II diabetes. PLoS One. 2020;15: e0238764.

30. Reitmeier S, Kiessling S, Clavel T, List M, Almeida EL, Ghosh TS, et al. Arrhythmic Gut Microbiome Signatures Predict Risk of Type 2 Diabetes. Cell Host Microbe. 2020;28: 258–272.e6.

31. Sparvoli LG, Cortez RV, Daher S, Padilha M, Sun SY, Nakamura MU, et al. Women's multisite microbial modulation during pregnancy. Microb Pathog. 2020;147: 104230.

32. Gao B, Zhong M, Shen Q, Wu Y, Cao M, Ju S, et al. Gut microbiota in early pregnancy among women with Hyperglycaemia vs. Normal blood glucose. BMC Pregnancy Childbirth. 2020;20: 284.

33. Cancello R, Turroni S, Rampelli S, Cattaldo S, Candela M, Cattani L, et al. Effect of Short-Term Dietary Intervention and Probiotic Mix Supplementation on the Gut Microbiota of Elderly Obese Women. Nutrients. 2019;11. doi:10.3390/nu11123011

34. Alemán JO, Bokulich NA, Swann JR, Walker JM, De Rosa JC, Battaglia T, et al. Fecal microbiota and bile acid interactions with systemic and adipose tissue metabolism in diet-induced weight loss of obese postmenopausal women. J Transl Med. 2018;16: 244.

35. Org E, Blum Y, Kasela S, Mehrabian M, Kuusisto J, Kangas AJ, et al. Relationships between gut microbiota, plasma metabolites, and metabolic syndrome traits in the METSIM cohort. Genome Biol. 2017;18: 70.

36. Guzmán-Castañeda SJ, Ortega-Vega EL, de la Cuesta-Zuluaga J, Velásquez-Mejía EP, Rojas W, Bedoya G, et al. Gut microbiota composition explains more variance in the host cardiometabolic risk than genetic ancestry. bioRxiv. 2018. p. 394726. doi:10.1101/394726

37. He Y, Wu W, Wu S, Zheng H-M, Li P, Sheng H-F, et al. Linking gut microbiota, metabolic syndrome and economic status based on a population-level analysis. Microbiome. 2018;6: 172.

38. Alcazar M, Escribano J, Ferré N, Closa-Monasterolo R, Selma-Royo M, Feliu A, et al. Gut microbiota is associated with metabolic health in children with obesity. Clin Nutr. 2022. doi:10.1016/j.clnu.2022.06.007

39. Sowah SA, Milanese A, Schübel R, Wirbel J, Kartal E, Johnson TS, et al. Calorie restriction improves metabolic state independently of gut microbiome composition: a randomized dietary intervention trial. Genome Med. 2022;14: 30.

40. Tavella T, Rampelli S, Guidarelli G, Bazzocchi A, Gasperini C, Pujos-Guillot E, et al. Elevated gut microbiome abundance of Christensenellaceae, Porphyromonadaceae and Rikenellaceae is associated with reduced visceral adipose tissue and healthier metabolic profile in Italian elderly. Gut Microbes. 2021;13: 1–19.

41. Chen Z, Radjabzadeh D, Chen L, Kurilshikov A, Kavousi M, Ahmadizar F, et al. Association of Insulin Resistance and Type 2 Diabetes With Gut Microbial Diversity: A Microbiome-Wide Analysis From Population Studies. JAMA Netw Open. 2021;4: e2118811.

42. Villaseñor-Aranguren M, Rosés C, Riezu-Boj JI, López-Yoldi M, Ramos-Lopez O, Barceló AM, et al. Association of the Gut Microbiota with the Host's Health through an Analysis of Biochemical Markers, Dietary Estimation, and Microbial Composition. Nutrients. 2022;14. doi:10.3390/nu14234966

43. Mazier W, Le Corf K, Martinez C, Tudela H, Kissi D, Kropp C, et al. A New Strain of Christensenella minuta as a Potential Biotherapy for Obesity and Associated Metabolic Diseases. Cells. 2021;10: 823.

44. Cani PD, Van Hul M, Lefort C, Depommier C, Rastelli M, Everard A. Microbial regulation of organismal energy homeostasis. Nature Metabolism. 2019;1: 34–46.

45. Zhang T, Yang Y, Liang Y, Jiao X, Zhao C. Beneficial Effect of Intestinal Fermentation of Natural Polysaccharides. Nutrients. 2018;10. doi:10.3390/nu10081055

46. Heiss CN, Olofsson LE. Gut Microbiota-Dependent Modulation of Energy Metabolism. J Innate Immun. 2018;10: 163–171.

47. Lai Y, Dhingra R, Zhang Z, Ball LM, Zylka MJ, Lu K. Toward Elucidating the Human Gut Microbiota-Brain Axis: Molecules, Biochemistry, and Implications for Health and Diseases. Biochemistry. 2021. doi:10.1021/acs.biochem.1c00656

48. Cryan JF, O'Riordan KJ, Cowan CSM, Sandhu KV, Bastiaanssen TFS, Boehme M, et al. The Microbiota-Gut-Brain Axis. Physiol Rev. 2019;99: 1877–2013.

49. Mayer EA, Nance K, Chen S. The Gut-Brain Axis. Annu Rev Med. 2021. doi:10.1146/annurev-med-042320-014032

50. Dohnalová L, Lundgren P, Carty JRE, Goldstein N, Wenski SL, Nanudorn P, et al. A microbiome-dependent gut-brain pathway regulates motivation for exercise. Nature. 2022;612: 739–747.

51. Scheiman J, Luber JM, Chavkin TA, MacDonald T, Tung A, Pham L-D, et al. Meta-omics analysis of elite athletes identifies a performance-enhancing microbe that functions via lactate metabolism. Nat Med. 2019;25: 1104–1109.

52. Miyazaki K, Itoh N, Yamamoto S, Higo-Yamamoto S, Nakakita Y, Kaneda H, et al. Dietary heat-killed Lactobacillus brevis SBC8803 promotes voluntary wheel-running and affects sleep rhythms in mice. Life Sci. 2014;111: 47–52.

53. Santarossa S, Sitarik AR, Johnson CC, Li J, Lynch SV, Ownby DR, et al. Associations of physical activity with gut microbiota in pre-adolescent children. Phys Act Nutr. 2021;25: 24–37.

54. Sun L, Yan Y, Yan S, Yang Y. Does physical activity associate with gut microbiome and survival outcomes of Chinese metastatic colorectal cancer patients? A secondary analysis of a randomized controlled trial. Heliyon. 2022;8: e11615.

55. Liu T-W, Park Y-M, Holscher HD, Padilla J, Scroggins RJ, Welly R, et al. Physical Activity Differentially Affects the Cecal Microbiota of Ovariectomized Female Rats Selectively Bred for High and Low Aerobic Capacity. PLoS One. 2015;10: e0136150.

56. Park S-S, Kim S-H, Kim C-J, Shin M-S, Park Y-J, Kim T-W. Effects of exercise and microbiota transplant on the memory of obesity-induced mice. Eur J Cardiovasc Prev Rehabil. 2022;18: 162–170.

57. Ruaud A, Esquivel-Elizondo S, de la Cuesta-Zuluaga J, Waters JL, Angenent LT, Youngblut ND, et al. Syntrophy via Interspecies H2 Transfer between Christensenella and Methanobrevibacter Underlies Their Global Cooccurrence in the Human Gut. MBio. 2020;11. doi:10.1128/mBio.03235-19

58. Luo M, Lu J, Li C, Wen B, Chu W, Dang X, et al. Hydrogen improves exercise endurance in rats by promoting mitochondrial biogenesis. Genomics. 2022;114: 110523.

59. Botek M, Krejčí J, McKune AJ, Sládečková B, Naumovski N. Hydrogen Rich Water Improved Ventilatory, Perceptual and Lactate Responses to Exercise. Int J Sports Med. 2019;40: 879–885.

60. Eda N, Tsuno S, Nakamura N, Sone R, Akama T, Matsumoto M. Effects of Intestinal Bacterial Hydrogen Gas Production on Muscle Recovery following Intense Exercise in Adult Men: A Pilot Study. Nutrients. 2022;14: 4875.

61. Flynn CR, Albaugh VL, Cai S, Cheung-Flynn J, Williams PE, Brucker RM, et al. Bile diversion to the distal small intestine has comparable metabolic benefits to bariatric surgery. Nat Commun. 2015;6: 7715.

62. Weir JBDEB. New methods for calculating metabolic rate with special reference to protein metabolism. J Physiol. 1949;109: 1–9.

63. Ndahimana D, Kim E-K. Measurement Methods for Physical Activity and Energy Expenditure: a Review. Clin Nutr Res. 2017;6: 68–80.

64. Burnett CML, Grobe JL. Direct calorimetry identifies deficiencies in respirometry for the determination of resting metabolic rate in C57Bl/6 and FVB mice. Am J Physiol Endocrinol Metab. 2013;305: E916–24.

65. Walsberg GE, Hoffman TCM. Direct calorimetry reveals large errors in respirometric estimates of energy expenditure. J Exp Biol. 2005;208: 1035–1043.

66. Szentirmai É, Millican NS, Massie AR, Kapás L. Butyrate, a metabolite of intestinal bacteria, enhances sleep. Sci Rep. 2019;9: 7035.

67. Burcelin R, Luche E, Serino M, Amar J. The gut microbiota ecology: a new opportunity for the treatment of metabolic diseases? Front Biosci . 2009;14: 5107–5117.

68. Bäckhed F, Ley RE, Sonnenburg JL, Peterson DA, Gordon JI. Host-bacterial mutualism in the human intestine. Science. 2005;307: 1915–1920.

69. Clauss M, Gérard P, Mosca A, Leclerc M. Interplay Between Exercise and Gut Microbiome in the Context of Human Health and Performance. Front Nutr. 2021;8: 637010.

70. Martens ME, Peterson PL, Lee CP. In vitro effects of glucocorticoid on mitochondrial energy metabolism. Biochim Biophys Acta. 1991;1058: 152–160.

71. Jimeno B, Hau M, Verhulst S. Corticosterone levels reflect variation in metabolic rate, independent of “stress.” Sci Rep. 2018;8: 13020.

72. Turnbaugh PJ, Ley RE, Mahowald MA, Magrini V, Mardis ER, Gordon JI. An obesity-associated gut microbiome with increased capacity for energy harvest. Nature. 2006;444: 1027–1031.

73. Murphy EF, Cotter PD, Healy S, Marques TM, O’Sullivan O, Fouhy F, et al. Composition and energy harvesting capacity of the gut microbiota: relationship to diet, obesity and time in mouse models. Gut. 2010;59: 1635–1642.

74. Tschöp MH, Speakman JR, Arch JRS, Auwerx J, Brüning JC, Chan L, et al. A guide to analysis of mouse energy metabolism. Nat Methods. 2011;9: 57–63.

75. Speakman JR, Fletcher Q, Vaanholt L. The “39 steps”: an algorithm for performing statistical analysis of data on energy intake and expenditure. Dis Model Mech. 2013;6: 293–301.

76. Hill JO, Wyatt HR, Peters JC. The Importance of Energy Balance. Eur Endocrinol. 2013;9: 111–115.

77. Luo Y, Zeng B, Zeng L, Du X, Li B, Huo R, et al. Gut microbiota regulates mouse behaviors through glucocorticoid receptor pathway genes in the hippocampus. Transl Psychiatry. 2018;8: 187.

78. Oraha J, Enriquez RF, Herzog H, Lee NJ. Sex-specific changes in metabolism during the transition from chow to high-fat diet feeding are abolished in response to dieting in C57BL/6J mice. Int J Obes . 2022. doi:10.1038/s41366-022-01174-4

79. Broida J, Svare B. Sex differences in the activity of mice: modulation by postnatal gonadal hormones. Horm Behav. 1984;18: 65–78.

80. Geary CG, Wilk VC, Barton KL, Jefferson PO, Binder T, Bhutani V, et al. Sex differences in gut microbiota modulation of aversive conditioning, open field activity, and basolateral amygdala dendritic spine density. J Neurosci Res. 2021;99: 1780–1801.

81. Bridgewater LC, Zhang C, Wu Y, Hu W, Zhang Q, Wang J, et al. Gender-based differences in host behavior and gut microbiota composition in response to high fat diet and stress in a mouse model. Sci Rep. 2017;7: 10776.

82. Holder MK, Peters NV, Whylings J, Fields CT, Gewirtz AT, Chassaing B, et al. Dietary emulsifiers consumption alters anxiety-like and social-related behaviors in mice in a sex-dependent manner. Sci Rep. 2019;9: 172.

83. Davis DJ, Hecht PM, Jasarevic E, Beversdorf DQ, Will MJ, Fritsche K, et al. Sex-specific effects of docosahexaenoic acid (DHA) on the microbiome and behavior of socially-isolated mice. Brain Behav Immun. 2017;59: 38–48.

84. Gao H, Shu Q, Chen J, Fan K, Xu P, Zhou Q, et al. Antibiotic Exposure Has Sex-Dependent Effects on the Gut Microbiota and Metabolism of Short-Chain Fatty Acids and Amino Acids in Mice. mSystems. 2019;4. doi:10.1128/mSystems.00048-19

85. Shi Y, Wei L, Xing L, Wu S, Yue F, Xia K, et al. Sex Difference is a Determinant of Gut Microbes and Their Metabolites SCFAs/MCFAs in High Fat Diet Fed Rats. Curr Microbiol. 2022;79: 347.

86. Moisan M-P. Sexual Dimorphism in Glucocorticoid Stress Response. Int J Mol Sci. 2021;22. doi:10.3390/ijms22063139

87. Mauvais-Jarvis F, Arnold AP, Reue K. A Guide for the Design of Pre-clinical Studies on Sex Differences in Metabolism. Cell Metab. 2017;25: 1216–1230.

88. Kim N. Sex Difference of Gut Microbiota. In: Kim N, editor. Sex/Gender-Specific Medicine in the Gastrointestinal Diseases. Singapore: Springer Nature Singapore; 2022. pp. 363–377.

89. Cuevas-Sierra A, Romo-Hualde A, Aranaz P, Goni L, Cuervo M, Martínez JA, et al. Diet- and sex-related changes of gut microbiota composition and functional profiles after 4 months of weight loss intervention. Eur J Nutr. 2021;60: 3279–3301.

90. Karp NA, Reavey N. Sex bias in preclinical research and an exploration of how to change the status quo. Br J Pharmacol. 2019;176: 4107–4118.

91. Karasov TL, Almario J, Friedemann C, Ding W, Giolai M, Heavens D, et al. Arabidopsis thaliana and Pseudomonas Pathogens Exhibit Stable Associations over Evolutionary Timescales. Cell Host Microbe. 2018;24: 168–179.e4.

92. Droop AP. fqtools: an efficient software suite for modern FASTQ file manipulation. Bioinformatics. 2016;32: 1883–1884.

93. Jiang H, Lei R, Ding S-W, Zhu S. Skewer: a fast and accurate adapter trimmer for next-generation sequencing paired-end reads. BMC Bioinformatics. 2014;15: 182.

94. Ewels P, Magnusson M, Lundin S, Käller M. MultiQC: summarize analysis results for multiple tools and samples in a single report. Bioinformatics. 2016;32: 3047–3048.

95. Wood DE, Lu J, Langmead B. Improved metagenomic analysis with Kraken 2. Genome Biol. 2019;20: 257.

96. Lu J, Breitwieser FP, Thielen P, Salzberg SL. Bracken: estimating species abundance in metagenomics data. PeerJ Comput Sci. 2017;3: e104.

97. Youngblut ND, Ley RE. Struo2: efficient metagenome profiling database construction for ever-expanding microbial genome datasets. PeerJ. 2021;9: e12198.

98. Beghini F, McIver LJ, Blanco-Míguez A, Dubois L, Asnicar F, Maharjan S, et al. Integrating taxonomic, functional, and strain-level profiling of diverse microbial communities with bioBakery 3. Elife. 2021;10. doi:10.7554/eLife.65088

99. Mallick H, Rahnavard A, McIver LJ, Ma S, Zhang Y, Nguyen LH, et al. Multivariable association discovery in population-scale meta-omics studies. PLoS Comput Biol. 2021;17: e1009442.

100. Almeida AM, Castel-Branco MM, Falcão AC. Linear regression for calibration lines revisited: weighting schemes for bioanalytical methods. J Chromatogr B Analyt Technol Biomed Life Sci. 2002;774: 215–222.

101. Tautenhahn R, Patti GJ, Rinehart D, Siuzdak G. XCMS Online: a web-based platform to process untargeted metabolomic data. Anal Chem. 2012;84: 5035–5039.

102. Pang Z, Chong J, Zhou G, de Lima Morais DA, Chang L, Barrette M, et al. MetaboAnalyst 5.0: narrowing the gap between raw spectra and functional insights. Nucleic Acids Res. 2021;49: W388–W396.

103. Chambers MC, Maclean B, Burke R, Amodei D, Ruderman DL, Neumann S, et al. A cross-platform toolkit for mass spectrometry and proteomics. Nat Biotechnol. 2012;30: 918–920.

104. Furuhashi T, Sugitate K, Nakai T, Jikumaru Y, Ishihara G. Rapid profiling method for mammalian feces short chain fatty acids by GC-MS. Anal Biochem. 2018;543: 51–54.

105. Kuznetsova A, Brockhoff PB, Christensen RHB. lmerTest package: tests in linear mixed effects models. J Stat Softw. 2017;82: 1–26.

106. Varian BJ, Poutahidis T, Levkovich T, Ibrahim YM, Lakritz JR, Chatzigiagkos A, et al. Beneficial bacteria stimulate youthful thyroid gland activity. J Obes Weight Loss Ther. 2014;4. Available: https://www.cabdirect.org/cabdirect/abstract/20153424026

107. Spaggiari G, Brigante G, De Vincentis S, Cattini U, Roli L, De Santis MC, et al. Probiotics Ingestion Does Not Directly Affect Thyroid Hormonal Parameters in Hypothyroid Patients on Levothyroxine Treatment. Front Endocrinol . 2017;8: 316.

108. Liu QF, Kim H-M, Lim S, Chung M-J, Lim C-Y, Koo B-S, et al. Effect of probiotic administration on gut microbiota and depressive behaviors in mice. Daru. 2020;28: 181–189.

109. Theoharides TC. On the Gut Microbiome-Brain Axis and Altruism. Clin Ther. 2015;37: 937–940.

110. Chen H, Nwe P-K, Yang Y, Rosen CE, Bielecka AA, Kuchroo M, et al. A Forward Chemical Genetic Screen Reveals Gut Microbiota Metabolites That Modulate Host Physiology. Cell. 2019;177: 1217–1231.e18.

111. Luck B, Horvath TD, Engevik KA, Ruan W, Haidacher SJ, Hoch KM, et al. Neurotransmitter Profiles Are Altered in the Gut and Brain of Mice Mono-Associated with Bifidobacterium dentium. Biomolecules. 2021;11. doi:10.3390/biom11081091

112. Zheng P, Zeng B, Liu M, Chen J, Pan J, Han Y, et al. The gut microbiome from patients with schizophrenia modulates the glutamate-glutamine-GABA cycle and schizophrenia-relevant behaviors in mice. Sci Adv. 2019;5: eaau8317.

113. Bravo JA, Forsythe P, Chew MV, Escaravage E, Savignac HM, Dinan TG, et al. Ingestion of Lactobacillus strain regulates emotional behavior and central GABA receptor expression in a mouse via the vagus nerve. Proc Natl Acad Sci U S A. 2011;108: 16050–16055.

114. Sudo N, Chida Y, Aiba Y, Sonoda J, Oyama N, Yu X-N, et al. Postnatal microbial colonization programs the hypothalamic-pituitary-adrenal system for stress response in mice. J Physiol. 2004;558: 263–275.

115. Modigh K. Effects of L-tryptophan on motor activity in mice. Psychopharmacologia. 1973;30: 123–134.

116. O'Mahony SM, Clarke G, Borre YE, Dinan TG, Cryan JF. Serotonin, tryptophan metabolism and the brain-gut-microbiome axis. Behav Brain Res. 2015;277: 32–48.

117. Luo J, Wang T, Liang S, Hu X, Li W, Jin F. Ingestion of Lactobacillus strain reduces anxiety and improves cognitive function in the hyperammonemia rat. Sci China Life Sci. 2014;57: 327–335.

SUPPLEMENTARY MATERIAL

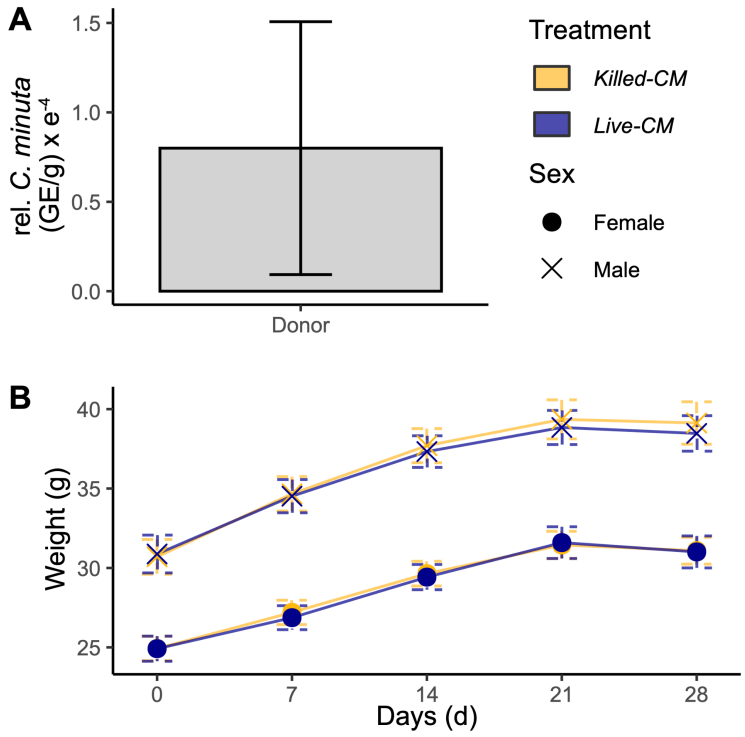

Figure S1 - *C. minuta* in donor stool and murine body weight gain over the duration of the experiment. (A) Relative abundance of *C. minuta* in the donor stool. Values are obtained from two independent DNA extractions and metagenomic sequencing runs. (B) Murine weight gain during the experiment.

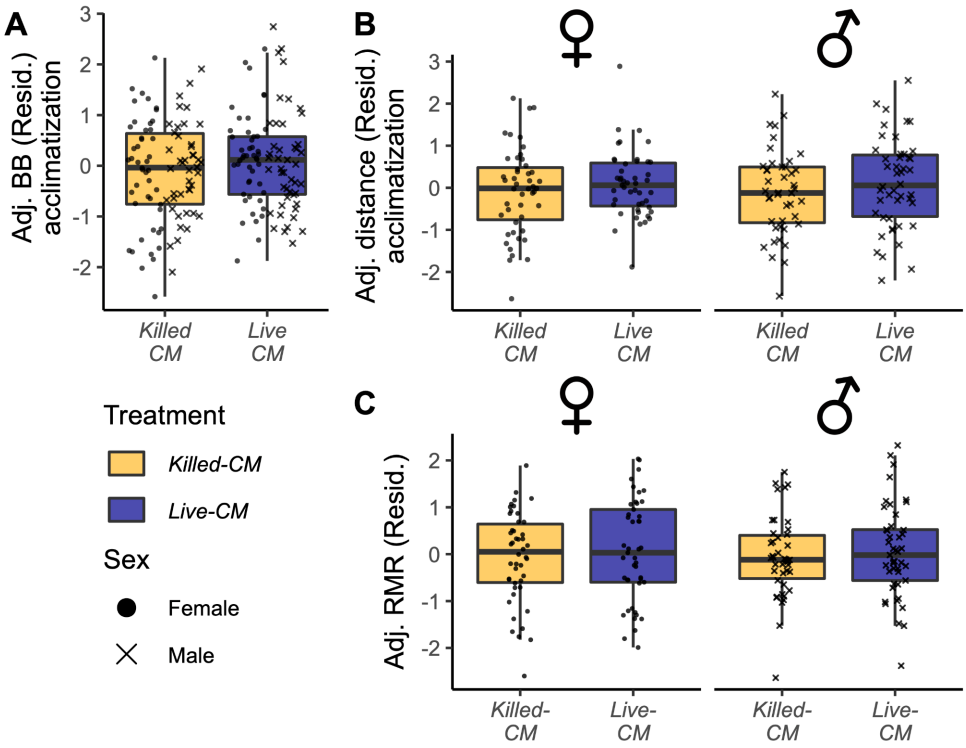

Figure S2 - Murine activity during acclimatization and average RMR. (A-B) Residual activity metrics, (A) number of beam breaks, (B) adjusted for batch and sex effects. Activity metrics with (A) overall activity and (B) total distance traveled, during the first 24 hours in the behavioral phenotyping respirometry cage system. (C) Residual average RMR adjusted for weight, sex and batch measured by indirect calorimetry during the last 48 hours in the behavioral phenotyping respirometry cage system. Adj. = adjusted; BB = beam breaks; Resid. = residuals; RMR = resting metabolic rate.

Table S1: Literature linking target metabolites to the gut-microbiome-brain axis.

Pathway	Compounds	Literature
Hypothalamic–pituitary–thyroid axis	T4 (thyroxine)	[106] Probiotic administration increases locomotor activity and improves thyroid function [107] Probiotic administration increase levothyroxine availability and stabilizes thyroid function
Hypothalamic–pituitary–adrenal axis	Corticosterone	[108] Probiotic administration alleviated depressive-like behaviors and decreased corticosterone level in mice subjected to restraint stress [77] Probiotic administration alleviated behavioral changes of germfree mice and modulated glucocorticoid pathway genes in the brain and serum cortisol concentrations
Histamine - Neurotransmitter	Histamine	[109] Histamine is critical for learning, memory, cognition, and motivation [110] Various gut microbes can produce histamine
GABA - Neurotransmitter	γ-aminobutyric acid (GABA), Glutamine, Glutamate	[111] Various probiotics can synthesize GABA, glutamine and glutamate in vitro and change GABA levels in murine feces [112] Fecal transplant experiments from schizophrenic human donors resulted in lower GABA levels in the brain and schizophrenia-related behaviors in recipient mice compared to controls [113] Probiotic administration affects GABA receptor expression in the brain, reduces stress-induced corticosterone levels and anxiety- and depression-related behavior in mice [114] Colonization of germfree mice normalized anxiety-like behavior and brain BDNF levels, associated with an expression of the GluN2A subunit (Glutamate-Receptor)
Tryptophan metabolism	Kynurenine, Kynurenic acid, Tryptophan, Indole lactic acid, Serotonin	[115] High dosage of tryptophan decreased murine activity [116] Serum serotonin and tryptophan metabolite concentrations depend on host colonization status [117] Probiotic administration improved cognitive and anxiety-like behavior and affected central serotonin levels as well as metabolites of the kynurenine pathway

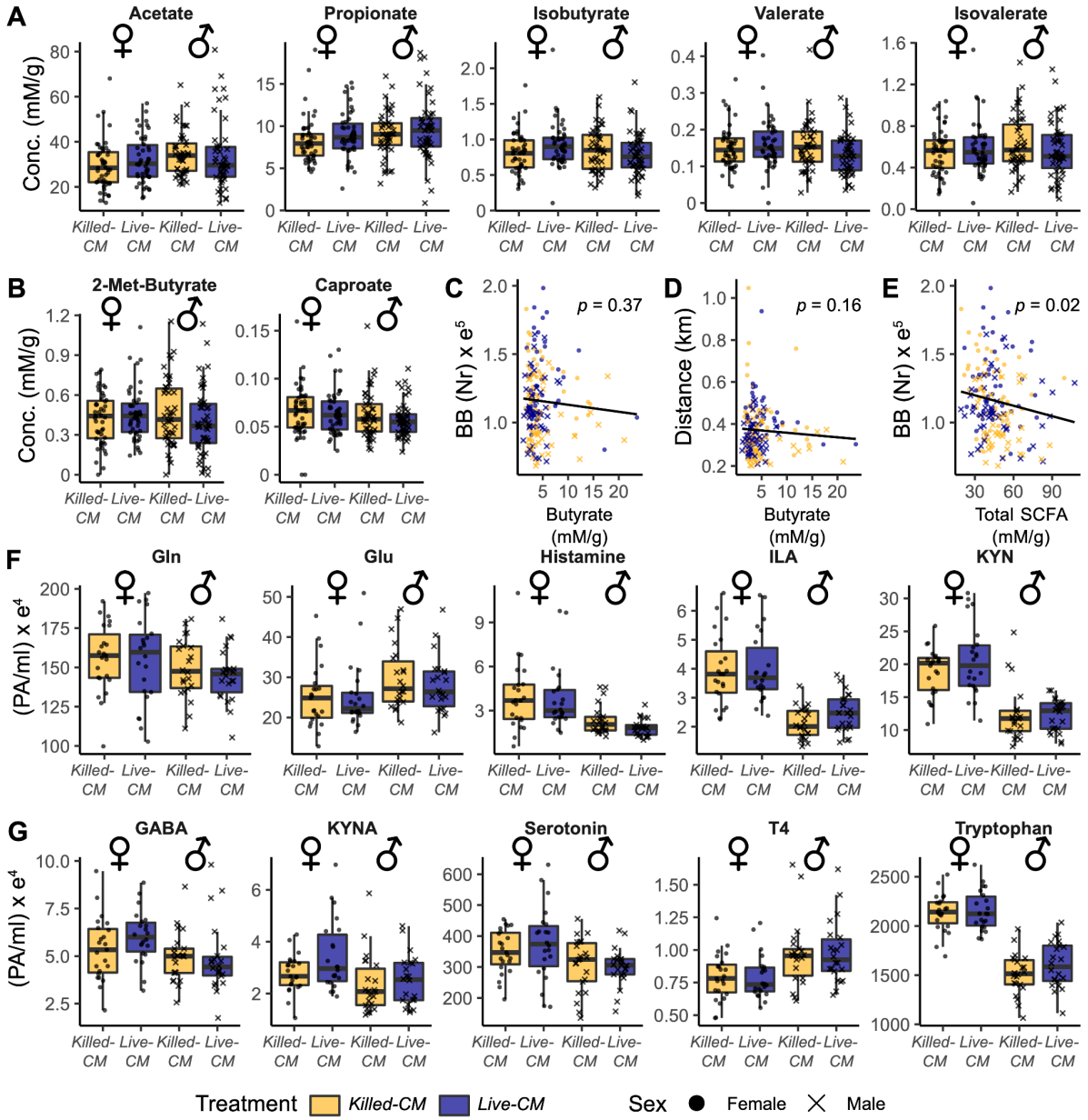

Figure S3 - Targeted metabolites in murine serum samples and cecal contents. (A-E) SCFA and branched-chain fatty acid concentrations in murine cecal contents on day 28 post-inoculation measured via GC-MS. (B) Butyrate concentrations correlated to (C) murine overall activity and (D) locomotion. (E) Sum of all SCFA correlated to murine overall activity. (F-G) Targeted metabolites in murine sera measured via LC-MS. GABA = γ-Aminobutyric acid; Gln = Glutamine; Glu = Glutamic acid; ILA = Indole lactic acid; KYN = Kynurenine; KYNA = Kynurenic acid; PA = peak area; T4 = Thyroxine.

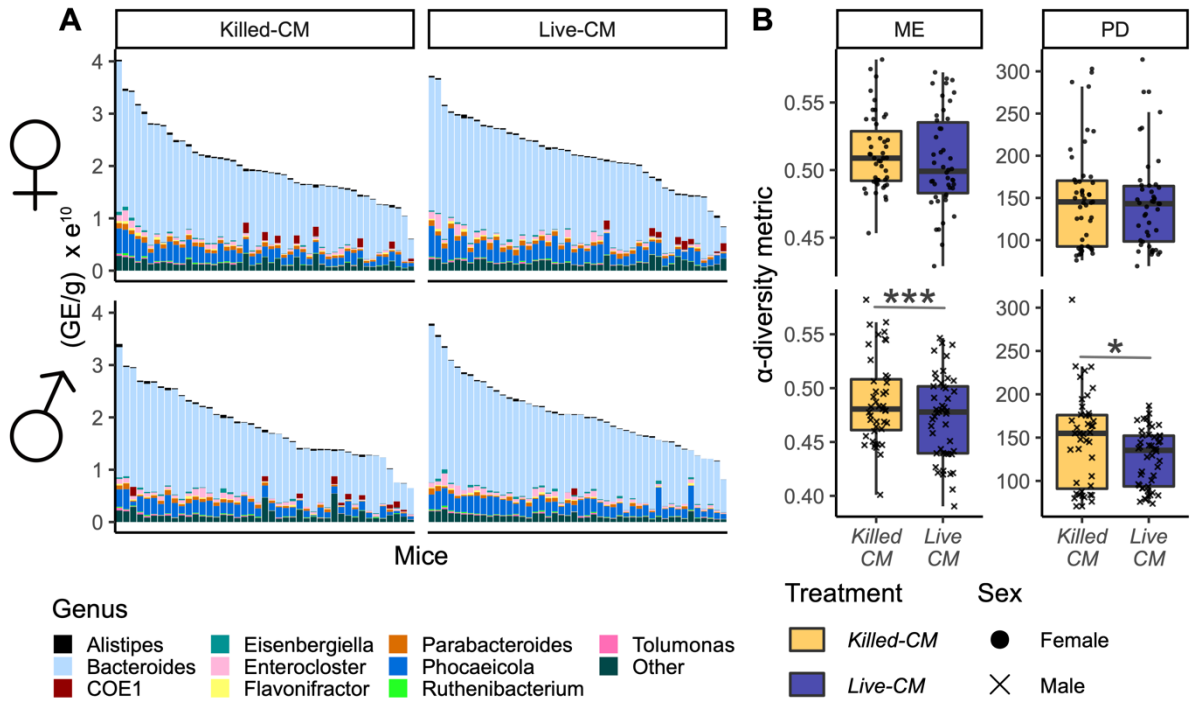

Figure S4 - Microbial composition per mouse and α-diversity. (A,B) Analyses of phylogenetically-profiled metagenomic cecal sequences normalized by microbial biomass quantified via qPCR. (A) Taxa bar plots for each mouse. (B) Comparison of α-diversity metrics, microbial evenness (ME) and phylogenetic diversity (PD) between treatment groups. Asterisks indicate statistical significance of the linear mixed model correcting for sex and batch. * : $p < 0.1$; *** : $p < 0.001$. GE = genome equivalents; ME = microbial evenness; PD = phylogenetic diversity.

4.4. Conclusion

This final results chapter incorporated the main project of my doctoral thesis. Here, I provided first evidence of *C. minuta* influencing host physical activity and energy expenditure, a possible mechanism for its causal role in decreasing host adiposity and its constant associations with host metabolic health. Moreover, I identified several sex-dependent effect of *C. minuta* on the host, a phenomenon not reported until now. These results provide a strong foundation for further studies of *C. minuta's* influence on host health and the underlying mechanism.

Chapter 5: Discussion

Despite global associations of *Christensenellaceae* with a lean human BMI and metabolic health, and the demonstrated causal role of *C. minuta* in reduced host adiposity gain, knowledge of this microbe and its microbial family remains scarce. To address this gap, I studied how the addition of *C. minuta* impacts the microbial community (Chapters 2-4) and the host (Chapter 4) using mice with a simplified microbial community (Chapter 2) and with a complex community established via fecal transplantation from an obese human donor to recipient germfree mice (Chapters 3-4). I found that the fitness of *C. minuta* increases with the presence of other microbial species in the murine gut (Chapter 2) but has only a minor effect on the overall microbial community composition (Chapters 3-4). Moreover, the addition of living *C. minuta* affected murine physical activity and metabolic energy expenditure, a possible explanation for its reported association with host metabolic health and BMI (Chapter 4). In this chapter, I evaluate the advantages and disadvantages of using the mouse model organism to study the gut microbiome based on its adoption across all experiments presented in this dissertation (Chapters 2-4). Furthermore, I address a common pattern in the effect of *C. minuta* on certain members of the microbial community evident in both my experiments and those conducted by Jillian Waters (Chapters 3-4).

5.1. The mouse as a model organism to study microbial species of interest

A major obstacle in gut microbiome research is reproducing the natural environment of the gut microbe(s) in a controlled laboratory setting. The natural environment of the gut microbiome is the host intestine, with its changing environmental conditions such as pH, oxygen concentrations, and the composition and thickness of the mucus layer along the length of the intestinal tract [141]. Multiple host cell types are present in this environment and interact with the microbial community in the intestine, including immune cells [141]. In addition, gut peristalsis moves the gut content, rendering it a non-stationary environment [141]. The complex combination of these factors is currently not fully reproducible *in vitro*, although many

potentially applicable technologies are advancing rapidly, for example organoids [142] and complex bioreactors [143]. Many studies thus use a model organism to ensure these complex factors are included when investigating the gut microbiome and its interactions with the host. Especially when microbial interactions with the host expand to influence host behavior, a research area called the gut-microbiome-brain axis, no *in-vitro* alternatives are applicable [144].

Of all the model organisms used in microbiome research, the mouse is easy to handle, cost-effective, and closely related to humans [145,146]. Germ-free mice in particular represent a strong model for microbiome research, offering the power to control the exact number and types of microbes within the host to study those microbes in a simplified scenario *in vivo* [Chapter 2] [144]. It is also possible to "humanize" the murine microbiota to some extent via fecal transplants, giving us the opportunity to study the whole complex human microbial community *in vivo* [Chapters 3 & 4] [144]. In humanization experiments described in the literature mice mirrored disease phenotypes and conditions from the human fecal donor, revealing a causal role of the gut microbiome in diseases and conditions, including cancer immunity, autoimmunity, and obesity [147]. Such experimental breakthroughs would not have been possible without a suitable *in vivo* model organism, highlighting the suitability of the mouse for microbiome research. Especially in the gut-microbiota-brain research area the mouse is a widely used model system, with multiple protocols to evaluate behavioral modulations [144,148].

However, the mouse as a model organism in microbiome research harbors several drawbacks in terms of translating study results to humans. The anatomy of the murine and human intestinal tracts differ markedly, e.g. in terms of the distribution of specific cell types and the intestinal compartment sizes relative to body size [146]. More importantly, not all gut microbes are present in both humans and mice, with some not transferable between the two [147,149]. Thus, a complete "humanization" of the murine gut microbiome is impossible. Moreover, studies have reported developmental deficits in germfree mice, making it possibly unsuitable for a number of specific scientific questions, including brain neurogenesis and social cognition behaviors [144].

In the context of my studies, studying *C. minuta* in mice expanded our knowledge of its growing role in the microbial community *in vivo*, including (i) a potential growth limit in the murine intestines (Chapter 2) and (ii) a substantial increase of the total microbial biomass (Chapter 4). (iii) Further, my results suggest a possible mechanism of its association with host health via host energy homeostasis, including changes in voluntary physical activity and metabolic energy expenditure (Chapter 4). (iv) Moreover, I detected that all the effects of *C. minuta in vivo* depend on mouse sex, indicating an interaction with host sex hormones.

All these new findings have raised questions expanding beyond the scope of this thesis. In the following, I list possible follow-up experiments exploring these questions. (i) To test the growth modulations of *C. minuta* by microbial and host-derived products, an initial assay of potential substances *in vitro* is possible. Adding these substances to media containing *C. minuta* and tracking its growth helps to identify several selected candidates. Supplementing drinking water or food with the candidate substances can verify the growth-modulating effects in mice mono-colonized with *C. minuta*. (ii) To investigate how *C. minuta* increases total microbial biomass, I suggest a top-down approach *in vitro*. First, mimicking the increase in microbial biomass by adding *C. minuta* to a microbial community is required. Here, I would suggest using a simple microbial community in batch cultures. Transcriptomics or proteomics data comparisons of cultures amended with *C. minuta* and controls without *C. minuta* identifies candidate metabolites to test in batch experiments (iii) As already stated in this chapter, germfree mice depict a few irreversible developmental deficits of the brain, with the possibility of affecting murine behavior post-microbial-colonization. Therefore, replication of the experiment in Chapter 4, followed by breeding of the inoculated mice within the treatment groups and examining murine behaviors in the F2 generation, helps to estimate the validity of my results. (iv) Literature reported higher abundances of *C. minuta* in females [47,61,137], giving a first hint of the influence of sex hormones on *C. minuta*. But it is unknown if *C. minuta* itself can influence host sex hormones. Similar to the experiments performed by Lombardi et al. [150], an expanded *in vitro* assay can test the ability of *C. minuta* to metabolize androgens or estrogens.

In summary, the mouse represents a relatively easy-to-handle and cost-effective organism to study the gut microbiome *in vivo* and its interactions with the host. It improves research due to the inability to model the complex *in vivo* environment *in vitro*, and the possibility to study its interactions with the host starting from the cellular levels and expanding to complex interactions as behavior.

5.2. Selective effect of *Christensenella minuta* on the microbial community composition

Despite the sparsity of *Christensenellaceae* in the human gut microbiome [5], they are consistently associated with human health [5,45–85]. This opens the question of how such low abundant microbes are capable of influencing human health. In Chapter 3 I already stated my hypothesis of an indirect effect of *C. minuta* on the host via the microbial community, possibly via the production of hydrogen.

I investigated the effect of *C. minuta* on complex microbial communities in multiple murine pilot studies (Chapter 3) and in experiments conducted by me (Chapter 4). Taking these two chapters together, *C. minuta* had only minor effects on the microbial community composition. Instead, a large proportion of the variance in both studies was found to be associated with the experimental batches, despite the use of the same protocol to prepare the inoculum in all experiments with the same stool sample of one donor. An explanation for these batch effects thus remains elusive. Although no marked effect on the overall microbial community composition was visible between the study groups in both chapters, differential abundance analyses revealed significant differentially-abundant taxa between the *C. minuta*-related study groups of each study. Most of the taxa belonged to the family of *Lachnospiraceae,* of which most showed lower abundances in the mice with live *C. minuta* compared to the control mice in the corresponding study. Contrary to my hypothesis of a community shaping effect of *C. minuta* via its hydrogen production, literature states enrichment of *Lachnospiraceae* by hydrogen [151,152], not a decrease which I observed.

My results showed the ability of *C. minuta* to reduce the abundance of multiple *Lachnospiraceae* in the murine guts. If this reduction in *Lachnospiraceae* contributes to the positive effects associated with *C. minuta* needs to be investigated, including the mechanism driving this influence of *C. minuta* on specific members of the gut microbiome.

5.3. General conclusion

This thesis aimed at investigating a member of the health-associated *Christensenellaceae*, *C. minuta*, *in vivo* examining its interactions with other gut microbes and the host. Here I showed that *C. minuta* benefits from the presence of other microbes in the gastrointestinal tract of the host [Chapter 2]. Even though *C. minuta* had only a minor influence on the overall composition of the gut microbiome [Chapters 3 & 4], it was capable of influencing host physical activity and metabolism [Chapter 4]. My findings broaden the understanding in this particular species and reinforce associations of *C. minuta* with host health. Further, my results lay the groundwork for further investigations of *C. minuta* in context of the gut-microbiome-brain axis and its effects in dependence of host sex.

Appendix Chapter 2: Detailed DNA extraction protocol

This protocol is optimized for input samples with low DNA-amount and contains comments to ensure the proper procedure.

Reagents:

- freshly prepared (on the day of extraction) lysis solution
- PCR grade water/Nuclease free water
- Proteinase K (20 mg/ml)
- Phenol/Chloroform-Isoamyl Alcohol (PCI)
- Chloroform-Isoamyl Alcohol (CI)
- Cold EtOH 75% (molecular grade)
- (Cold) EtOH 100% (molecular grade)
- 3M Na Acetate (pH 7)
- Qiagen Blood and Tissue Kit

Table : 8x Lysis Solution

Add reagents in the order written in the table

Total Volume	**2.5 mL**	**1.25 mL**
PCR grade water/Nuclease free water	1150 µL	575 µL
3M Na Acetate (pH 7)	265 µL	132.5 µL
20 % SDS	1000 µL	500 µL
0.5 M EDTA (pH 8)	80 µL	40 µL

Procedure:

Lysis

1. Prepare lysis solution freshly and heat it up 60 °C
2. Add 800 µL PCR grade water/Nuclease free water and 115 µL LysSol to each bead tube
3. Incubate for 30 min @ 60 °C
4. Cool samples on ice
5. Bead-beating of samples with the parameters:
   7 m/s, 90 s, 2 cycles, 30 s pause in-between
6. Cool samples on ice
7. Centrifuge tubes for 30 s @ 10.000 rpm
8. Add 20 µL of Proteinase K (20 mg/ml)
9. Incubate for 30 min @ 60 °C

Extraction

10. Centrifuge tubes for 30 s @ 10.000 rpm
11. Pipette supernatant into a 2 mL Eppendorf tube – *estimate volume (~800 µL) Safe stopping point – store tubes at -20 °C. As the lysis buffer crystallizes at low temperatures, before continuing with the protocol the tubes need to be heated for 1 min at 60 °C to get the buffer back to solution*
12. Add the same volume of PCI to supernatant
13. Mix on thermomixer gently (300 rpm) for 5 min @ RT
14. Centrifuge for 15 min with 10.000 rpm @ RT
15. Carefully remove top (aqueous) phase containing DNA and transfer into a new 2 mL tube
16. Repeat steps 13-16 till no white precipitate is at the interface (2x or more)
17. Add equal volume CI
18. Mix on thermomixer gently (300 rpm) for 2 min @ RT
19. Centrifuge for 1 min with 10.000 rpm @ RT
20. Carefully remove top (aqueous) phase containing DNA and transfer into new 2 mL tube

Precipitation

21. Add 2.5 x Volume ice-cold 100% EtOH and 0.1 x Volume 3M Na Acetate (pH 7)
22. Mix gently and place overnight in -20 °C
23. Prepare 75% EtOH and put it on ice
24. Centrifuge the tubes for 20 min with max speed @ 4 °C
25. Remove the supernatant, add 1 mL EtOH and invert tubes for 2-3 times carefully
26. Centrifuge the tubes for 10 min with max speed @ 4 °C
27. Repeat step 26-27
28. Dry pellet in the flow hood @ RT

Clean up (DNeasy® Blood & Tissue Kit)

29. Dissolve pellet in 220 µL PCR grade water/Nuclease free water
    After a Phenol/Chloroform purification it is hard to get the DNA back to solution -> pipette up and down until the pellet is not visible anymore. Heat the solutions in a thermomixer up to 65 °C with 300 rpm for 5 min. Afterward it is better to let it sit at RT for a while
30. Add 200 µL Buffer AL (without added ethanol) to the sample, and mix thoroughly by vortexing.
31. Add 200 µL ethanol (96–100%). Mix thoroughly by vortexing.
32. Pipette the mixture into a DNeasy Mini spin column placed in a 2 ml collection tube. Centrifuge at ≥6000 x g (8000 rpm) for 1 min. Discard the flow-through and collection tube.
33. Place the spin column in a new 2 mL collection tube. Add 500 µL Buffer AW1. Centrifuge for 1 min at ≥6000 x g. Discard the flow-through and collection tube.
34. Place the spin column in a new 2 mL collection tube, add 500 µL Buffer AW2 and centrifuge for 3 min at 20,000 x g (14,000 rpm). Discard the flow-through and collection tube.
    It is important to dry the membrane of the DNeasy Mini spin column, since residual ethanol may interfere with subsequent reactions. This centrifugation step ensures that no residual ethanol will be carried over during the following elution. Following the centrifugation step, remove the DNeasy Mini spin

column carefully so that the column does not come into contact with the flow-through since this will result in a carryover of ethanol. If the carryover of ethanol occurs, empty the collection tube, then reuse it for another centrifugation for 1 min at 20,000 x g (14,000 rpm).

35. Transfer the spin column to a new 1.5 mL microcentrifuge tube.
36. Elute the DNA by adding 50 µL PCR grade water/Nuclease free water to the center of the spin column membrane. Incubate for 1 min at room temperature (15–25°C). Centrifuge for 1 min at ≥6000 x g

    Don't use Buffer AE when working with qPCR as it contains EDTA, which can inhibit the PCR reaction

References

1. O'Hara AM, Shanahan F. The gut flora as a forgotten organ. EMBO Rep. 2006;7: 688–693.

2. Sekirov I, Russell SL, Antunes LCM, Finlay BB. Gut microbiota in health and disease. Physiol Rev. 2010;90: 859–904.

3. Sanmiguel C, Gupta A, Mayer EA. Gut Microbiome and Obesity: A Plausible Explanation for Obesity. Curr Obes Rep. 2015;4: 250–261.

4. Morotomi M, Nagai F, Watanabe Y. Description of Christensenella minuta gen. nov., sp. nov., isolated from human faeces, which forms a distinct branch in the order Clostridiales, and proposal of Christensenellaceae fam. nov. Int J Syst Evol Microbiol. 2012;62: 144–149.

5. Goodrich JK, Waters JL, Poole AC, Sutter JL, Koren O, Blekhman R, et al. Human genetics shape the gut microbiome. Cell. 2014;159: 789–799.

6. Ley RE, Goodrich J, Waters J. Modulation of fat storage in a subject by altering population levels of christensenellaceae in the gi tract. European Patent. 3134509:A4, 2017. Available: https://patentimages.storage.googleapis.com/0a/6a/fa/bede395c5e73a8/US10206958.pdf

7. Sender R, Fuchs S, Milo R. Revised Estimates for the Number of Human and Bacteria Cells in the Body. PLoS Biol. 2016;14: e1002533.

8. Berg G, Rybakova D, Fischer D, Cernava T, Vergès M-CC, Charles T, et al. Microbiome definition re-visited: old concepts and new challenges. Microbiome. 2020;8: 103.

9. Farhadi A, Banan A, Fields J, Keshavarzian A. Intestinal barrier: an interface between health and disease. J Gastroenterol Hepatol. 2003;18: 479–497.

10. David LA, Maurice CF, Carmody RN, Gootenberg DB, Button JE, Wolfe BE, et al. Diet rapidly and reproducibly alters the human gut microbiome. Nature. 2014;505: 559–563.

11. Janzon A, Goodrich JK, Koren O, TEDDY Study Group, Waters JL, Ley RE. Interactions between the Gut Microbiome and Mucosal Immunoglobulins A, M, and G in the Developing Infant Gut. mSystems. 2019;4. doi:10.1128/mSystems.00612-19

12. Suzuki TA, Ley RE. The role of the microbiota in human genetic adaptation. Science. 2020;370. doi:10.1126/science.aaz6827

13. Ramakrishna BS. Role of the gut microbiota in human nutrition and metabolism. J Gastroenterol Hepatol. 2013;28 Suppl 4: 9–17.

14. Reid G, Howard J, Gan BS. Can bacterial interference prevent infection? Trends Microbiol. 2001;9: 424–428.

15. Parekh PJ, Balart LA, Johnson DA. The Influence of the Gut Microbiome on Obesity, Metabolic Syndrome and Gastrointestinal Disease. Clin Transl Gastroenterol. 2015;6: e91.

16. Chassaing B, Koren O, Goodrich JK, Poole AC, Srinivasan S, Ley RE, et al. Dietary emulsifiers impact the mouse gut microbiota promoting colitis and metabolic syndrome. Nature. 2015;519: 92–96.

17. Kozhieva M, Naumova N, Alikina T, Boyko A, Vlassov V, Kabilov MR. Primary progressive multiple sclerosis in a Russian cohort: relationship with gut bacterial diversity. BMC Microbiol. 2019;19: 309.

18. Zackular JP, Baxter NT, Iverson KD, Sadler WD, Petrosino JF, Chen GY, et al. The gut microbiome modulates colon tumorigenesis. MBio. 2013;4: e00692–13.

19. Lai Y, Dhingra R, Zhang Z, Ball LM, Zylka MJ, Lu K. Toward Elucidating the Human Gut Microbiota-Brain Axis: Molecules, Biochemistry, and Implications for Health and Diseases. Biochemistry. 2021. doi:10.1021/acs.biochem.1c00656

20. Cryan JF, O'Riordan KJ, Cowan CSM, Sandhu KV, Bastiaanssen TFS, Boehme M, et al. The Microbiota-Gut-Brain Axis. Physiol Rev. 2019;99: 1877–2013.

21. Mayer EA, Nance K, Chen S. The Gut-Brain Axis. Annu Rev Med. 2021. doi:10.1146/annurev-med-042320-014032

22. de Groot P, Scheithauer T, Bakker GJ, Prodan A, Levin E, Khan MT, et al. Donor metabolic characteristics drive effects of faecal microbiota transplantation on recipient insulin sensitivity, energy expenditure and intestinal transit time. Gut. 2020;69: 502–512.

23. Cheng S, Ma X, Geng S, Jiang X, Li Y, Hu L, et al. Fecal Microbiota Transplantation Beneficially Regulates Intestinal Mucosal Autophagy and Alleviates Gut Barrier Injury. mSystems. 2018;3. doi:10.1128/mSystems.00137-18

24. Turnbaugh PJ, Ley RE, Mahowald MA, Magrini V, Mardis ER, Gordon JI. An obesity-associated gut microbiome with increased capacity for energy harvest. Nature. 2006;444: 1027–1031.

25. Ridaura VK, Faith JJ, Rey FE, Cheng J, Duncan AE, Kau AL, et al. Gut microbiota from twins discordant for obesity modulate metabolism in mice. Science. 2013;341: 1241214.

26. Obesity. [cited 23 Jan 2023]. Available: https://www.who.int/news-room/facts-in-pictures/detail/6-facts-on-obesity

27. Dinsa GD, Goryakin Y, Fumagalli E, Suhrcke M. Obesity and socioeconomic status in developing countries: a systematic review. Obes Rev. 2012;13: 1067–1079.

28. van der Vossen EWJ, de Goffau MC, Levin E, Nieuwdorp M. Recent insights into the role of microbiome in the pathogenesis of obesity. Therap Adv Gastroenterol. 2022;15: 17562848221115320.

29. Hall KD, Sacks G, Chandramohan D, Chow CC, Wang YC, Gortmaker SL, et al. Quantification of the effect of energy imbalance on bodyweight. The Lancet. 2011. pp. 826–837.

30. Cani PD, Van Hul M, Lefort C, Depommier C, Rastelli M, Everard A. Microbial regulation of organismal energy homeostasis. Nature Metabolism. 2019;1: 34–46.

31. Speakman JR. Measuring energy metabolism in the mouse - theoretical, practical, and analytical considerations. Front Physiol. 2013;4: 34.

32. Arnold PA, Delean S, Cassey P, White CR. Meta-analysis reveals that resting metabolic rate is not consistently related to fitness and performance in animals. J Comp Physiol B. 2021;191: 1097–1110.

33. Gordon CJ. Thermal physiology of laboratory mice: Defining thermoneutrality. J Therm Biol. 2012;37: 654–685.

34. Hill JO, Wyatt HR, Peters JC. The Importance of Energy Balance. Eur Endocrinol. 2013;9: 111–115.

35. Abreu-Vieira G, Xiao C, Gavrilova O, Reitman ML. Integration of body temperature into the analysis of energy expenditure in the mouse. Mol Metab. 2015;4: 461–470.

36. Pang G, Xie J, Chen Q, Hu Z. Energy intake, metabolic homeostasis, and human health. Food Science and Human Wellness. 2014;3: 89–103.

37. Tilg H, Moschen AR, Kaser A. Obesity and the microbiota. Gastroenterology. 2009;136: 1476–1483.

38. Bäckhed F, Ding H, Wang T, Hooper LV, Koh GY, Nagy A, et al. The gut microbiota as an environmental factor that regulates fat storage. Proc Natl Acad Sci U S A. 2004;101: 15718–15723.

39. Li B, Li L, Li M, Lam SM, Wang G, Wu Y, et al. Microbiota Depletion Impairs Thermogenesis of Brown Adipose Tissue and Browning of White Adipose Tissue. Cell Rep. 2019;26: 2720–2737.e5.

40. Asadi A, Shadab Mehr N, Mohamadi MH, Shokri F, Heidary M, Sadeghifard N, et al. Obesity and gut-microbiota-brain axis: A narrative review. J Clin Lab Anal. 2022; e24420.

41. Scheiman J, Luber JM, Chavkin TA, MacDonald T, Tung A, Pham L-D, et al. Meta-omics analysis of elite athletes identifies a performance-enhancing microbe that functions via lactate metabolism. Nat Med. 2019;25: 1104–1109.

42. Miyazaki K, Itoh N, Yamamoto S, Higo-Yamamoto S, Nakakita Y, Kaneda H, et

al. Dietary heat-killed Lactobacillus brevis SBC8803 promotes voluntary wheel-running and affects sleep rhythms in mice. Life Sci. 2014;111: 47–52.

43. Dohnalová L, Lundgren P, Carty JRE, Goldstein N, Wenski SL, Nanudorn P, et al. A microbiome-dependent gut-brain pathway regulates motivation for exercise. Nature. 2022;612: 739–747.

44. Wang J, Jia H. Metagenome-wide association studies: fine-mining the microbiome. Nat Rev Microbiol. 2016;14: 508.

45. Turnbaugh PJ, Hamady M, Yatsunenko T, Cantarel BL, Duncan A, Ley RE, et al. A core gut microbiome in obese and lean twins. Nature. 2009;457: 480–484.

46. Peters BA, Shapiro JA, Church TR, Miller G, Trinh-Shevrin C, Yuen E, et al. A taxonomic signature of obesity in a large study of American adults. Sci Rep. 2018;8: 9749.

47. Brooks AW, Priya S, Blekhman R, Bordenstein SR. Gut microbiota diversity across ethnicities in the United States. PLoS Biol. 2018;16: e2006842.

48. López-Contreras BE, Morán-Ramos S, Villarruel-Vázquez R, Macías-Kauffer L, Villamil-Ramírez H, León-Mimila P, et al. Composition of gut microbiota in obese and normal-weight Mexican school-age children and its association with metabolic traits. Pediatr Obes. 2018;13: 381–388.

49. Jackson MA, Bonder MJ, Kuncheva Z, Zierer J, Fu J, Kurilshikov A, et al. Detection of stable community structures within gut microbiota co-occurrence networks from different human populations. PeerJ. 2018;6: e4303.

50. Ferrer M, Ruiz A, Lanza F, Haange S-B, Oberbach A, Till H, et al. Microbiota from the distal guts of lean and obese adolescents exhibit partial functional redundancy besides clear differences in community structure. Environ Microbiol. 2013;15: 211–226.

51. Fu J, Bonder MJ, Cenit MC, Tigchelaar EF, Maatman A, Dekens JAM, et al. The Gut Microbiome Contributes to a Substantial Proportion of the Variation in Blood Lipids. Circ Res. 2015;117: 817–824.

52. Kummen M, Holm K, Anmarkrud JA, Nygård S, Vesterhus M, Høivik ML, et al. The gut microbial profile in patients with primary sclerosing cholangitis is distinct from patients with ulcerative colitis without biliary disease and healthy controls. Gut. 2017;66: 611–619.

53. Stanislawski MA, Dabelea D, Wagner BD, Sontag MK, Lozupone CA, Eggesbø M. Pre-pregnancy weight, gestational weight gain, and the gut microbiota of mothers and their infants. Microbiome. 2017;5: 113.

54. Lim MY, You HJ, Yoon HS, Kwon B, Lee JY, Lee S, et al. The effect of heritability and host genetics on the gut microbiota and metabolic syndrome. Gut. 2017;66: 1031–1038.

55. Yun Y, Kim H-N, Kim SE, Heo SG, Chang Y, Ryu S, et al. Comparative analysis

of gut microbiota associated with body mass index in a large Korean cohort. BMC Microbiol. 2017;17: 151.

56. Oki K, Toyama M, Banno T, Chonan O, Benno Y, Watanabe K. Comprehensive analysis of the fecal microbiota of healthy Japanese adults reveals a new bacterial lineage associated with a phenotype characterized by a high frequency of bowel movements and a lean body type. BMC Microbiol. 2016;16: 284.

57. Li X, Yuan X, Pang L, Miao Y, Wang S, Zhang X, et al. Gut Microbiota markers for antipsychotics induced metabolic disturbance in drug naïve patients with first episode schizophrenia – A 24 weeks follow-up study. bioRxiv. medRxiv; 2021. doi:10.1101/2020.12.26.20248886

58. Vujkovic-Cvijin I, Sklar J, Jiang L, Natarajan L, Knight R, Belkaid Y. Host variables confound gut microbiota studies of human disease. Nature. 2020;587: 448–454.

59. Nogacka AM, de Los Reyes-Gavilán CG, Martínez-Faedo C, Ruas-Madiedo P, Suarez A, Mancabelli L, et al. Impact of Extreme Obesity and Diet-Induced Weight Loss on the Fecal Metabolome and Gut Microbiota. Mol Nutr Food Res. 2021;65: e2000030.

60. Dhakal S, McCormack L, Dey M. Association of the Gut Microbiota with Weight-Loss Response within a Retail Weight-Management Program. Microorganisms. 2020;8. doi:10.3390/microorganisms8081246

61. Li X, Li Z, He Y, Li P, Zhou H, Zeng N. Regional distribution of Christensenellaceae and its associations with metabolic syndrome based on a population-level analysis. PeerJ. 2020;8: e9591.

62. Cuevas-Sierra A, Riezu-Boj JI, Guruceaga E, Milagro FI, Martínez JA. Sex-Specific Associations between Gut Prevotellaceae and Host Genetics on Adiposity. Microorganisms. 2020;8. doi:10.3390/microorganisms8060938

63. McCann JR, Bihlmeyer NA, Roche K, Catherine C, Jawahar J, Kwee LC, et al. The pediatric obesity microbiome and metabolism study (POMMS): Methods, baseline data, and early insights. bioRxiv. medRxiv; 2020. doi:10.1101/2020.06.09.20126763

64. Ikeda T, Aida M, Yoshida Y, Matsumoto S, Tanaka M, Nakayama J, et al. Alteration in faecal bile acids, gut microbial composition and diversity after laparoscopic sleeve gastrectomy. Br J Surg. 2020;107: 1673–1685.

65. Gong J, Shen Y, Zhang H, Cao M, Guo M, He J, et al. Gut Microbiota Characteristics of People with Obesity by Meta-Analysis of Existing Datasets. Nutrients. 2022;14. doi:10.3390/nu14142993

66. Stefura T, Zapała B, Gosiewski T, Skomarovska O, Dudek A, Pędziwiatr M, et al. Differences in Compositions of Oral and Fecal Microbiota between Patients with Obesity and Controls. Medicina . 2021;57. doi:10.3390/medicina57070678

67. Allin KH, Tremaroli V, Caesar R, Jensen BAH, Damgaard MTF, Bahl MI, et al.

Aberrant intestinal microbiota in individuals with prediabetes. Diabetologia. 2018;61: 810–820.

68. Castro-Mejía JL, Khakimov B, Krych Ł, Bülow J, Bechshøft RL, Højfeldt G, et al. Physical fitness in community-dwelling older adults is linked to dietary intake, gut microbiota, and metabolomic signatures. Aging Cell. 2020;19: e13105.

69. Yuan X, Chen R, McCormick KL, Zhang Y, Lin X, Yang X. Metabolically healthy obese children and the role of the gut Microbiota. Research Square. Research Square; 2020. doi:10.21203/rs.3.rs-127205/v1

70. Kim M-H, Yun KE, Kim J, Park E, Chang Y, Ryu S, et al. Gut microbiota and metabolic health among overweight and obese individuals. Sci Rep. 2020;10: 19417.

71. Calderón-Pérez L, Llauradó E, Companys J, Pla-Pagà L, Pedret A, Rubió L, et al. Interplay between dietary phenolic compound intake and the human gut microbiome in hypertension: A cross-sectional study. Food Chem. 2021;344: 128567.

72. Radwan S, Gilfillan D, Eklund B, Radwan HM, El Menofy NG, Lee J, et al. A comparative study of the gut microbiome in Egyptian patients with Type I and Type II diabetes. PLoS One. 2020;15: e0238764.

73. Reitmeier S, Kiessling S, Clavel T, List M, Almeida EL, Ghosh TS, et al. Arrhythmic Gut Microbiome Signatures Predict Risk of Type 2 Diabetes. Cell Host Microbe. 2020;28: 258–272.e6.

74. Sparvoli LG, Cortez RV, Daher S, Padilha M, Sun SY, Nakamura MU, et al. Women's multisite microbial modulation during pregnancy. Microb Pathog. 2020;147: 104230.

75. Gao B, Zhong M, Shen Q, Wu Y, Cao M, Ju S, et al. Gut microbiota in early pregnancy among women with Hyperglycaemia vs. Normal blood glucose. BMC Pregnancy Childbirth. 2020;20: 284.

76. Cancello R, Turroni S, Rampelli S, Cattaldo S, Candela M, Cattani L, et al. Effect of Short-Term Dietary Intervention and Probiotic Mix Supplementation on the Gut Microbiota of Elderly Obese Women. Nutrients. 2019;11. doi:10.3390/nu11123011

77. Alemán JO, Bokulich NA, Swann JR, Walker JM, De Rosa JC, Battaglia T, et al. Fecal microbiota and bile acid interactions with systemic and adipose tissue metabolism in diet-induced weight loss of obese postmenopausal women. J Transl Med. 2018;16: 244.

78. Org E, Blum Y, Kasela S, Mehrabian M, Kuusisto J, Kangas AJ, et al. Relationships between gut microbiota, plasma metabolites, and metabolic syndrome traits in the METSIM cohort. Genome Biol. 2017;18: 70.

79. Guzmán-Castañeda SJ, Ortega-Vega EL, de la Cuesta-Zuluaga J, Velásquez-Mejía EP, Rojas W, Bedoya G, et al. Gut microbiota composition explains more

variance in the host cardiometabolic risk than genetic ancestry. bioRxiv. 2018. p. 394726. doi:10.1101/394726

80. He Y, Wu W, Wu S, Zheng H-M, Li P, Sheng H-F, et al. Linking gut microbiota, metabolic syndrome and economic status based on a population-level analysis. Microbiome. 2018;6: 172.

81. Alcazar M, Escribano J, Ferré N, Closa-Monasterolo R, Selma-Royo M, Feliu A, et al. Gut microbiota is associated with metabolic health in children with obesity. Clin Nutr. 2022. doi:10.1016/j.clnu.2022.06.007

82. Sowah SA, Milanese A, Schübel R, Wirbel J, Kartal E, Johnson TS, et al. Calorie restriction improves metabolic state independently of gut microbiome composition: a randomized dietary intervention trial. Genome Med. 2022;14: 30.

83. Tavella T, Rampelli S, Guidarelli G, Bazzocchi A, Gasperini C, Pujos-Guillot E, et al. Elevated gut microbiome abundance of Christensenellaceae, Porphyromonadaceae and Rikenellaceae is associated with reduced visceral adipose tissue and healthier metabolic profile in Italian elderly. Gut Microbes. 2021;13: 1–19.

84. Chen Z, Radjabzadeh D, Chen L, Kurilshikov A, Kavousi M, Ahmadizar F, et al. Association of Insulin Resistance and Type 2 Diabetes With Gut Microbial Diversity: A Microbiome-Wide Analysis From Population Studies. JAMA Netw Open. 2021;4: e2118811.

85. Villaseñor-Aranguren M, Rosés C, Riezu-Boj JI, López-Yoldi M, Ramos-Lopez O, Barceló AM, et al. Association of the Gut Microbiota with the Host's Health through an Analysis of Biochemical Markers, Dietary Estimation, and Microbial Composition. Nutrients. 2022;14. doi:10.3390/nu14234966

86. Papa E, Docktor M, Smillie C, Weber S, Preheim SP, Gevers D, et al. Non-Invasive Mapping of the Gastrointestinal Microbiota Identifies Children with Inflammatory Bowel Disease. PLoS One. 2012;7: e39242.

87. Rajilić-Stojanović M, Shanahan F, Guarner F, de Vos WM. Phylogenetic analysis of dysbiosis in ulcerative colitis during remission. Inflamm Bowel Dis. 2013;19: 481–488.

88. Palm NW, de Zoete MR, Cullen TW, Barry NA, Stefanowski J, Hao L, et al. Immunoglobulin A Coating Identifies Colitogenic Bacteria in Inflammatory Bowel Disease. Cell. 2014;158: 1000–1010.

89. Jalanka-Tuovinen J, Salojärvi J, Salonen A, Immonen O, Garsed K, Kelly FM, et al. Faecal microbiota composition and host–microbe cross-talk following gastroenteritis and in postinfectious irritable bowel syndrome. Gut. 2014;63: 1737–1745.

90. Palma GD, De Palma G, Lynch MDJ, Lu J, Dang VT, Deng Y, et al. Transplantation of fecal microbiota from patients with irritable bowel syndrome alters gut function and behavior in recipient mice. Sci Transl Med. 2017;9:

eaaf6397.

91. Zhang L, Bahl MI, Roager HM, Fonvig CE, Hellgren LI, Frandsen HL, et al. Environmental spread of microbes impacts the development of metabolic phenotypes in mice transplanted with microbial communities from humans. ISME J. 2017;11: 676–690.

92. Turpin W, Espin-Garcia O, Xu W, Silverberg MS, Kevans D, Smith MI, et al. Association of host genome with intestinal microbial composition in a large healthy cohort. Nat Genet. 2016;48: 1413–1417.

93. Rosa BA, Hallsworth-Pepin K, Martin J, Wollam A, Mitreva M. Genome Sequence of Christensenella minuta DSM 22607 ^{T}. Genome Announcements. 2017. doi:10.1128/genomea.01451-16

94. Waters JL, Ley RE. The human gut bacteria Christensenellaceae are widespread, heritable, and associated with health. BMC Biol. 2019;17: 83.

95. Ruaud A, Esquivel-Elizondo S, de la Cuesta-Zuluaga J, Waters JL, Angenent LT, Youngblut ND, et al. Syntrophy via Interspecies H2 Transfer between Christensenella and Methanobrevibacter Underlies Their Global Cooccurrence in the Human Gut. MBio. 2020;11. doi:10.1128/mBio.03235-19

96. Mazier W, Le Corf K, Martinez C, Tudela H, Kissi D, Kropp C, et al. A New Strain of Christensenella minuta as a Potential Biotherapy for Obesity and Associated Metabolic Diseases. Cells. 2021;10: 823.

97. Rajilić-Stojanović M, de Vos WM. The first 1000 cultured species of the human gastrointestinal microbiota. FEMS Microbiol Rev. 2014;38: 996–1047.

98. Awany D, Allali I, Dalvie S, Hemmings S, Mwaikono KS, Thomford NE, et al. Host and Microbiome Genome-Wide Association Studies: Current State and Challenges. Front Genet. 2018;9: 637.

99. Spor A, Koren O, Ley R. Unravelling the effects of the environment and host genotype on the gut microbiome. Nat Rev Microbiol. 2011;9: 279–290.

100. Clavel T, Lagkouvardos I, Blaut M, Stecher B. The mouse gut microbiome revisited: From complex diversity to model ecosystems. Int J Med Microbiol. 2016;306: 316–327.

101. Mark Welch JL, Hasegawa Y, McNulty NP, Gordon JI, Borisy GG. Spatial organization of a model 15-member human gut microbiota established in gnotobiotic mice. Proc Natl Acad Sci U S A. 2017;114: E9105–E9114.

102. Elzinga J, van der Oost J, de Vos WM, Smidt H. The Use of Defined Microbial Communities To Model Host-Microbe Interactions in the Human Gut. Microbiol Mol Biol Rev. 2019;83. doi:10.1128/MMBR.00054-18

103. Balish E, Warner T. Enterococcus faecalis induces inflammatory bowel disease in interleukin-10 knockout mice. Am J Pathol. 2002;160: 2253–2257.

104. Devkota S, Wang Y, Musch MW, Leone V, Fehlner-Peach H, Nadimpalli A, et al. Dietary-fat-induced taurocholic acid promotes pathobiont expansion and colitis in Il10-/- mice. Nature. 2012;487: 104–108.

105. Kernbauer E, Ding Y, Cadwell K. An enteric virus can replace the beneficial function of commensal bacteria. Nature. 2014;516: 94–98.

106. Ukena SN, Singh A, Dringenberg U, Engelhardt R, Seidler U, Hansen W, et al. Probiotic Escherichia coli Nissle 1917 inhibits leaky gut by enhancing mucosal integrity. PLoS One. 2007;2: e1308.

107. Sugahara H, Odamaki T, Fukuda S, Kato T, Xiao J-Z, Abe F, et al. Probiotic Bifidobacterium longum alters gut luminal metabolism through modification of the gut microbial community. Sci Rep. 2015;5: 13548.

108. Van den Abbeele P, Gérard P, Rabot S, Bruneau A, El Aidy S, Derrien M, et al. Arabinoxylans and inulin differentially modulate the mucosal and luminal gut microbiota and mucin-degradation in humanized rats. Environ Microbiol. 2011;13: 2667–2680.

109. Spichak S, Guzzetta KE, O'Leary OF, Clarke G, Dinan TG, Cryan JF. Without a bug's life: Germ-free rodents to interrogate microbiota-gut-neuroimmune interactions. Drug Discov Today Dis Models. 2019.

110. Norin E, Midtvedt T. Intestinal microflora functions in laboratory mice claimed to harbor a "normal" intestinal microflora. Is the SPF concept running out of date? Anaerobe. 2010;16: 311–313.

111. Martínez I, Maldonado-Gomez MX, Gomes-Neto JC, Kittana H, Ding H, Schmaltz R, et al. Experimental evaluation of the importance of colonization history in early-life gut microbiota assembly. Elife. 2018;7. doi:10.7554/eLife.36521

112. Datta MS, Sliwerska E, Gore J, Polz MF, Cordero OX. Microbial interactions lead to rapid micro-scale successions on model marine particles. Nat Commun. 2016;7: 11965.

113. Rey FE, Faith JJ, Bain J, Muehlbauer MJ, Stevens RD, Newgard CB, et al. Dissecting the in vivo metabolic potential of two human gut acetogens. J Biol Chem. 2010;285: 22082–22090.

114. Wymore Brand M, Wannemuehler MJ, Phillips GJ, Proctor A, Overstreet A-M, Jergens AE, et al. The Altered Schaedler Flora: Continued Applications of a Defined Murine Microbial Community. ILAR J. 2015;56: 169–178.

115. Claassen-Weitz S, Gardner-Lubbe S, Mwaikono KS, du Toit E, Zar HJ, Nicol MP. Optimizing 16S rRNA gene profile analysis from low biomass nasopharyngeal and induced sputum specimens. BMC Microbiol. 2020;20: 113.

116. Eisenhofer R, Minich JJ, Marotz C, Cooper A, Knight R, Weyrich LS. Contamination in Low Microbial Biomass Microbiome Studies: Issues and Recommendations. Trends Microbiol. 2019;27: 105–117.

117. Brankatschk R, Bodenhausen N, Zeyer J, Bürgmann H. Simple absolute quantification method correcting for quantitative PCR efficiency variations for microbial community samples. Appl Environ Microbiol. 2012;78: 4481–4489.

118. Barker K. At the Bench: A Laboratory Navigator. Cold Spring Harbor Laboratory Press, NY; 1998.

119. Flynn CR, Albaugh VL, Cai S, Cheung-Flynn J, Williams PE, Brucker RM, et al. Bile diversion to the distal small intestine has comparable metabolic benefits to bariatric surgery. Nat Commun. 2015;6: 7715.

120. Bacchetti De Gregoris T, Aldred N, Clare AS, Burgess JG. Improvement of phylum- and class-specific primers for real-time PCR quantification of bacterial taxa. J Microbiol Methods. 2011;86: 351–356.

121. Staroscik A. Calculator for determining the number of copies of a template. 29 Jan 2004 [cited 4 Jun 2019]. Available: https://cels.uri.edu/gsc/cndna.html

122. Spiess A-N. qpcR: Modelling and Analysis of Real-Time PCR Data. 2018. Available: https://CRAN.R-project.org/package=qpcR

123. Collet C, Gaudard O, Péringer P, Schwitzguébel J-P. Acetate production from lactose by Clostridium thermolacticum and hydrogen-scavenging microorganisms in continuous culture--effect of hydrogen partial pressure. J Biotechnol. 2005;118: 328–338.

124. Smith NW, Shorten PR, Altermann EH, Roy NC, McNabb WC. Hydrogen cross-feeders of the human gastrointestinal tract. Gut Microbes. 2019;10: 270–288.

125. Ríos-Covián D, Ruas-Madiedo P, Margolles A, Gueimonde M, de Los Reyes-Gavilán CG, Salazar N. Intestinal Short Chain Fatty Acids and their Link with Diet and Human Health. Front Microbiol. 2016;7: 185.

126. Bernalier A, Willems A, Leclerc M, Rochet V, Collins MD. Ruminococcus hydrogenotrophicus sp. nov., a new H2/CO2-utilizing acetogenic bacterium isolated from human feces. Arch Microbiol. 1996;166: 176–183.

127. Wolf PG, Biswas A, Morales SE, Greening C, Gaskins HR. H2 metabolism is widespread and diverse among human colonic microbes. Gut Microbes. 2016;7: 235–245.

128. Kostic AD, Howitt MR, Garrett WS. Exploring host-microbiota interactions in animal models and humans. Genes Dev. 2013;27: 701–718.

129. Zarrinpar A, Chaix A, Yooseph S, Panda S. Diet and feeding pattern affect the diurnal dynamics of the gut microbiome. Cell Metab. 2014;20: 1006–1017.

130. Bolyen E, Rideout JR, Dillon MR, Bokulich NA, Abnet CC, Al-Ghalith GA, et al. Reproducible, interactive, scalable and extensible microbiome data science using QIIME 2. Nat Biotechnol. 2019;37: 852–857.

131. Caporaso JG, Kuczynski J, Stombaugh J, Bittinger K, Bushman FD, Costello EK, et al. QIIME allows analysis of high-throughput community sequencing data. Nat Methods. 2010;7: 335–336.

132. Anderson MJ. A new method for non-parametric multivariate analysis of variance. Austral Ecology. 2001. pp. 32–46. doi:10.1111/j.1442-9993.2001.01070.pp.x

133. Oksanen J, Blanchet FG, Kindt R, Legendre P, Minchin PR, O'Hara RB, et al. vegan: community ecology package. 2013. Available: https://CRAN.R-project.org/package=vegan

134. Mallick H, Rahnavard A, McIver LJ, Ma S, Zhang Y, Nguyen LH, et al. Multivariable association discovery in population-scale meta-omics studies. PLoS Comput Biol. 2021;17: e1009442.

135. Turnbaugh PJ, Ridaura VK, Faith JJ, Rey FE, Knight R, Gordon JI. The effect of diet on the human gut microbiome: a metagenomic analysis in humanized gnotobiotic mice. Sci Transl Med. 2009;1: 6ra14.

136. Liang Y, Dong T, Chen M, He L, Wang T, Liu X, et al. Systematic Analysis of Impact of Sampling Regions and Storage Methods on Fecal Gut Microbiome and Metabolome Profiles. mSphere. 2020;5. doi:10.1128/mSphere.00763-19

137. Davis DJ, Hecht PM, Jasarevic E, Beversdorf DQ, Will MJ, Fritsche K, et al. Sex-specific effects of docosahexaenoic acid (DHA) on the microbiome and behavior of socially-isolated mice. Brain Behav Immun. 2017;59: 38–48.

138. Heisel T, Montassier E, Johnson A, Al-Ghalith G, Lin Y-W, Wei L-N, et al. High-Fat Diet Changes Fungal Microbiomes and Interkingdom Relationships in the Murine Gut. mSphere. 2017;2. doi:10.1128/mSphere.00351-17

139. Liu Z, Wang N, Ma Y, Wen D. Hydroxytyrosol Improves Obesity and Insulin Resistance by Modulating Gut Microbiota in High-Fat Diet-Induced Obese Mice. Front Microbiol. 2019;10: 390.

140. Lin H, An Y, Hao F, Wang Y, Tang H. Correlations of Fecal Metabonomic and Microbiomic Changes Induced by High-fat Diet in the Pre-Obesity State. Sci Rep. 2016;6: 21618.

141. Aguilar-Rojas A, Olivo-Marin J-C, Guillen N. Human intestinal models to study interactions between intestine and microbes. Open Biol. 2020;10: 200199.

142. Poletti M, Arnauts K, Ferrante M, Korcsmaros T. Organoid-based Models to Study the Role of Host-microbiota Interactions in IBD. J Crohns Colitis. 2021;15: 1222–1235.

143. Jin Z, Ng A, Maurice CF, Juncker D. The Mini Colon Model: a benchtop multi-bioreactor system to investigate the gut microbiome. Gut Microbes. 2022;14: 2096993.

144. Luczynski P, McVey Neufeld K-A, Oriach CS, Clarke G, Dinan TG, Cryan JF.

Growing up in a Bubble: Using Germ-Free Animals to Assess the Influence of the Gut Microbiota on Brain and Behavior. Int J Neuropsychopharmacol. 2016;19. doi:10.1093/ijnp/pyw020

145. Hugenholtz F, de Vos WM. Mouse models for human intestinal microbiota research: a critical evaluation. Cell Mol Life Sci. 2018;75: 149–160.

146. Nguyen TLA, Vieira-Silva S, Liston A, Raes J. How informative is the mouse for human gut microbiota research? Dis Model Mech. 2015;8: 1–16.

147. Park JC, Im S-H. Of men in mice: the development and application of a humanized gnotobiotic mouse model for microbiome therapeutics. Exp Mol Med. 2020;52: 1383–1396.

148. Moulin TC, Covill LE, Itskov PM, Williams MJ, Schiöth HB. Rodent and fly models in behavioral neuroscience: An evaluation of methodological advances, comparative research, and future perspectives. Neurosci Biobehav Rev. 2021;120: 1–12.

149. Ley RE, Bäckhed F, Turnbaugh P, Lozupone CA, Knight RD, Gordon JI. Obesity alters gut microbial ecology. Proc Natl Acad Sci U S A. 2005;102: 11070–11075.

150. Lombardi P, Goldin B, Boutin E, Gorbach SL. Metabolism of androgens and estrogens by human fecal microorganisms. J Steroid Biochem. 1978;9: 795–801.

151. Gagen EJ, Padmanabha J, Denman SE, McSweeney CS. Hydrogenotrophic culture enrichment reveals rumen Lachnospiraceae and Ruminococcaceae acetogens and hydrogen-responsive Bacteroidetes from pasture-fed cattle. FEMS Microbiol Lett. 2015;362. doi:10.1093/femsle/fnv104

152. Ge L, Qi J, Shao B, Ruan Z, Ren Y, Sui S, et al. Microbial hydrogen economy alleviates colitis by reprogramming colonocyte metabolism and reinforcing intestinal barrier. Gut Microbes. 2022;14: 2013764.